Lateral Heterogeneity in Compressional Mountain Belt Settings

Bibek Giri and Mary Hubbard

Department of Earth Sciences, Montana State University, Bozeman

Corresponding author: Bibek Giri (bibekgiri@montana.edu)

Key Points

- Lateral heterogeneity, expressed as sharp lateral variations, has been observed in most orogens and often coincides with cross structures.
- Major controls are basement structures, lateral changes in sedimentary facies, varying crustal rheology, and changing plate dynamics.
- Lateral heterogeneities impact orogenic evolution and have geomorphic, seismic, and economic implications.

Abstract

Convergent orogens are typically linear with laterally continuous, orogen-parallel folds and thrusts. Over the years, geoscience research has revealed evidence for important orthogonal/cross structures as well as lateral heterogeneity in deformation style, igneous activity, metamorphic grade, geomorphology, and seismic activity. To assess the occurrence, causal mechanisms, and implications of these lateral heterogeneities, a selection of convergent orogens, with different tectonic settings and history are reviewed. The Appalachians, the North American Cordillera, the Alps, the Himalayas, the Zagros, the Andes, and several other belts all exhibit a degree of lateral heterogeneity. Major factors driving the lateral heterogeneity and/or cross structures include the pre-existing deformational history of the cratonic blocks involved, lateral change in lithology of crustal rocks, variations in crustal/lithospheric rheologic properties, or changes in plate kinematics. The Appalachian orogenic front mimics the Iapetan rift margin. Pre-existing basement structures have control on pre- and syn-orogenic sedimentation, which subsequently impacts how an orogenic wedge evolves. A thicker sedimentary column generally evolves into a salient (as opposed to a recess), which is further enhanced by the presence of weak horizons as seen in the Zagros and the Cordillera. Lateral variation in sedimentary facies also creates changes in thrust-ramp geometry. During orogenic contraction, inherited basement structures can be preferentially reactivated based on their orientation. Several cross faults in the Himalayas spatially coincide with orogen-perpendicular, lower plate, basement structures. In a similar way, oceanic subducting plate physiography can also influence deformation in the overriding plate. Along-strike variations in subduction dynamics have been reflected in the Andean deformation. Orogenic extension in the Alps has been accompanied by a system of orogen-parallel strike slip faults and extensional cross faults. It is evident that lateral heterogeneities can form crucial control on the evolution of orogenic belts and can influence seismic rupture patterns, resource occurrence, and landslide-related natural hazards.

1 Introduction

Many of the world's major mountain belts are found along modern or former convergent plate boundaries and they are typically dominated by major thrust structures (Elliott, 1976; Chapple, 1978; Boyer & Elliott, 1982; Dahlen, 1990). The terms 'continental collision or terrane accretion' have been used for convergent boundaries when both the involved plates are continental, though mountain building also occurs along convergent plate boundaries where an oceanic plate is subducting beneath continental crust (e.g.; Dewey & Bird, 1970). In both tectonic settings, compressive stress is accommodated through imbrication and shortening of upper crustal material as thrust sheets and/or nappes, within a system of fault surfaces, which generally strike perpendicular to the direction of compression (or parallel to the orogen). In general, these faults and related structures are laterally continuous both temporally and spatially. Detailed geological and geophysical research, however, has found that while these convergent mountain belts exhibit overall lateral continuity, there are also lateral heterogeneities that have made an important contribution to the development of the mountain belt. Driven by various mechanisms, these lateral changes serve to induce important structural, geological, and geomorphological lateral heterogeneities along mountains belts that may (or may have) influence(d) igneous or seismic processes or even the occurrence of economic resources. Commonly, significant along-strike changes are known to occur across structures, which strike orthogonal to the overall trend of the orogen. In this article, the term 'cross structure' has been utilized to refer to all generic, syn and post orogenic structural features that bound lateral changes along a mountain belt, though the terms 'cross-strike structural discontinuities' (CSD), 'transverse zones', and 'cross faults' have all been utilized to describe large-scale structures that strike across convergent mountain belts (Drahovzal & Thomas, 1976; Wheeler, 1980; Hubbard et al., 2018; Hubbard et al., 2021). Thomas (1990) suggested that transverse zones (TZ) along fold and thrust belts are domains of several, structurally aligned 'lateral connectors', which encompass transverse/tear faults, lateral ramps, and displacement transfer faults/zones. In general, the term 'transverse zone' has been used in the literature to denote large-scale, inherited basement features with a high-angled orientation to the evolving orogen. Lateral connecters like tear faults, lateral ramps, and transfer faults/zones form during thrust propagation and are rather localized, only spanning across a few thrust sheets. Formed during the propagation of thrust belts, these lateral connectors could be spatially controlled by the inherited structures in the crystalline basement as well as the overlying stratigraphy of the

evolving thrust sheet (Thomas, 1990). During orogenesis, inherited basement structures are commonly reactivated or inverted and impart a great control on the tectonic and structural evolution of mountain belts (e.g.; Tavarnelli et al., 2004; Butler et al., 2006). Evidence has also been presented suggesting that oceanic transform faults or seamounts in a subducting oceanic plate can influence the structural development of the mountain belt in the overriding continental plate, thus causing lateral heterogeneity or the presence of cross structures (e.g.; Gutscher et al., 2000; Chapin, 2012).

Mountain belts formed in convergent plate tectonic settings at different time periods in Earth's history all exhibit some degree of lateral heterogeneity. The following review explores a selection of mountain belts from convergent boundaries, examining the proposed driving mechanisms and implications of lateral heterogeneities and the presence of cross structures during and after orogenesis. The Appalachians, the North American Cordillera, the Alps, the Himalayas, the Zagros, and the Andes have been looked at in detail, and several other mountain belts are briefly discussed (Figure 1). This selection represents some of the most well studied and prominent mountain belts around the world and presents a wide array of tectonic settings. Within each mountain belt, presented examples of lateral heterogeneities and cross structures are representative of the lateral variability for that orogen. For each mountain belt, we present a brief introduction of the tectonic setting, observed lateral heterogeneities, and proposed causal factors for those heterogeneities. It is noted that lateral heterogeneities can be expressed in several ways including: 1) along-strike changes in deformation style; 2) variation in igneous activity or metamorphic grade; 3) variation in seismic activity; 4) changes in geomorphology; or 5) abrupt lateral stratigraphic change. Drivers of these along-strike changes can include irregularities along continental margin, inherited basement structures of an overriding plate, features from a subducting plate (oceanic) or footwall block (continental), lateral variation in lithospheric or crustal properties, lateral changes in thickness and facies of the deforming sedimentary sequence, lateral variation in dynamic plate tectonic setting or a combination of these factors. Apart from their influence in the structural/tectonic evolution of the mountain belt, the lateral heterogeneity may also have important seismic, geomorphic, and economic implications.

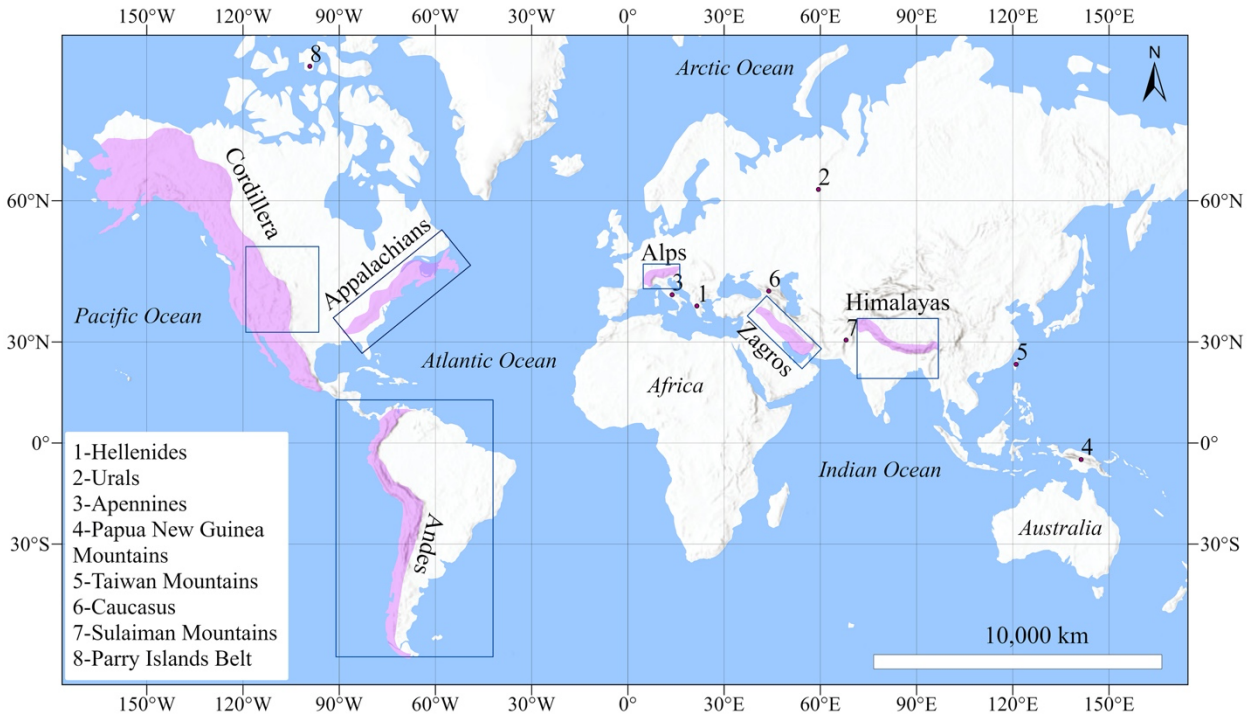

Figure 1: Map of the world showing locations of mountain belts described in this review. The pink shades are spatial extent of respective orogenic belts. Rectangular boxes indicate the extent of tectonic maps presented in the following sections. Numbered areas are other convergent orogens mentioned in the text.

2 Appalachians

2.1 Tectonic Setting and Lateral Heterogeneities

The Appalachian orogenic belt, along the eastern margin of the North American continent, is the structural culmination of a prolonged tectonic history consisting of multiple episodes of subduction, terrain accretion, continental collision, and rifting (Figure 2). The prominent Grenville orogeny (1.3-0.9 Ga; Li et al., 2008; Hynes & Rivers, 2010; Rivers, 2012)) was the coalescence of the Laurentian (modern day North American continent) and Amazonian cratons, which formed the Rodinia supercontinent (Li et al., 2008; Rivers, 2008, 2015). Following the Grenville orogeny, the Laurentian craton remained tectonically inactive for about 250 Ma before being detached from the Rodinia craton in various episodes from 759±12 Ma to 530 Ma (Thomas, 1991; Aleinikoff et al., 1995; Hogan & Gilbert, 1998). The Iapetan rifting, during which the Iapetus ocean opened between the Laurentian and Amazonian (Gondwana) cratons (Domeier, 2016), marked the end of

this series of tectonic events (Rankin, 1976; Thomas, 1977; O'Brien & van der Pluijm, 2012). The Middle Ordovician to Late Silurian Taconian orogeny represents the aggregate contractional tectonic activity along the boundary between the Laurentian and Iapetan plates (Hatcher, 1972; Drake et al., 1989; van Staal et al., 2007; Hatcher, 2010). The Late Silurian to Devonian Acadian orogeny has been interpreted to have formed along an Andean-type margin (flat slab subduction) following the accretion of Avalonia to the Laurentia margin (Keppie & Krogh, 1999; Murphy & Keppie, 2005). The youngest event in the building of the Appalachians was the Late Mississippian to Late Permian Alleghenian orogeny (Laurentia and Gondwana) (Hatcher et al., 1989), which also marked the formation of the Pangean supercontinent. In the Mesozoic, the modern day North American plate rifted westward from the African continent. Dominant structures from all of these convergent and divergent tectonic events are range-parallel faults and fold axes. Close inspection, however, reveals lateral heterogeneity that includes changes in the mountain belt orientation, structural style, metamorphic grade, and the presence of cross structures.

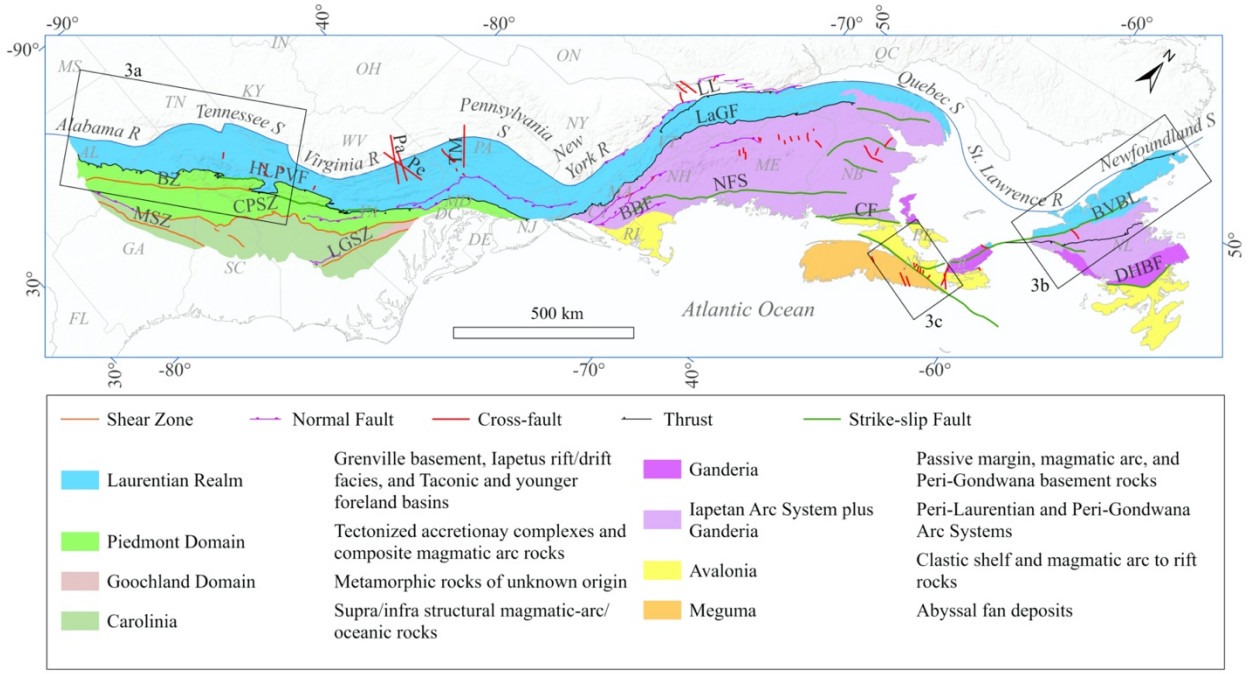

Figure 2: Simplified tectonic map of the Appalachians belt showing the major faults, the salient (S) and recesses (R), and the extent of the Appalachian deformation front. Insets show the locations of figures 3a, 3b, and 3c (simplified from: Southworth, 1986; Hibbard et al., 2006; Waldron et al., 2015).

147 Acronyms: BBF: Bloody Bluff Fault; BVBL: Baie Verte-Brompton Line; BZ: Brevard Zone; CF:
148 Caledonia Fault; CPSZ: Central Piedmont Shear Zone; DHBF: Dover Hermitage Bay Fault;
149 HLPVF: Hollins Line-Pleasant Valley Fault System; LaGF: La Gaudaloupe Fault; LGSZ: Lake
150 Gordon Shear Zone; LL: Logan's Line; MSZ: Modoc Shear Zone; NFS: Norumbega Fault System;
151 Pa: Parson's Lineament; Pe: Petersburg Lineament; TM: Tyrone-Mount Union lineament.
152

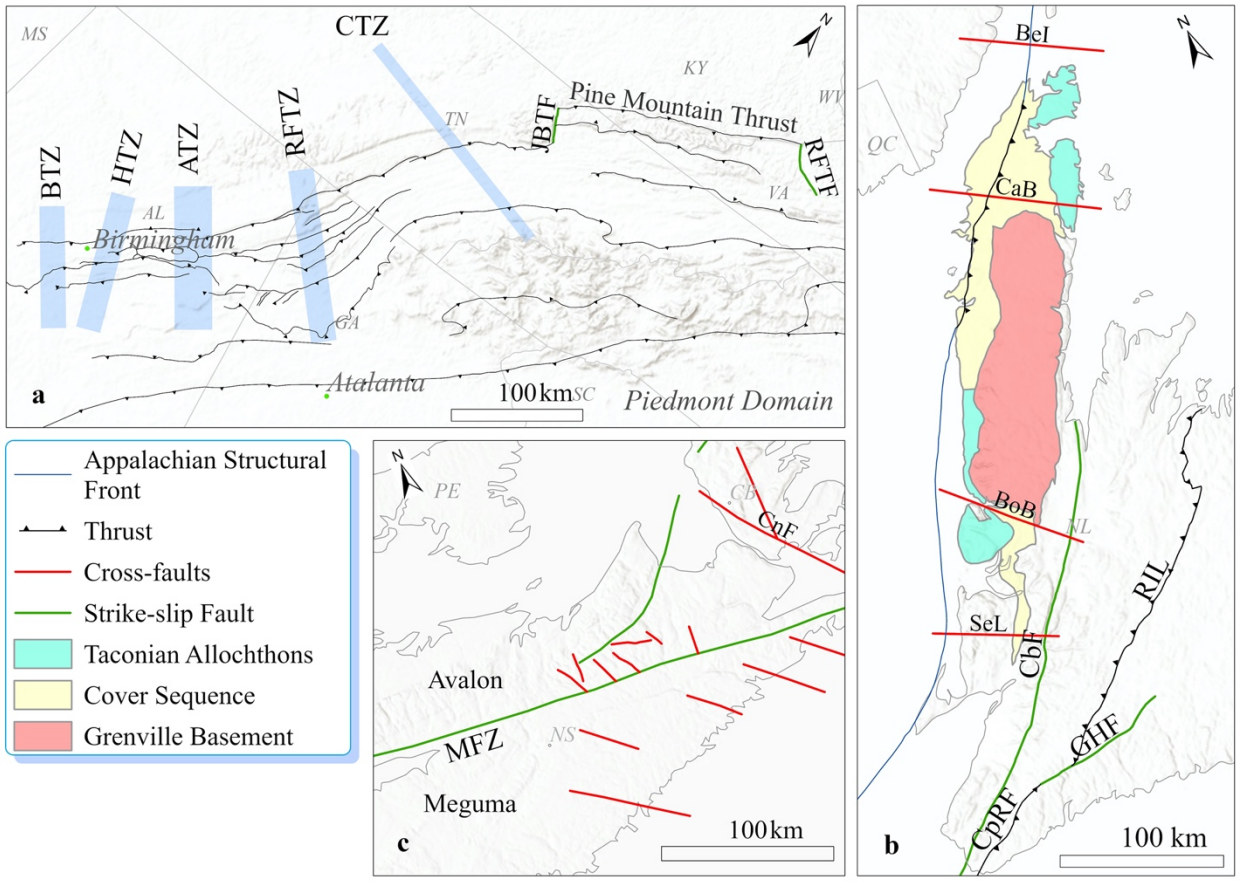

153
154

155 Figure 3: Cross structures along the Appalachians. a) Map of the Alleghenian fold and thrust belt
156 in the Alabama recess and the Tennessee salient showing the major transverse zones (light blue
157 rectangles) and the tear faults on either side of the Pine Mountain (source:Mitra, 1988; Cook &
158 Thomas, 2009). b) Tectonic-sketch map of the Newfoundland Island showing the major cross-
159 faults. Note the lateral termination of the Grenville basement inliers at the Bonne Bay cross-strike
160 discontinuity (BoB) and the Canada Bay (CaB) cross-strike discontinuity. (source: Cawood &
161 Botsford, 1991; Hibbard et al., 2006; Waldron et al., 2015). c) The Minas Fault Zone (MFZ)

between the Avalon and Meguma terranes and its conjugate faults including the Canso Fault (CnF) (source: Hibbard et al., 2006; Waldron et al., 2015).

Acronyms: ATZ: Anniston Transverse Zone; BeI: Belle Isle cross-strike discontinuity; BoB: Bonne Bay cross-strike discontinuity; BTZ: Bessemer Transverse Zone; CaB: Canada Bay cross-strike discontinuity; CbF: Cabot Fault; CnF: Canso Fault; CpRF: Cape Ray Fault; CTZ: Cartersville Transverse Zone, GHF: Gunflap Hills Fault; HTZ: Happersville Transverse Zone; JBTF: Jacksboro Tear Fault; MFZ: Minas Fault Zone; RFTF: Russel Fork Tear Fault; RFTZ: Rising Fawn Transverse Zone; RIL: Red Indian Line; SeL: Serpentine Lake cross-strike discontinuity.

One of the obvious heterogeneities in topography is the fact that the NE-trending Appalachian mountain front curves around a series of recesses and salients along the length of its western margin (Figure 2). These recesses and salient are proposed to be bound by broad transverse structures that offset or truncate thrust structures (Thomas, 1990). In the southern Appalachians, the large-scale thrust faults and related structures are predominantly striking northeast and verging towards the northwest (Bayona et al., 2003). Abrupt along-strike terminations of these structures are known to spatially coincide with these transverse zones (TZ). In the Alabama recess (Figure 3a), major TZs include the Bessemer Transfer Zone (TZ), the Happersville TZ, the Anniston TZ, and the Rising Fawn TZ from southwest to northeast respectively (Thomas, 1990; Bayona et al., 2003; Brewer, 2004). In general, these transfer zones are tens of kilometers wide, hundreds of kilometers long, and cut into the Proterozoic basement rocks (Thomas & Bayona, 2002; Brewer, 2004). Thrust-related structures plunge into these TZs, abruptly terminate at lateral or oblique ramps, show offsets along transverse faults (tear faults), or break into en-echelon segments of transfer zones (Thomas & Bayona, 2002; Thomas, 2007; Cook & Thomas, 2009). Structural strike deviates within these TZs, while propagating over oblique/lateral ramp and irregular basement and at junctions between lateral/oblique and frontal ramps (Bayona et al., 2003). Above a lateral/oblique ramp, hanging wall rocks are generally folded into upright, isoclinal folds driven by local-scale, ramp perpendicular contraction in the hanging wall due to crowding of materials along that trend (Cook and Thomas 2009). Across the Cartersville TZ, deformation style, metamorphic grade, and thrust sheet stratigraphy show sharp contrast between the Alabama recess and the Tennessee salient (Tull & Holm, 2005). In the salient, passive margin and foreland

193 sedimentary sequences are much thicker and have been deformed and metamorphosed (biotite
194 grade of the Barrovian metamorphic series) more strongly than in the recess (Tull & Holm, 2005).
195 Towards the adjoining Virginia recess, a section of the Pine Mountain belt, bounded by the left-
196 lateral Jacksboro tear fault and the right lateral Russel Fork tear fault (Figure 3a), demonstrates a
197 double ramp geometry in the middle section, while a single ramp geometry around the edges
198 (Mitra, 1988). Presence of the orogen-parallel, large-scaled (about 35 km wide, (Brewer, 2004))
199 Birmingham graben beneath the southern Alleghenian thrust belt also had major controls on the
200 foreland sedimentation and subsequent propagation of the thrust sheet (Thomas, 2007). Transverse
201 zones in the southern Appalachians have been interpreted as inherited transform fault related to
202 the Iapeton rifting along the continental margin of Laurentia (e.g.; Figure 4) (Rankin, 1976;
203 Thomas, 1977, 2014).

204 Cross-structures in the Appalachians of Pennsylvania and West Virginia (central
205 Appalachians) such as the Parsons, Petersburg, and Tyrone-Mount Union lineaments (Figure 2)
206 also have similar effects on the orogen-parallel structures as is seen in the southern Appalachians
207 (Wheeler, 1980; Southworth, 1986). In the northern Appalachians, however, genesis of cross-
208 structures presents much more diversity. The Serpentine Lake cross-strike discontinuity (CSD),
209 the Bonne Bay CSD, the Canada Bay CSD, and Belle Isle CSD in Newfoundland mark the

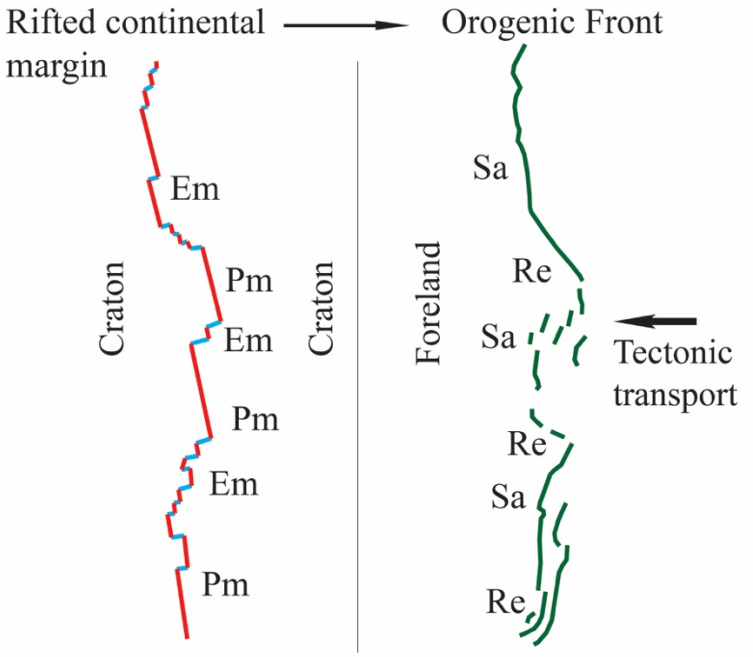

210

211 Figure 4: Impact of the continental margin geometry on the geometry of an orogenic front.
212 Embayments (Em) evolve into salients (Sa) and Promontories (Pm) evolve into recesses (Re).

213

214 boundaries of second-order salients and recesses and had controls on the Taconic and younger
215 orogenic events (Figure 3b) (Cawood & Botsford, 1991). Across these structures, the depositional
216 facies and structural style of the rock units overlying the Grenville basement change abruptly
217 suggesting these faults have Precambrian roots. The Grenville basement inlier terminates
218 southward at the Bonne Bay CSD (Figure 3b), which also delineates the southern limit of the
219 Acadian uplift of the Grenville Inlier (Cawood & Botsford, 1991). North of the Bonne Bay CSD,
220 thrusts and associated structures are west verging, while towards the south the vergence reverses
221 (Williams & Cawood, 1986). In southern Newfoundland and the Cape Breton islands, the Silurian
222 tectonic wedging of the Avalon craton into the Laurentian craton has resulted in a very narrow
223 Appalachian central mobile belt characterized by stronger syncollisional deformation, high-grade
224 Barrovian metamorphism ('Kyanite and Sillimanite grade, 700˚-750˚C at 6-10 Kbar (Plint &
225 Jamieson, 1989), 5 kbar elsewhere'), and a greater volume of Silurian magmatism than elsewhere
226 (Lin et al., 1994). This intensely deformed and metamorphosed narrow band is bound by the NW-
227 striking Canso fault (Figure 3c) to the southwest and the E-striking Gunflap Hills fault to the
228 northwest, interpreted as transverse, right lateral wrench faults that accommodated the differential
229 movement on either side of the wedging (Lin et al., 1994). In its western end, the Gunflap Hills
230 fault (Colman-Sadd et al., 1992) merges with the NW-striking Cape Ray fault zone (Figure 3b).
231 In eastern Nova Scotia, several NW-striking, transverse, left-lateral strike-slip faults (e.g. the
232 Country Harbour Fault) have been described as conjugates of the Minas Fault Zone (Figure 3c)
233 (Waldron et al., 2015), which is an E-W striking 300 km long, continental transform fault in New
234 Brunswick and Nova Scotia that marks the boundary between the Avalon and Meguma terranes
235 (Murphy et al., 2011). Towards the west, the Paleozoic Norumbega Fault System (Figure 2)
236 demonstrates the effect of the subducting plate physiography on the upper plate structures. This
237 NE-striking, 300 km long, transpressive, dextral fault system (West Jr & Hubbard, 1997; Hubbard,
238 1999) has recently been interpreted to be a result of subduction of an oceanic ridge and related
239 transform fault (Kuiper, 2016; Kuiper & Wakabayashi, 2018). Around the orogenic front in
240 Quebec and northern Vermont, cross structures were formed due to reactivation of earlier-formed

241 transverse, normal faults with an oblique thrust-sense or served as an oblique ramp during the
242 westward thrusting of the Lower to Middle Ordovician shelf-carbonates (Séjourné & Malo, 2007).

243

244 **2.2 Proposed Factors Controlling Lateral Heterogeneities**

245 Lateral heterogeneity along the Appalachians has largely been controlled by the irregularities
246 along pre-collisional continental margins and by inherited basement structures. The eastern
247 continental margin of Laurentia went through a series of rifting events including the Iapetan rifting,
248 all of which acted in concert to develop a series of embayments (concave oceanward) and
249 promontories (convex oceanward) separated by transform faults (Rankin, 1976; Thomas, 1977,
250 2014). During subsequent orogenic events (Taconic, Acadian, and Alleghenian orogenies),
251 embayments evolved into salients (convex towards the foreland), promontories evolved into
252 recesses (concave towards the foreland), and the transform fault boundaries evolved into transverse
253 zones (Figure 4). As Tull and Holm (2005) noted, foreland sedimentary sections along salients are
254 much thicker than along recesses, which has a great control on the geometry and deformation style
255 of the evolving thrust sheets (discussed in detail in the North American Cordillera section of this
256 article). Irregularity along continental margins also has another important control, which results in
257 a sharp lateral heterogeneity along an orogen. A collisional event between two promontories (of
258 two different landmasses) results in a narrower but stronger orogenic deformation and a higher
259 grade of metamorphism that a promontory-embayment collision (Lin et al., 1994). The evolution
260 of rift-related transform faults into transverse zones also had a profound impact on the evolution
261 of the Appalachians mountains by creating barriers or zones that truncated or offset major thrust
262 faults. Along the range front, transverse zones have served as nucleation sites for cross structures
263 in the form of lateral ramps or tear faults.

264

265 **3 Cordillera**

266 **3.1 Tectonic Setting and Lateral Heterogeneities**

267 The North American Cordilleran orogenic system records the Jurassic (and possibly earlier) to
268 Paleogene history of terrane accretion and the eastward convergence of the Farallon and Kula
269 plates beneath the western margin of Laurentia (North American continent) (Oldow et al., 1989;
270 Burchfiel et al., 1992; Saleeby et al., 1992; DeCelles, 2004; Dickinson, 2004). This convergence

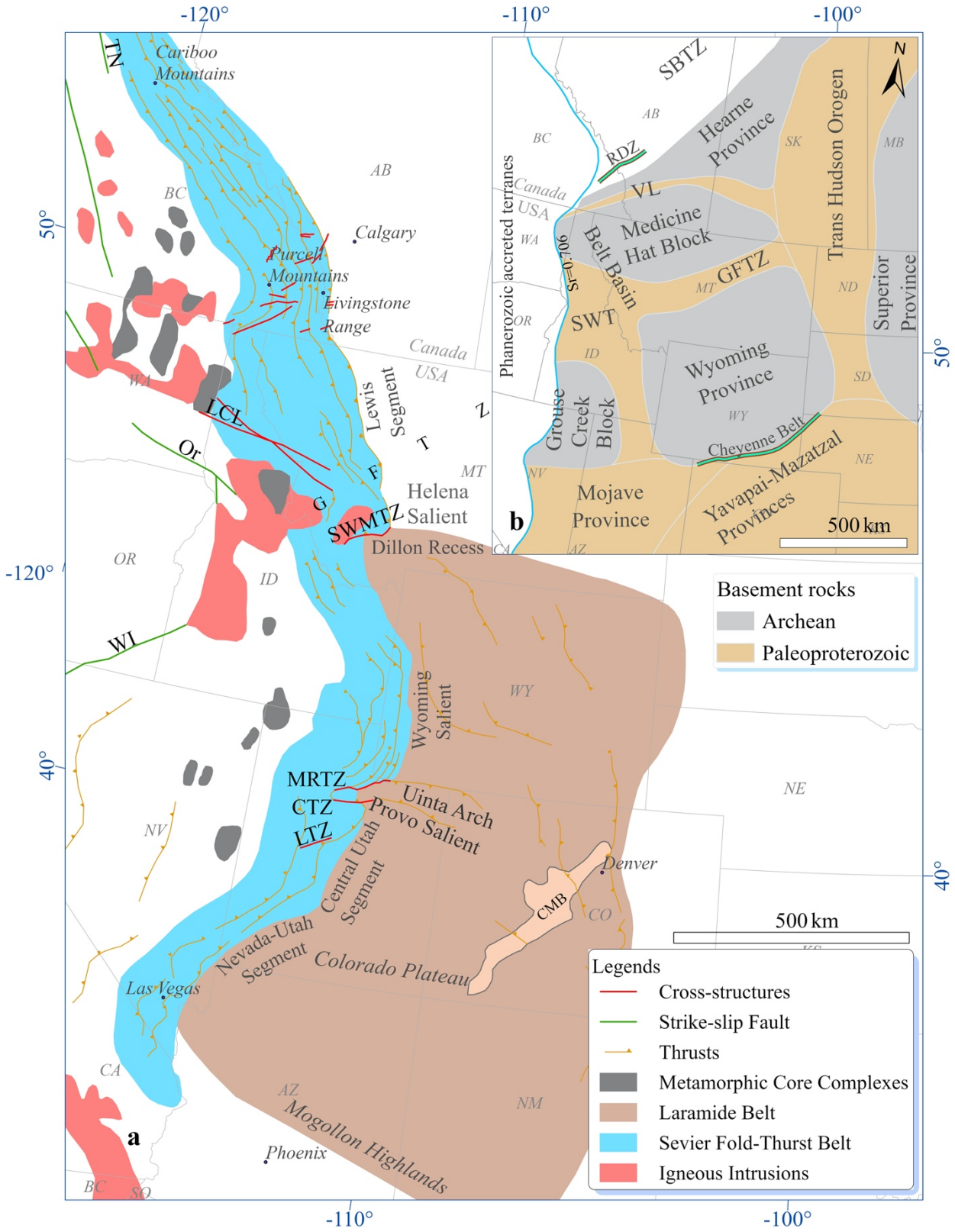
-120°
-110°
-100°
50°
40°
TL
Cariboo Mountains
AB
BC
Calgary
Purcell Mountains
Livingstone Range
Canada
USA
WA
LCL
Or
Lewis Segment
T
F
G
MT
Helena Salient
SWMTZ
Dillon Recess
OR
ID
WI
Wyoming Salient
WY
MRTZ
CTZ
LTZ
Uinta Arch
Provo Salient
Central Utah Segment
Nevada-Utah Segment
Colorado Plateau
Denver
CO
CMB
NE
NV
Las Vegas
CA
AZ
NM
Mogollon Highlands
Phoenix
a
BC
SO
500 km
Legends
Cross-structures
Strike-slip Fault
Thrusts
Metamorphic Core Complexes
Laramide Belt
Sevier Fold-Thurst Belt
Igneous Intrusions
SBTZ
N
AB
BC
RDZ
Hearne Province
SK
MB
Trans Hudson Orogen
Canada
USA
WA
VL
Medicine Hat Block
Belt Basin
Sr=0.706
GFTZ
MT
ND
Superior Province
Phanerozoic accreted terranes
OR
SWT
ID
Wyoming Province
SD
Grouse Creek Block
WY
Cheyenne Belt
NE
NV
Mojave Province
Yavapai-Mazatzal Provinces
b
500 km
CA
AZ
Basement rocks
Archean
Paleoproterozoic

271

Figure 5: Simplified tectonic and basement map around the western North American Cordilleran belt. a) Tectonic map of the US and Southern Canadian Cordillera showing the major orogenic curvature and the major cross-structures (modified from: Moffat & Spang, 1984; McGugan, 1987; Kwon & Mitra, 2006; Cooley et al., 2011; McMechan, 2012; Whisner et al., 2014; Yonkee & Weil, 2015) b) Generalized basement map of the western North America. The Sr=0.706 line represents the eastern boundary of the accreted terranes (source: Foster et al., 2006; Whitmeyer & Karlstrom, 2007; McMechan, 2012; Yonkee & Weil, 2015; Ronemus et al., 2020).
Acronyms: CMB: Colorado Mineral Belt; CTZ: Charleston Transverse Zone; GFTZ: Great Falls Tectonic Zone; LCL: Lewis and Clark Line; LTZ: Leamington Transverse Zone; MRTZ: Mount Raymond Transverse Zone; Or: Orfino Shear Zone; RDZ: Red Deer Zone; SBTZ: Snowbird Tectonic Zone (the Thorsby Low is located within the SBTZ); SWMTZ: Southwestern Montana Transverse Zone; SWT: Selway Terrance; TN: Tintina-Rocky Mountain Shear Zone; VL: Vulcan Low; WI: West-Idaho Fault.

resulted in a number of different ranges including the Sierra Nevada, the Rocky Mountains, and the various mountain systems of Alaska (Figure 5a). Changing plate dynamics has resulted in varied deformation style and distribution throughout the Cordilleran evolution. The Late Cretaceous (Beck et al., 1988; Decelles et al., 1991) transition of deformation style from the thin-skinned, taper-wedge in the US Sevier fold-thrust belt to predominantly thick-skinned, basement-involved Laramide orogenesis is one of the remarkable changes. Initiation of the Laramide system uplifts has generally been correlated to the subduction of a flat-slab segment (e.g.; Coney & Reynolds, 1977; Dickinson & Snyder, 1978; Saleeby, 2003; Chapin, 2012). North of the Canadian border, the Laramide-style deformation is absent. Orogenic collapse of the Cordilleran system, focused on the Sevier belt, initiated during Middle to Late Eocene due to the change in relative plate kinematics and has resulted in the active Basin and Range province of extensional deformation (e.g.; Constenius, 1996; Yonkee & Weil, 2015). The contractional phase of deformation resulted in spectacular range-parallel fold and thrust belts (Yonkee & Weil, 2015), yet there are important lateral heterogeneities and a number of cross structures along the Cordillera.

Basement provinces and their suture zones and major faults along the western margin of the North American continent include the Snowbird Tectonic Zone (Ross et al., 1991; Hope &

Eaton, 2002), the Archean Hearne Province (Hope & Eaton, 2002), the Archean Medicine Hat Block (Ross et al., 1991; Lemieux et al., 2000); the Archean Wyoming Province (Wooden & Mueller, 1988; Mogk et al., 1992), and the Paleoproterozoic Yavapai and Mazatzal Provinces (Foster et al., 2006; Whitmeyer & Karlstrom, 2007), from north to the south (Figure 5b). The Trans-Hudson Orogen and the Superior Craton lie towards the east, around the central region of the North America. Towards the west, the basement block include the Archean Grouse Creek Block and the Selway Terrane (Foster et al., 2006).

Transverse crustal boundaries between these provinces and the other Archean/Paleoproterozoic transverse basement structures are one of the primary causes of lateral heterogeneity in the Cordillera due to their influence in the subsequent sedimentary and deformational history (e.g.; Paulsen & Marshak, 1999; Sears & Hendrix, 2004; McMechan, 2012). Significant crustal-scale, transverse boundaries around the southeastern Canadian Cordilleran front (Alberta) include the Thorsby Low, a crustal suture within the Snowbird tectonic zone (Ross et al., 1991; Hope & Eaton, 2002), the Red Deer zone, the northern boundary of the Hearne Province (Hope & Eaton, 2002), and the Vulcan Low, a crustal suture between the Medicine Hat Block and Hearne Province (Figure 5b) (Hoffman, 1988; Ross et al., 1991). These structures and terrane boundaries served as loci for activation of transverse zones during the deposition of the Mesoproterozoic Belt-Purcell sequence (Benvenuto & Price, 1979; Foo, 1979; Root, 1987; Anderson & Davis, 1995; McMechan, 2012). Multiple other transverse structures were also initiated in Mississippian and Triassic as normal faults above these transverse boundaries (Cooley et al., 2011; McMechan, 2012). Segments of some of these transverse zones were reactivated as dextral, oblique reverse faults or as tear faults during Jurassic to Eocene in response to compressional stresses (Bielenstein, 1969; Foo, 1979; Price, 1981; McMechan & Price, 1982; McMechan, 2000; Cooley et al., 2011). Similar impacts of basement structures on the evolution of thrust belts have been reported from other domains in the Canadian Cordillera (e.g.; Pride et al., 1986; Thompson, 1989; Pilkington et al., 2000; Berger et al., 2008). In northern British Columbia, a geometric inversion of the northern end of a NW-trending “basement uplift” during the Sevier contraction resulted in the formation of NE to E-trending (transverse) contractional structures, which were superimposed on the regional NW-striking structures (McMechan, 2007). Aside from their influence in the sedimentary and deformational history, these basement structures and terrane

boundaries also formed suitable conduits for melt transport and served as loci for igneous intrusions and mineralization (McMechan, 2012).

The Sevier FTB is generally classified into the Main Ranges, the Front Ranges, and the Foothills, from the hinterland to the foreland, in the northern US and the southern Canada. Cross structures have been observed in all these sub-divisions at different scales. In the Main Ranges of British Columbia (Purcell Mountains), Mesoproterozoic and Eocambrian synsedimentary faults have been reactivated as dextral, east-striking, transverse, thrust faults (Figure 5a) during Mesozoic and Cenozoic (Höy & Heyden, 1988; Larson et al., 2006; McMechan, 2012). Several transverse faults have also been identified in the Front Ranges (e.g.; Moffat & Spang, 1984; McGugan, 1987; Fermor, 1999; McMechan, 2001; Norris, 2001). In the foothills, the north to NW-trending Livingstone Range anticlinorium consists of en-echelon, chevron-style fault-propagation folds, which have been compartmentalized by multiple tear faults and transverse zones of intense fracturing (Cooley et al., 2011). Anticlines plunge into these tear faults and form domal culminations. Tear faults also mark along-strike changes in fold-style, from chevron to concentric and changes in the presence or absence of back-thrusts. These tears are thought to be the results of syn-thrusting reactivation of preexisting NE-striking Paleoproterozoic basement faults, some of which were active during Mississippian (Cooley et al., 2011).

The Great Falls Tectonic Zone (GFTZ; Figure 5) in Montana is a NE-trending, transverse (in relation to the Cordillera) crustal suture between the Medicine Hat Block and the Wyoming Craton (O'Neill & Lopez, 1985). This deformation zone was initiated prior to ~1.9 Ga as a convergent boundary and subsequently evolved into a transpressive boundary in response to the eastward movement of the Wyoming Craton (Dahl et al., 1999; Mueller et al., 2002; Gifford et al., 2014). Cenozoic alkali magmatism, belonging to the Montana Alkali Province, occurred within this zone (Gifford et al., 2014). In central Montana and Idaho, the Mesoproterozoic Belt rifting most likely led to the initiation of the Lewis and Clark fault zone from the southern margin of the GFTZ (Harrison et al., 1974; Reynolds, 1979; Wallace et al., 1990; Sears & Hendrix, 2004; Foster et al., 2006). The Lewis and Clark fault zone (Figure 5a) is a WNW-trending, >800 km long, system of 'steeply dipping strike-slip, oblique-slip, and dip-slip faults', which obliquely cuts across the Sevier belt (Foster et al., 2007). During the Mesozoic-Cenozoic Cordilleran orogeny, this fault zone deformed as a ca. 40 km wide, sinistral shear zone with 'transpressional flower structures' (Hyndman et al., 1988; Sears et al., 2000; Sears & Hendrix, 2004). With the onset of the Basin and

Range extension in the Eocene, polarity of the fault movement reversed, and this zone served as a dextral, extensional, TZ that facilitated the exhumation of metamorphic core complexes (Figure 5a) (Foster et al., 2007).

In the Sevier FTB (USA), the geometry of basement structures had first-order control on the formation of orogenic curvatures and on the evolution of their transverse boundaries (e.g.; Paulsen & Marshak, 1999). A deeper basin generally corresponds to a thicker sedimentary column and more material available to be incorporated into the deforming taper, which results in a wider wedge (salient) (e.g.; Marshak & Wilkerson, 1992; Boyer, 1995). The Helena salient likely formed over an E-trending, asymmetrical depositional trough of the Middle Proterozoic Belt basin called the Helena embayment (Figure 5b) (Harrison et al., 1974). A north-dipping Middle Proterozoic normal fault on the southern edge of the embayment probably evolved into the Southwest Montana Transverse Zone (SWMTZ), which forms the southern boundary of the salient with the Dillon recess (Whisner et al., 2014). Thrusts and related structures in the southern domain of this salient are strongly converging into the right-lateral, reverse faults within the SWMTZ, due to a gradual clockwise rotation of the shortening direction during their evolution (Whisner et al., 2014).

Further south, controls of the basin boundary geometry on the evolution of transverse zones have been exemplified by the Mount Raymond Transverse Zone (MRTZ) and the Charleston TZ. The MRTZ and the Charleston TZ form the northern and the southern boundaries of the Uinta/Cottonwood arch (recess) with the Wyoming Salient and the Provo Salient respectively (Figure 5a) (Paulsen & Marshak, 1997, 1998). Paulsen and Marshak (1999) noted contrasting structural styles between these two zones and explained this contrast in light of corresponding basement structures. An east-west trending asymmetric basement high, with a gentle northern flank and a steep southern flank, existed just north of the present Uinta/Cottonwood arch, along the boundary between the Archean Wyoming province (north) and Proterozoic terranes (south) (Paulsen & Marshak, 1999). A gentler northern flank meant that the sedimentary thickness gradually increased northwards from the Uinta recess into the Wyoming Salient. The MRTZ initiated above this flank as NNE-trending thrusts along the southern margin of the Wyoming salient, which were later tilted northward creating an E-W strike during the uplift of the Uinta/Cottonwood arch (Paulsen & Marshak, 1997). The steeper southern flank, however, marked an abrupt increase in sedimentary thickness towards the south and thereby formed the boundary between two contrasting taper wedges. The Charleston TZ (Figure 5a) served as zone of lateral

ramp between the two contrasting tapers and gradually evolved into a left-lateral strike slip zone, which accommodated the differential motion between the Uinta recess and the Provo salient (Paulsen & Marshak, 1998 and references therein). The southern boundary of the Provo salient with the central Utah segment is the Leamington TZ, which is an ENE trending, >50 m long, complex, cross structure (Lawton et al., 1997; Kwon & Mitra, 2006). In the salient, an initial E-directed vergence over the TZ rotated clockwise during subsequent deformational phases, which likely reflects the interaction between a deforming wedge and an oblique ramp (Lawton et al., 1997; Paulsen & Marshak, 1999; Kwon & Mitra, 2006).

In southern Wyoming, the E- to NE-trending Cheyenne belt (Figure 5b) represents the transverse, crustal suture/ transpressional shear zone between the Wyoming and Yavapai-Mazatzal Provinces, across which the Precambrian geology, metamorphism, and metallogenesis abruptly change between adjacent blocks (Karlstrom & Houston, 1984). During the Laramide orogeny, this weak crustal zone was reactivated as a left-lateral transpressional structure and subsequently as a right-lateral transtensional zone during the Tertiary extension (Bader, 2008). Just to the south, east-west trending Precambrian basement fault zones, genetically linked to the Cheyenne belt (Sims et al., 2001; Whitmeyer & Karlstrom, 2007), have been identified to influence Laramide uplift resulting in accumulation of oil and gas resources (Bader, 2009).

A peculiar feature in the Laramide belt of Colorado is a 500-km long, 25-50 km-wide, linear zone of numerous magmatic intrusions, known as the Colorado Mineral Belt (Figure 5a). This zone marks an abrupt along-strike change in: 1) the structural trend of the Laramide uplifts (north-trending in the southern region versus NW-trending northwards); 2) the thickness of the Late Cretaceous and Paleogene sedimentary sequences; and 3) the composition of the Laramide plutons (Chapin, 2012). This economically valuable belt has been interpreted to have formed over an extensional boundary between two adjacent segments of the underlying Farallon flat slab (Chapin, 2012), which serves to demonstrate the effects of the down-going plate features and processes on the upper plate structures. In the Laramide belt, preexisting basement structures and lateral heterogeneities are suggested to have a control on the stress-field and thereby led to the development of structures with an orientation different from the regional trend (Weil et al., 2016).

3.2 Proposed Factors Controlling Lateral Heterogeneities

Along the Cordillera (primarily along the Sevier FTB), pre-existing basement features/structures likely had the greatest impact on creating lateral heterogeneity, which has generally manifested as curvatures along the orogenic front and as variation in the geometry of cross structures. Prior to the Cordilleran orogeny, transverse crustal boundaries served as loci for activation of transverse zones during various rift-related extensional features (McMechan, 2012). Subsequently, these transverse zones were reactivated as cross structures during the orogenic contraction/extension and served to partition or distort deformation of the evolving crustal wedge. Both transverse structures and irregular basement topography further added lateral heterogeneity through their profound control on the lateral continuity of facies and thickness of the pre and syn orogenic sedimentary succession. Abrupt lateral changes in the facies and thickness of the sedimentary column caused the deforming wedge to partition into segments, which are separated by cross structures of various geometries and genesis. As Paulsen and Marshak (1999) explained, a thicker sedimentary column corresponds to a farther propagation of the deforming wedge (salients) than a thinner column (recesses). Further the geometry of the basement irregularities and transverse structures dictate the geometry of cross structures. A near vertical transverse structure is more likely to evolve into a tear fault, whereas, an inclined structure evolves into a lateral ramp (Paulsen & Marshak, 1999). And finally, features of the subducting plate (Farallon) may have influenced the development of cross structures and lateral heterogeneity along the range (e.g.; Chapin, 2012).

4 Alps

4.1 Tectonic Setting and Lateral Heterogeneities

The European Alps formed during a Late Cretaceous collision between the European and African plates following the closure of the Alpine Tethys, which consisted of the northern Valais ocean and the southern Piemont-Liguria ocean, separated by continental crust in the middle known as the Brianconnais (Tricart, 1984; Stampfli & Borel, 2002; Schmid et al., 2004; Handy et al., 2010). The European side of the collision was the lower plate with the Apulian/Adriatic blocks of the African plate forming the upper plate (Dewey et al., 1998; Handy et al., 2010). The Apulian plate refers to all continental domains located south of the Alpine Tethys. The Adriatic micro-plate or Adriatic indenter, a part of the Apulian plate, is situated south of the modern-day Periadriatic Fault System (PA; Stampfli & Borel, 2002; Schmid et al., 2004; Handy et al., 2010). Today this

orogen trends approximately east-west in the Eastern and Central Alps and has a NE-SW orientation in the Western Alps (Figure 6). Major range-parallel lithotectonic units of the Alpine orogen are from north to south, the European foreland, Jura Mountains, Molasse Basin (Oligocene-Miocene Foreland), Helvetics, Penninic zone, Austroalpine, Southern Alpine, and Po Basin (retro-arc basin for the Alps and foreland basin for the Apennines) (Pfiffner, 2014). The Helvetic domains are derived from the Mesozoic and Cenozoic shelf and upper slope deposits along the southern European plate margin, and in places include the Pre-Triassic basement (Zerlauth et al., 2014). For simplicity, the classic term 'Penninic nappes/zone' has been largely used in the literature to denote the tectonic units derived from the subducted European margin, the Valais ocean, the Piemont-Liguria ocean, and the Brianconnais continental crust (e.g.; Schmid et al., 2004; Pfiffner, 2014). Parts of the Apulian plate to the north and south of the PA are represented by the Austoalpine and Southern Alpine units respectively (Polinski & Eisbacher, 1992; Schmid et al., 2004). While the Austroalpine unit dominates the eastern Alps, this unit has fully eroded away in the Western Alps, exposing up to blueschist to eclogite facies rocks of the Penninic unit and sub-greenschist facies rocks of the Helvetics (Pfiffner, 2014). The rheologically strong Dolomites, the Adriatic indenter, lie within the Southern Alpine unit.

Following the initial collision, the eastern Alps underwent E-W directed orogen parallel extension in the Miocene (Oligocene; Ring, 1994; Steck, 2008). This extension has been referred to as "lateral extrusion" (Ratschbacher et al., 1991). The lateral extrusion has been interpreted as; i) coupling of compression and gravitational collapse (Ratschbacher et al., 1991), ii) upper plate extension due to roll back of a subduction zone beneath the Carpathian orogen (Royden et al., 1983; Royden, 1993; Horváth & Cloetingh, 1996; Sperner et al., 2002), iii) northward indentation of the southern Dolomites (Rosenberg et al., 2004; Rosenberg & Garcia, 2011; Reiter et al., 2018), and iv) an extension related to the roll back of the Mediterranean plate in the west (Ring & Gerdes, 2016). This Miocene extension has been accommodated along a series of orogen-parallel, strike-slip faults and orogen-perpendicular, normal faults. Modern-day topographic evolution was largely controlled by these faults as much of the lateral heterogeneity we see along the range (Bartosch et al., 2017). Major orogen-parallel strike-slip faults in the Eastern and Central Alps are the Periadriatic Fault System (PA), the Defreggen-Antholz-Vals Fult (DAV), Salzach-Ennstal-Mariazell-Puchberg Fault (SEPM), Inntal Fault (IN), and Mur-Murz Valley Fault (MM) (Figure 6). The PA trends E-W for ~700 km and forms a rheological boundary between the weaker Eastern

Alps and the relatively stronger Southern Alps (Robl & Stüwe, 2005). From the west to east, the PA consists of the Tonale (or Insubric) Line, Giudicarie Fault System, Mauls, Puresetral, and Gailtal segments (Figure 6). Different segments of the PA were active during 32-29 Ma and 22-16 Ma (Müller et al., 2001). North of the PA (Pustertal and Mauls segments), the sinistral, normal DAV runs E-W, for ~80 km and forms the southern boundary of alpine metamorphism (Müller et al., 2000; Bartosch et al., 2017). Within the Austroalpine domain, the EW-striking, ~400 km long, SEPM has a cumulative left-lateral slip of about 60 km (Urbanek et al., 2002) and separates the Mesozoic Northern Calcareous Alps (NCA) from the Middle Austroalpine basement rocks (Bartosch et al., 2017). The NE-striking, sinistral MM was active during 17-13 Ma (Dunkl et al., 2005) as a conjugate of the NNW-striking, dextral Pols-Lavanttal fault system (PL) (Bartosch et al., 2017).

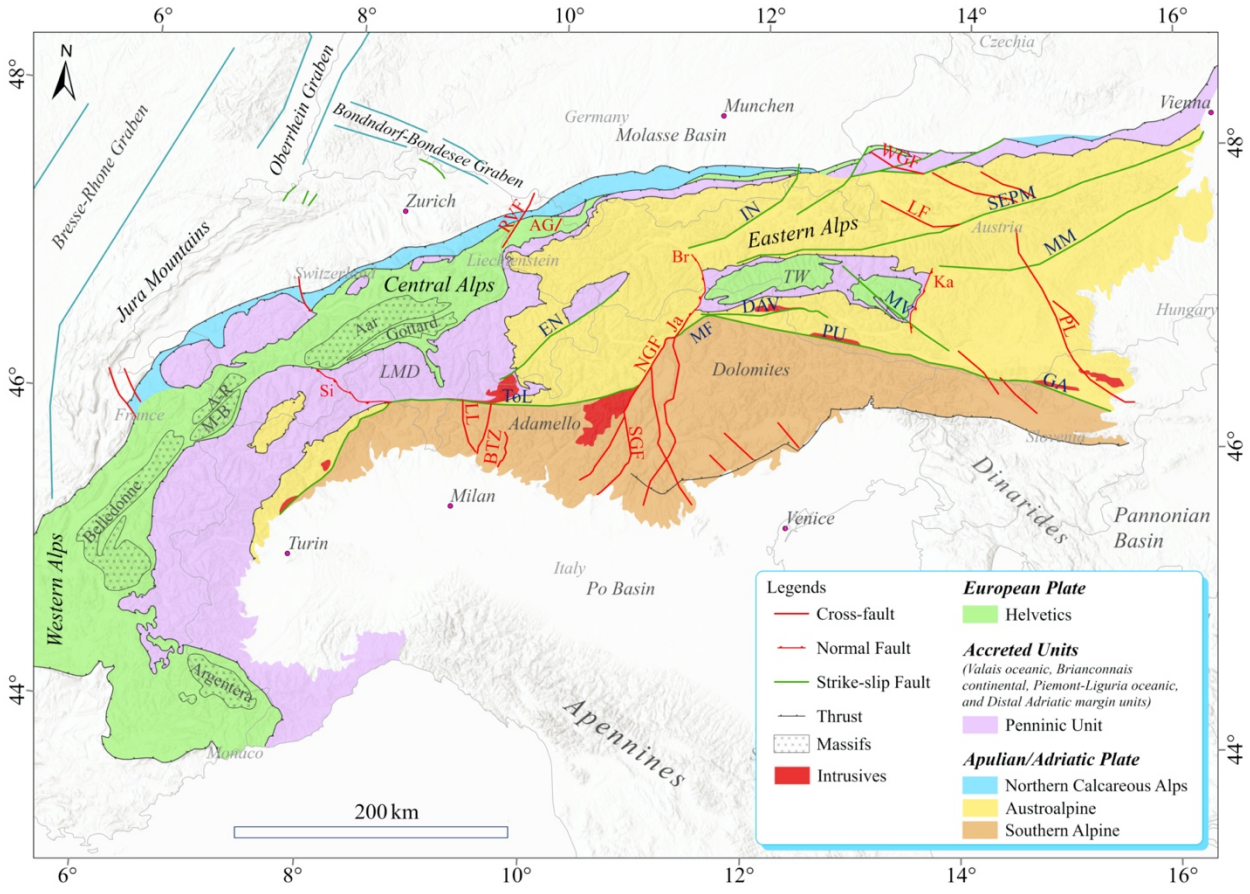

Figure 6: Geological map of the Alps showing the major lithotectonic units, major strike-slip faults (golden lines), and major cross-faults (red lines) (after Laubscher, 1985; Polinski & Eisbacher,

1992; Schönborn, 1992; Linzer et al., 1995; Castellarin et al., 2006; Pfiffner, 2014; Zerlauth et al., 2014; Ring & Gerdes, 2016; Bartosch et al., 2017).

Acronyms: AG: Alpenrhein Graben; A-R: Aiguilles Rouges Massif; Br: Brenner Fault; BTZ: Ballabio-Barzio Transfer Zone; EN: Enagdin Fault; GA: Gailtal Fault; IN: Inntal Fault; Ja: Jaufen Fault; Ka: Katschberg Faults; LF: Lammertal Fault; LL: Lecco Line; LMD: Lepontine Metamorphic Dome; M-B: Mont-Blanc Massif; MF: Meran-Mauls Fault; MM: Murz-Valley Fault; MV: Moll Valley Fault; NGF: North Giudicarie Fault System; PL: Pols-Lavanttal fault system; PU: Purestal Fault; RVF: Rhine Valley Fault; SEPM: Salzach-Ennstal-Mariazell-Puchberg Fault; SGF: South Giudicarie Fault System; Si: Simplon Fault Zone; ToL: Tonale (Insurbic) Line; TW: Tauern Window; WGF: Wolfgangsee Fault.

4.1.1 Cross Structures in the Eastern and Central Alps

Major transverse, normal faults in the eastern and central Alps are the Simplon Fault Zone (Si), the Pols-Lavanttal fault system (PL), the Brenner Fault (Br), the Moll Valley Fault (MV), and the Katschberg Faults (Ka) (Figure 6). The Brenner and Katschberg Faults mark the western and eastern edges of the Tauern Window respectively (Behrmann, 1988; Selverstone, 1988; Fiigenschuh et al., 1997), where blue-schist and eclogitic facies rocks of the Penninic zone have been exposed (Pfiffner, 2014). Exhumation of the Tauern Window has been widely linked to Miocene extension. Rosenberg and Garcia (2011) argue that localized intensive folding deformation due to an irregular geometry of the Dolomite indenter coupled with erosion can also exhume deep-seated rocks without a significant crustal extension. The southern edge of the window has been cut by the NW-striking dextral, normal MV fault. Gently west-dipping mylonitic fabric, with top-to-the-west shear along the Brenner Fault (Behrmann, 1988; Selverstone, 1988), has been overprinted by steeply west-dipping cataclastic zones (Prey, 1989). Much like the Brenner Fault, the Simplon Fault zone is a low-angle, SW-dipping, extensional fault that exhumes the Lepontine Metamorphic Dome in its footwall. Mylonitic shearing that formed the Simplon Fault zone initiated at 30 Ma (Campani et al., 2010) and was overprinted by brittle detachment faults of the Simplon Line from 14.5-10 Ma until 3-5 Ma (Hubbard & Mancktelow, 1992; Mancktelow, 1992; Grosjean et al., 2004; Campani et al., 2010). Both the Brenner and Simplon Faults expose a telescoped crustal section via an initial ductile shearing and subsequent brittle faulting (Grosjean et al., 2004; Campani et al., 2010; Mancktelow et al., 2015). It has been

533 proposed that Brenner and Simplon extension may be related to step-overs in the range-parallel
534 dextral strike-slip deformation in the Neogene (Schmid et al., 1989; Hubbard & Mancktelow,
535 1992).
536 Around the eastern Alpine periphery, the NW-trending, NE-verging, Paleogene folds in
537 Permo-Mesozoic cover of the Austroalpine are cut by sets of NE-striking, high-angle, cross-faults
538 (Figure 6) (Polinski & Eisbacher, 1992). In the Miocene, both the Austroalpine and Southern
539 Alpine units were folded into NE-trending folds, which are dissected by a system of NW-trending
540 high angle, dextral cross-faults, which includes the 150 km long PL. These Miocene cross faults
541 either offset or merge into the PA and partition deformation between the contractional Alpine
542 domain and the extensional Pannonian basin (Polinski & Eisbacher, 1992). In the western Alps,
543 NE to E-striking transverse faults are represented by the Neogene normal faults with a few faults
544 showing minor left-lateral reactivation (Sue & Tricart, 2003) and the late to post Oligocene right-
545 lateral, strike-slip faults (Malusà, 2004; Perello et al., 2004; Perrone et al., 2011). Anti-clockwise
546 rotation of the Apulian plate has been attributed as the cause of the orogen-parallel dextral
547 displacement and the NE to SW extension (Hubbard & Mancktelow, 1992; Calais et al., 2002).
548 The Giudicarie Fault System (GFS) is a system of WNW-NW dipping fault-links between
549 the Tonale and Pustertal line of the PA (Castellarin & Cantelli, 2000; Mancktelow et al., 2001;
550 Müller et al., 2001; Viola et al., 2001). The Meran-Mauls (MF) and the Northern Giudicarie Fault
551 (NGF) within the GFS form the trace of the PA, while the Southern Giudicarie Fault (SGS) is
552 entirely located in the Southern Alps. The Jaufen Fault, as a secondary fault within the GFS, has
553 been considered as a potential continuity of the Brenner Fault (Rosenberg & Garcia, 2011). An
554 explanation of the genesis of the GFS assumes evolution of an initially curved section of the PA,
555 which underwent Neogene sinistral transpression over an inherited NE-trending horst and graben
556 structure (Castellarin & Cantelli, 2000; Müller et al., 2001; Viola et al., 2001). A second
557 explanation, however, considers an initially straight PA bent by the Late Oligocene to Early
558 Miocene, northward movement of the Dolomite indenter. The MF represents a section of the bend,
559 which was subsequently cut by the NGS (Laubscher, 1971; Schmid et al., 1996; Frisch et al., 1998;
560 Pomella et al., 2012). The SGF has been interpreted as a Serravallian-Tortonian transfer fault
561 between the Guidicarie belt and the pre-Adamello belt of the Southern Alps (Castellarin et al.,
562 2006). The Adamello batholith is an Upper Eocene and Lower Oligocene batholith, the northern
563 rim of which has been sheared by the Tonale line (Brack, 1981; Laubscher, 1985; Zanchetta et al.,

2011). Just to the east of the NGS, a shallow, NNE-striking, sinistral transpressive fault has been mapped in the Southern Alps (Fondriest et al., 2015).

4.1.2 Cross Structures in the Southern Alps

Basement rocks in the Southern Alps have undergone extension in the Permian, resulting in ENE-trending faults in Triassic, NS-trending faults, and in Jurassic and Cretaceous EW-trending faults (Gaetani et al., 1986; Schumacher, 1990; Bertotti et al., 1993; Picotti et al., 1997; Festa et al., 2020). During the south-verging tectonic transport, these basement structures acted as lateral/oblique ramps, initiated more lateral ramps, and produced complex geometries like en-echelon ramp folds and back thrusting (Schönborn, 1992). In the central Southern Alps, inherited transfer zones cut through decoupling surfaces, partition thrust sheets into discrete blocks, and thereby serve to generate a laterally heterogenous deformation style (Laubscher, 1985; Schönborn, 1992). Several transverse structures that have been identified in this area include the Lecco Line and Ballabio-Barzio TZ (Figure 6) (Laubscher, 1985; Schönborn, 1992; Zanchi et al., 2012). The central Southern Alpine thrust belt has been compartmentalized by these transverse zones (Schönborn, 1992). Moreover, many upper Triassic to Jurassic (Bernoulli, 2007), orogen-perpendicular (e.g.; Berra & Carminati, 2010), normal faults were reactivated during the Neo-Alpine deformation (Oligocene-Miocene; Castellarin & Cantelli, 2000) along with nucleation of several transverse, sinistral, strike-slip faults (Prosser, 1998; Zanchi et al., 2012).

4.1.3 Cross Structures in the Northern Calcareous Alps (a subdivision of the Austroalpine unit)

The Permo-Mesozoic sedimentary succession (3-5 km thick) of the Northern Calcareous Alps were deformed into roughly NE-trending contractional structures during Early Cretaceous to Late Eocence (Gaupp & Batten, 1983; Kralik et al., 1987). The synchronous, en echelon, WNW-striking dextral, tear/transfer faults cut these contractional structures at all scales (Linzer et al., 1995). Some examples include the Lammertal and Wolfgangsee fault systems in the northeastern Alps (Figure 6). Linzer et al. (1995) observed a peculiar deformation decoupling between the sedimentary cover and basement during the ongoing oblique convergence. The sedimentary cover accommodated the convergence obliquity via deformation partitioning between the contractional and strike-slip structures, while the basement deformed through ‘crystal-plastic flow’ (Linzer et

595 al., 1995). Together these displacement transfer faults and deformation decoupling caused a 30˚
596 clockwise rotation of the entire NCA belt about a vertical axis (Linzer et al., 1995). Moreover, tear
597 faults related to the synorogenic inversion of a Jurassic rift-related graben shoulder have also been
598 identified in the NCA (Oswald et al., 2019). The Miocene, extensional, NE-trending, sinistral,
599 strike-slip faults, such as the SEPM and IN, cut all the earlier structures and divide the NCA into
600 a number of rhombohedral crustal blocks (Linzer et al., 1995).
601
602 **4.1.4 Cross Structures in the Helvetics**
603 In the Helvetic units, NW to N-striking tear faults were formed due to lateral variation in
604 shortening of the nappe stack, primarily during 35-30 Ma (Hunziker et al., 1986). Nappe
605 imbrication in the Helvetics changes laterally due to the absence or presence of a decoupling layer
606 (Zerlauth et al., 2014). The Permo-Carboniferous and Jurassic extensional structures along the
607 European margin resulted in these along-strike facies changes, which subsequently controlled the
608 deformation style. During the nappe formation, syn-sedimentary normal faults were also
609 reactivated as lateral ramps (e.g.; the Rhine Valley Fault) and tear faults (Zerlauth et al., 2014). In
610 the Oligocene, the NW-trending, sinistral, transtensional Alpenrhein graben was formed in the
611 Helvetics (Ring & Gerdes, 2016). It's conjugate, the Bonndorf-Bodensee in the Jura Mountains is
612 a NE-trending graben formed due to dextral transtension prior to 18 Ma (Hofmann et al., 2000;
613 Ring & Gerdes, 2016). The Bresse-Rhone and Oberrhien grabens in the Alpine foreland are related
614 to the European Cenozoic Rift System (Ring & Gerdes, 2016).
615
616 **4.2 Proposed Factors Controlling Lateral Heterogeneities**
617 The Eastern and Western Alps show remarkable heterogeneity in timing of major orogenic
618 events (Late Cretaceous in the Eastern Alps Cenozoic in the Western Alps), timing of the regional
619 metamorphism (older in the Eastern Alps and younger in the Western Alps), and overall direction
620 of tectonic transport (NW- to W-directed in the Eastern Alps vs N to NW directed transport in the
621 Western Alps) (Handy et al., 2010, page 123 and references therein). Within each lateral sub-
622 division of the Alps, several factors have contributed to the development of cross structures and
623 lateral heterogeneity. Extension of the upper plate has given rise to several cross faults such as the
624 Simplon and Brenner Faults, which serve as a large-scale, displacement transfer faults between
625 major, range-parallel, strike-slip faults (e.g.; Selverstone, 1988; Hubbard & Mancktelow, 1992).

Lateral connecters (tear faults, lateral ramps, and displacement transfer faults) are common in most of the tectonic units of the Alps. As observed in the North American Cordillera and the Appalachians, extension related basement structures, in both the European and Apulian plates, had controls on the lateral continuity of facies and thicknesses of sedimentary rocks and thereby on subsequent deformation, primarily in the Southern Alps and Helvetics (e.g.; Laubscher, 1985; Schönborn, 1992; Zanchi et al., 2012; Zerlauth et al., 2014). Lateral variability in the composition of the sedimentary section has influenced deformation style based on the presence or absence of decollement horizons. Oblique convergence coupled with partitioning of deformation between the basement and sedimentary cover has resulted in multiple cross faults in the Northern Calcareous Alps (Linzer et al., 1995).

5 Himalayas

5.1 Tectonic Setting and Lateral Heterogeneities

The Himalaya is our planet's most prominent example of a collisional mountain belt. While the geology of this orogen is generally presented in the context of range-parallel thrust faults that separate lithotectonic units of differing metamorphic grade (Figure 7; Hodges, 2000), there is also lateral heterogeneity in various aspects of the geology along the range and in some areas cross structures have played a role in the segmentation of the Himalaya (Mukul, 2010; Godin & Harris, 2014). Early geological and geophysical studies on the Indo-Gangetic plain presented evidence for lateral variations in sediment thickness and geophysical properties along the Himalayan foreland (Burrard, 1915; Oldham, 1917). In the 1970's new data from the oil and gas industry connected these lateral variations to a series of NE-trending basement ridges (Sastri, 1971; Rao, 1973; Raiverman, 1983). It was also proposed that these transverse basement structures may influence Himalayan deformation (Valdiya, 1976). In recent years, evidence from field surveys and laboratory analyses confirms the lateral heterogeneity and locates structural transfer zones and cross structures (Mugnier et al., 1999; Mukul, 2010; Godin & Harris, 2014; Hubbard et al., 2018; DeCelles et al., 2020; Duvall, 2020).

The Himalaya is characterized by range-parallel zones of differing geologic characteristics separated by north-dipping thrust faults (Figure 7). From south to north, the Indo-Gangetic plain is separated from the Sub-Himalaya by the active Main Frontal Thrust (MFT). The Sub-Himalaya is bound to the north by the Main Boundary Thrust (MBT). The hanging wall to the MBT is the

Lesser Himalayan zone, which is bound to the north by the Main Central Thrust (MCT). The unit that includes the highest peaks of the range is the Greater Himalayan Sequence (GHS). Geophysical data supports the merging of these thrusts into a master fault known as the Main Himalayan Thrust (Zhao, 1993; Avouac, 2003; Nabelek, 2009). There is an extensional fault system bounding the northern GHS, the South Tibetan Detachment System (STDS; Hodges, 2000). The hanging wall of the STDS is the Tibetan or Tethyan Sedimentary Sequence (Gansser, 1964; DeCelles et al., 2020). Each of these zones from the Sub-Himalaya to the Tibetan Sedimentary Sequence and their bounding structures exhibits some degree of lateral heterogeneity along the length of the range in either the expression of structural style, depositional history, geomorphology, or seismicity.

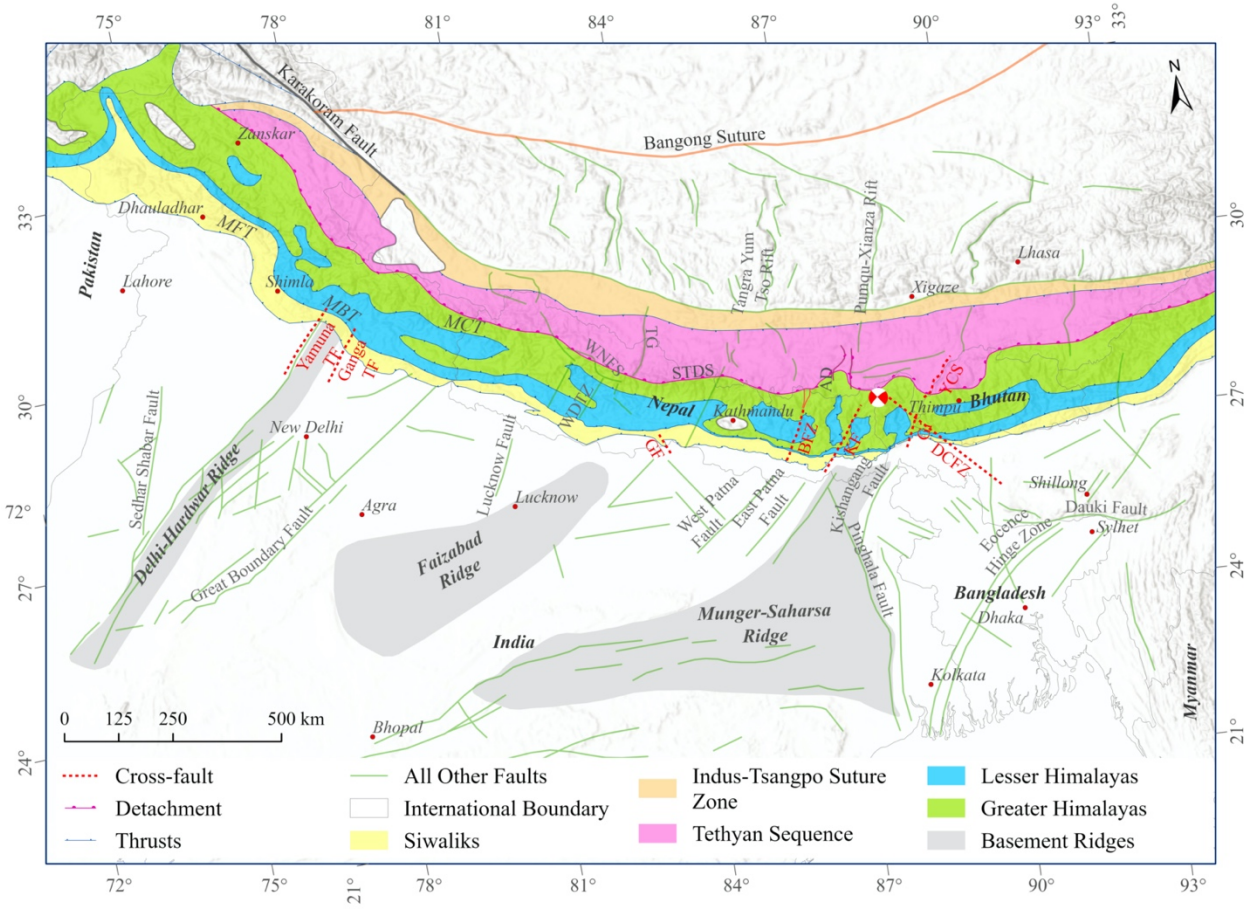

Figure 7: Simplified tectonic map of the Himalaya showing the major cross structures. The beach ball shows focal mechanism of the 2011 M_w 6.9 Sikkim Earthquake (source: the Department of Mines and Geology, Nepal; the Geological Survey of India; Gansser, 1964; Sastri, 1971; Mugnier

et al., 1999; Sahoo, 2000; Searle et al., 2003; Guillot et al., 2008; Jessup et al., 2008; Godin & Harris, 2014; Silver et al., 2015; Diehl, 2017; Mukul, 2018; Divyadarshini, 2019; Seifert, 2019). Acronyms: AD: Ama Drime Detachment; BFZ: Benkar Fault Zone; DCFZ: Dhurbi-Chungthan Fault Zone; GF: Gardi Tear Fault; Gi: Gish Fault; KF: Kosi Fault; MBT: Main Boundary Thrust, MCT: Main Central Thrust, MFT: Main Frontal Thrust, MMT: Main Mantle Thrust, MZB: Main Zanskar Back Thrust, STDS: South Tibetan Detachment System; TF: Tear Fault; WDTZ: Western Dang Transfer Zone; WNFS: Western Nepal Fault System; YCS: Yadong Cross Structure.

In the Sub-Himalayan there is notable variability in the morphology of the range front including the local presence of dun structures and a series of recesses and salients (Yeats, 1991; Mukul, 2010). In some areas the irregular mountain front has been linked to differences in shortening (Dubey, 2001) and in other areas there is a connection with cross faults that mark the transitions from salients to recesses. Examples of cross faults in the Sub-Himalaya include the Yamuna and Ganga Tear Faults in the NW Himalaya and the Kosi and Gish faults in eastern Nepal and Sikkim (India), respectively (Figure 7) (Sahoo, 2000; Srivastava, 2018). In the Lesser Himalaya, lateral heterogeneity is seen in topographic data, seismic data, and cooling history data (Harvey, 2015; van der Beek, 2016; Soucy La Roche, 2019). In western Nepal there is a zone of change in a variety of parameters that has led researchers to conclude that the MHT may have a ramp at that location, possibly coupled with a change in strike (Harvey, 2015; van der Beek, 2016; Soucy La Roche, 2019). This change also aligns with the proposed West Dang Transfer Zone (Figure 7) (Mugnier et al., 1999). Soucy La Roche (2019) propose a connection between this structural change and the NE-striking Lucknow fault in the Indian basement. In several areas, along-strike changes in the geometry of duplex structures in the Lesser Himalaya have also been noted (Hauck, 1998; DeCelles et al., 2001; Grujic, 2002; Long, 2011).

In the Greater Himalaya there is lateral heterogeneity in exhumation rates (Eugster, 2018), topographic profiles (Duncan et al., 2003), the presence of leucogranitic intrusions (Weinberg, 2016), and the presence or absence of discontinuities (Carosi, 2010; Larson, 2014). Hubbard et al. (2018) recently recognized a cross structure, the Benkar Fault zone, in the Greater Himalaya of eastern Nepal (Figure 7). This structure has dextral normal displacement and was active in the past ~12 Ma. The Benkar Fault zone may continue into the Lesser Himalaya, however it is yet to be mapped to the south.

Microseismicity in the Himalaya has occurred along cross-strike trends, has terminated at cross-strike zones, and has made other changes along cross-strike boundaries (Rajaure, 2013; Mugnier et al., 2017; Bilham, 2019; Mendoza, 2019). The aftershock seismicity from the 2015 Gorkha earthquake terminates along a sharp NE-striking boundary east of Kathmandu in Nepal (Hubbard et al., 2016; Mendoza, 2019). In the eastern Himalaya, several seismic events have been consistent with strike-slip displacement on transverse structures (Drukpa, 2006; Paul, 2015; Diehl, 2017). While a number of these events are minor, there have also been major earthquakes such as the 2011 M_w 6.9 Sikkim event that was interpreted to have occurred along a NW-striking (cross-strike) plane with dextral kinematics (Figure 7) (Paul, 2015). The Sikkim event and a number of the smaller events have originated at depths of ~50-60 km suggesting that rupture initiation was below the MHT (Drukpa, 2006; Paul, 2015) but possibly penetrating the hanging wall. Major historic thrust-related earthquake events are known to have had a finite rupture area (Bilham et al., 2001) and tracking of these areas has facilitated the recognition of seismic gaps that may represent regions with higher risk (Bilham, 2019). It has been proposed that cross structures may limit the seismic rupture area, thus contributing to the lateral heterogeneity in seismic activity (Mugnier et al., 2017; Hubbard et al., 2021).

5.2 Proposed Factors Controlling Lateral Heterogeneities

The combination of pre-existing transverse basement structures and the lateral variation in sedimentary history may both contribute to the lateral heterogeneity and cross structures that we see today in the Himalaya. Godin and Harris (2014) proposed a connection between variations in gravity data across a broad region in the Himalaya and Tibet to ridges in the Indian basement detected in the foreland. Soucy La Roche (2019) demonstrated lateral variations in cooling histories in western Nepal and proposed a cross structure in the form of a lateral ramp or tear fault separating the regions with differing cooling histories. This cross structure aligns with the Lucknow basement fault in the Indian foreland and these authors propose that the Himalayan cross structure is linked to the basement fault. Boundaries between salient and recesses in range front geomorphology has also been linked to basement faults (Hubbard et al., 2021). These basement faults in the foreland may also separate down-dropped blocks with thicker sedimentary sequences from higher blocks and these differences in sedimentary thickness may continue into the Himalaya, thus influencing lateral variations in structural style (DeCelles et al., 2020). Understanding the

nature of segmentation and segment boundaries may shed light on details of the mountain building process in collisional orogens but may also help us understand how convergence is accommodated and factors that control seismic energy propagation.

6 Zagros

6.1 Tectonic Setting and Lateral Heterogeneities

The Zagros orogenic belt runs for about 2000 km along the northeastern margin of the Arabian plate (Figure 8) and is the product of Miocene collision between the Arabian and Iranian continental plates and subsequent convergence (Allen & Armstrong, 2008; McQuarrie & van Hinsbergen, 2013). The eastern boundary is the dextral Zagros-Makran Transfer Zone (Regard et al., 2005), and it's western boundary is the sinistral East Anatolian Fault (Falcon, 1974; Haynes & McQuillan, 1974). During Permian to lower Cretaceous, the Neo-Tethys Ocean opened between the Arabian and Iranian plates. Closure of this short-lived ocean began in Late Cretaceous along with the tectonic emplacement of ophiolites and trench sediments on the Arabian plate (Haynes & Reynolds, 1980; Berberian & King, 1981). While there are dominant range-parallel thrust faults, there are also several important cross structures and other geologic features that vary along the length of the range.

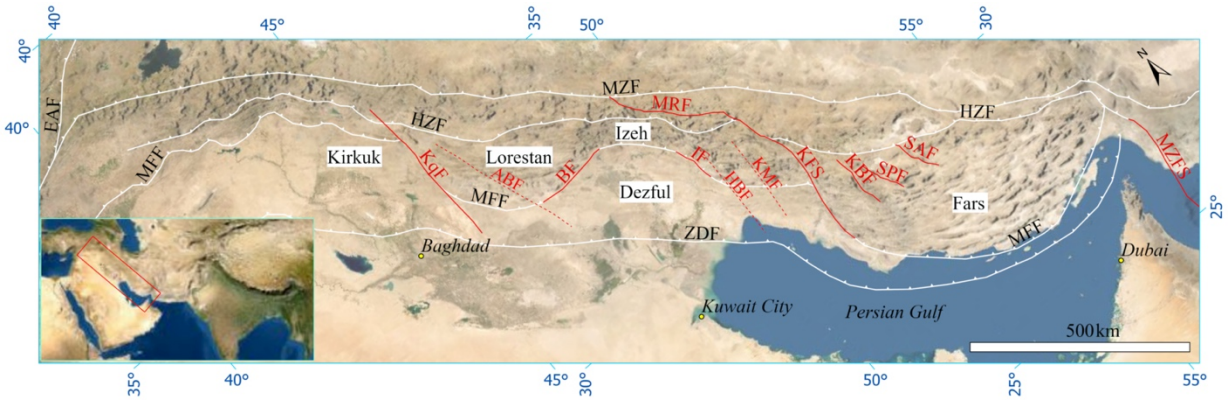

Figure 8: Simplified tectonic map of the Zagros mountains showing the major faults and the recesses and salients. The inset on the bottom-left corner shows the location of the larger map. The Minab-Zendan Fault System (MZFS) is a major fault of the Zagros-Makran Transfer Zone (modified from Authemayou et al., 2006; Farzipour-Saein et al., 2013; Joudaki et al., 2016; Le Garzic et al., 2019). The white lines are range parallel faults and red lines indicate cross structures.

Acronyms: ABF: Anaran Basement Fault; BF: Belarud Fault; EAF: East Anatolian Fault; HBF: Hendijan-Izeh Basement Fault; HZF: High Zagros Fault; IF: Izeh Fault; KBF: Kareh-Bas Fault; KFS: Kazerun Fault System; KMF: Khark-Mish Basement Fault; KqF: Khanequin Fault; MRF: Main Recent Fault; MZFS: Minab-Zendan Fault System; MZF: Main Zagros Reverse Fault; SAF: Saverstan Fault; SPF: Sabz Pushan Fault; ZDF: Zagros Deformation Front (also known as the Zagros Foredeep Fault).

The major, range-parallel tectonic elements in the Zagros have a NW-SE trend (Figure 8) and include the Main Zagros Reverse Fault (the continental suture), the Zagros Imbricate Zone, the High Zagros Faults, the Zagros Folded Belt, Mountain Front Fault, the Zagros Foredeep, and the Zagros Foredeep Fault, from NE to SW (Stocklin, 1968; Berberian, 1995). A peculiar feature in the Zagros is that crustal shortening has been accommodated by deep seated, high-angled reverse faults, which have been interpreted as reactivated, basement normal-faults initiated during the Neotethyan rifting and spreading (Falcon, 1974; Jackson, 1980; Chauvet et al., 2004; Mouthereau et al., 2012). Generally, these faults are segmented with about 85-100 km gaps in between segments and are confined in the Precambrian basement and the lower stratigraphic levels of the overlying sedimentary cover (Berberian, 1995; Bigi et al., 2018). The Cambrian to Pliocene sedimentary cover (~5-13 km thick) overlies the Proterozoic to early Cambrian Hormoz Salt (Stocklin, 1968; Falcon, 1974; Colman-Sadd, 1978). This incompetent salt unit acted as a decollement horizon between the thick-skinned deformation in the basement and the thin-skinned deformation in the sedimentary cover (e.g.; Berberian, 1995; Lacombe et al., 2006). Deformation initiated in the Zagros Imbricate Zone at about 20 Ma or earlier (Fakhari et al., 2008), propagated towards the SW and reached the Zagros Folded belt at 14 Ma (Khadivi et al., 2010).

Since the Neogene, a system of strike-slip faults has also been active in the Zagros (Berberian, 1995). The Main Recent Fault (MRF) was initiated in late Pliocene, which is an active, orogen-parallel, strike-slip fault that follows the trace of the Main Zagros Reverse Fault (Tchalenko & Braud, 1974; Berberian, 1995; Authemayou et al., 2006). Oblique convergence between the Iranian and Arabian plate is partially accommodated along this hinterland fault (Authemayou et al., 2006). At its southeastern end, the MRF diffuses into a series of N to NNW-striking right-lateral, basement-inherited faults, grouped as the Karezun Fault System (Authemayou et al., 2006). Major faults belonging to this zone are the Saverstan, Sabz Pushan,

787 and Kareh-Bas Faults (Figure 8) with an offset of about 100-150 km along each one (Berberian,
788 1995; Authemayou et al., 2006). During rifting of the Proto-Tethys and initial stages of the Neo-
789 Tethys, these faults were activated as right-lateral transform faults in the basement rocks (Talbot
790 & Alavi, 1996). Neogene reactivation of these transverse faults has produced a dragging effect on
791 the earlier-formed, orogen-parallel folds. These faults serve to transmit and distribute the slip along
792 the MRF towards the southeast into the Zagros Folded Belt and the Foredeep (Berberian, 1995;
793 Authemayou et al., 2006). Salt diapirs have been intruded along these faults at multiple locations,
794 which suggests that these faults cut into the top of the basement (e.g.; Kent, 1979; McQuillan,
795 1991; Talbot & Alavi, 1996). A certain degree of seismic hazard is associated with these transverse
796 faults (Berberian, 1995; Authemayou et al., 2006). West of the Karezun Fault System, important
797 transverse faults are the Izeh, Balarud Fault (E-W, 130 km left lateral), the Anaran Basement Fault,
798 and the Khanequin Fault (Figure 8) (Hessami et al., 2001; Joudaki et al., 2016; Sadeghi &
799 Yassaghi, 2016). All these transverse faults were active basin-bounding, normal faults, reactivated
800 as strike-slip faults, and had controls on pre and syn-orogenic sedimentation and subsequent
801 deformation in the Zagros (Sepehr & Cosgrove, 2004).

802 Along its strike, the Zagros curves into a series of salients and recesses bounded by the
803 transverse faults (Figure 8). Generally, these curvatures are grouped into domains and include the
804 Fars salient, the Dezful embayment, the Izeh zone (juxtaposed with the Dezful embayment in the
805 north), the Lorestan salient, and the Kirkuk recess from SE to NW (e.g.; Stocklin, 1968; Falcon,
806 1974; McQuarrie, 2004). The deformation zone is widest in the Fars salient and narrows towards
807 the NW. The style and distribution of deformation changes notably along these curvatures, mostly
808 driven by the presence or absence of decollement layers (e.g.; Bahroudi & Koyi, 2003).

809 Lateral heterogeneity in the Zagros is expressed through the transverse faults, the presence
810 of salt diapirs, and the salient and recesses on the mountain front as discussed above. Further
811 heterogeneity is also expressed in changes in fold geometry and the amount of shortening in
812 adjacent regions. The Fars salient is characterized by a very low taper angle, several salt intrusions,
813 and concentric folds with large amplitude (Talbot & Alavi, 1996; Sepehr et al., 2006; Mukherjee
814 et al., 2010). Towards the west, box folds and large concentric folds are dominant in the Izeh zone.
815 In the Dezful embayment, however, exposed folds are concentric folds with small wavelengths
816 and probably overlie large concentric folds beneath a detachment surface (Sepehr et al., 2006).
817 The presence of a paleo-basement high, bounded by the N-striking, Hendijan-Izeh and Khark-

818 Mish basement faults, has been suggested beneath the Izeh and Dezful domains (Farzipour-Saein
819 et al., 2013 and references therein). In the Lorestan salient, folds are rounded but with much smaller
820 wavelength than in the Fars salient (Sepehr et al., 2006). Several small-scale transverse faults have
821 also been identified around the inflection zone between the Lorestan salient and the Kirkuk recess
822 (e.g.; Sadeghi & Yassaghi, 2016). Amount of shortening in the Fars, Dezful, and Lorestan
823 segments are 67 km, 85 km, and 57 km respectively (McQuarrie, 2004).

824 Spatial changes in folding style have been linked to the mechanical anisotropy within the
825 deforming sedimentary column and the depth at which those anisotropies occur (e.g.; Sepehr et
826 al., 2006). Mechanical anisotropy (presence of an incompetent layer) has a major control on the
827 shape of the folds (lower anisotropy equals more rounded folds) and the depth of anisotropy
828 controls the fold wavelength (deeper anisotropy equals large folds) (Sepehr et al., 2006). The deep-
829 seated Cambrian Hormuz Salt is about 1-2 km thick beneath the Fars salient, and possibly present
830 in the Izeh zone, but absent beneath the sedimentary columns in the Lorestan and Dezful domains
831 (Bahroudi & Koyi, 2003). In contrast, the Mesozoic Kazhumdi shales or the Dashtak Evaporites
832 in the Lorestan, and the Miocene Gachsaran Formation in the Dezful Embayment act as higher
833 level decoupling surfaces, while the overlying sedimentary cover has a uniform mechanical
834 stratigraphy (Sepehr & Cosgrove, 2004; Sepehr et al., 2006). The presence of decollement horizons
835 at different structural levels in the Dezful and Izeh domains has generated a peculiar ramp and flat
836 geometry in the sedimentary cover in the central Zagros (McQuarrie, 2004; Sepehr et al., 2006).

837 Stratigraphy and deformation style are also generally different from the recesses to the
838 salients (Sepehr et al., 2006). It has been suggested that the Zagros foreland in the salient deform
839 by both thin-skinned and thick-skinned deformation, whereas, the foreland deformation in recesses
840 is accommodated only by thin-skinned tectonics (Malekzade et al., 2016). Around the central
841 Zagros foreland, both the intensity of deformation and the amount of shortening increases towards
842 the west and the deformation has been partitioned by left-lateral, blind tear faults reactivated on
843 preexisting basement structures (Sarkarinejad et al., 2018; Pash et al., 2020).

844

845 **6.2 Proposed Factors Controlling Lateral Heterogeneities**

846 Several ideas have been proposed to explain the sinuosity and lateral heterogeneity of
847 deformation style in the Zagros. These ideas include: 1) rotations of crustal blocks (Hessami et al.,
848 2001; Edey et al., 2020); 2) along strike variations in a viscous decollement horizon between the

849 basement and the sedimentary cover (Bahroudi & Koyi, 2003; McQuarrie, 2004); 3) the presence
850 of a lateral buttress that serves to partition deformation (Cotton & Koyi, 2000; Bahroudi & Koyi,
851 2003); 4) lateral variation in the degree of oblique convergence (McQuarrie et al., 2003; Vernant
852 et al., 2004; Vernant & Chéry, 2006); and 5) heterogenous rigidity along the plate margin
853 (Malekzade et al., 2016). The block rotation model suggests that adjacent crustal blocks rotate with
854 a reverse polarity along a vertical axis, driven by movements along strike-slip faults and the
855 presence of a rigid backstop (e.g.; Hessami et al., 2001; Edey et al., 2020). These strike-slip faults
856 were activated along N-S trending, inherited basement structures attributed to the Pan-African
857 tectonics (Koop & Stoneley, 1982; Husseini, 1988; Hessami et al., 2001) and subsequent Tethyan
858 rifting (Talbot & Alavi, 1996).

859 Along strike variation in the distribution of the Cambrian salt unit has a major control in the
860 deformation along the Zagros Fold Belt. The presence of this incompetent unit served as a viscous
861 detachment and deformation propagated much further where the salt was present than in the
862 domains where it is missing (Bahroudi & Koyi, 2003; McQuarrie, 2004; Farzipour-Saein et al.,
863 2013). The patchy arrangement of salt deposition has been attributed to the aforementioned,
864 inherited basement structures, which could have also created tear fault-type transverse structures
865 in the hanging walls of the thrust sheets. The style of deformation is also dependent on the nature
866 of detachment horizons. Above a viscous decollement, the overlying units generally deform by
867 ductile thickening, whereas above a frictional detachment, imbrication and folding deformation
868 dominates (Bahroudi & Koyi, 2003). During deformation, the presence of transverse basement
869 faults or a lateral change in facies can act as a lateral buttress and reorient local kinematics (Cotton
870 & Koyi, 2000; Bahroudi & Koyi, 2003). Obliquity of plate convergence and the frictional strength
871 along the MRF (a hinterland fault) together dictate if strike-slip partitioning initiates or not and
872 thereby can have controls on internal deformation in the Zagros belt (McQuarrie et al., 2003;
873 Vernant et al., 2004; Vernant & Chéry, 2006). Moreover, heterogenous plate-margin rigidity along
874 with the presence of embayments and indenters, can cause along-strike changes in deformation
875 patterns by affecting the local obliquity angle and favoring the escape of the upper crustal material
876 into adjacent reentrants (Malekzade et al., 2016).

877 It is likely that a number of factors have contributed to lateral heterogeneity in the Zagros. The
878 stratigraphy has played a role in terms of thickness changes causing differences in folding patterns
879 and fault geometry. The presence of localized salt layers and salt diapirs further contribute to

880 differences in thrust displacement and local geology. The geometry of the extensional or rifts
881 structures that pre-date collision may have impacted the geometry of post-collisional faults.
882

883 **7 Andes**

884 **7.1 Tectonic Setting and Lateral Heterogeneities**

885 The Andean mountain belt is a classic example of an active subduction margin and likely
886 represents processes that were active in the world's collisional mountain belts prior to collision.
887 Modern-day Andean topography is largely the manifestation of crustal shortening and thickening
888 in response to the ongoing oblique subduction of the Nazca oceanic plate beneath the South
889 American plate (e.g.; Mpodozis & Ramos, 1989). The two plates are currently converging along a
890 N78˚E vector at a rate of about 66 mm/yr (Angermann et al., 1999; Kendrick et al., 2003). The
891 Andean orogen follows a north-south trend along the western margin of the South American plate,
892 except in the Central Andes, where the orogen makes a curve known as the Arica bend (Figure
893 9a). Along the length of the mountain belt there is lateral heterogeneity exhibited at several scales.
894 Lateral heterogeneity along the range has been observed in terms of the upper and lower plate
895 dynamics, topography and deformation style of the retro-arc belt, nature of the foreland basin, and
896 igneous activity.
897 At a coarse scale, the Andes exhibit lateral heterogeneity in topographic changes from north to
898 south that has led to the characterization of the Northern Andes, the Central Andes, and the
899 Southern Andes (Figure 9a). The major visible difference is in the width of the mountain belt
900 where the Northern and Southern Andes are narrow while the Central Andes is much wider and
901 includes the Altiplano and Puna plateau regions. These general topographic differences are the
902 product of differences in their terrane accretion history and subduction zone dynamics. Other broad
903 differences seen along the range include the presence or absence of active volcanism which is
904 likely related to changes in the dip angle of the subduction slab (Ramos & Folguera, 2009). During
905 early Paleozoic, the southwestern margin of South America had a history of exotic terrane
906 accretion and subduction (e.g.; Ramos, 1988). The modern-day subduction margin initiated in late
907 Paleozoic (Giambiagi et al., 2012). The Late Permian to Early Jurassic tectonic history was

Figure 9: Tectonic map of the Andes. a) Map of the South American plate and the Nazca oceanic plate (west) showing major transverse features on the subducting Nazca oceanic plate. The red star

911 shows the epicenter of the M_w 8.4 2001 Peru earthquake. Red shades indicate volcanic zones. Note
912 the large-scale strike slip faults, indicated by yellow lines, in the Northern Andes. The inset shows
913 the extent of the 'Figure 9b' (modified from Gutscher et al., 2000; Robinson et al., 2006; Egbue &
914 Kellogg, 2010; Schepers et al., 2017). b) Geological map of the Central and Southern Andes
915 showing the location of major cross structures. The deformation style and distribution are quite
916 different from the Central to the Southern Andes. (modified from Ghiglione et al., 2009; Stanton-
917 Yonge et al., 2016; Schepers et al., 2017). The red lines in the 'Figure 9b' represent the Andean
918 Transverse Faults.
919 Acronyms: CCM: Calliqui-Copahue-Mandolegue Transfer Zone; CCVC: Cordon Caulle Volcanic
920 Complex; ChC: Chillan-Cortaderas Lineament; GFZ: Grijalva Fracture Zone; LATF: Lago
921 Argentino Transfer Fault; LOFS: Liquine-Ofqui Fault System; LVTF: Lago Videma Transfer
922 Fault; MFZ: Mendana Fracture Zone; MVFZ: Mocha-Villarrica Fault Zone; NFZ: Nazca Fracture
923 Zone; TPTF: Torres del Paine Transfer Fault; TSPP: Tarta-San Pedro-Pellado Volcanic
924 Alignment.
925
926 characterized by crustal extension and the associated volcanism (Llambías et al., 1993). In the
927 Southern Andean front, there was backarc extension from late Triassic to Early Jurassic (Vergani
928 et al., 1995; Giambiagi et al., 2012) while the Central Andes experienced extension from late
929 Jurassic to Early Cretaceous (Galliski & Viramonte, 1988; Salfity & Marquillas, 1994). The
930 resulting orogen-parallel, rift-related, normal faults and/or transfer faults were reactivated as
931 reverse faults with strike-slip components in Cretaceous to Paleogene (Kley et al., 2005; Mescua
932 & Giambiagi, 2012). In the Southern Andes, this Neogene inversion of the extensional basins led
933 to lateral variations in the thickness and facies of the sedimentary sequences, which were
934 subsequently reflected in heterogeneities of the deforming fold and thrust belt (e.g.; Ghiglione et
935 al., 2009; Likerman et al., 2013).
936 The style of subduction of the down-going Nazca Plate in the Central Andean margin
937 differs greatly from the adjacent margins to the north and south. The Central segment has had a
938 steep subducting plate while to the north and south the oceanic plate has been subducting at a low
939 angle since 12 Ma in the respective trench segments namely, the northern Peruvian and southern
940 Pampean flat slabs (Schepers et al., 2017). The trench retreat has greatly outpaced the slab roll
941 back and this difference has generated the 200-300 km long flat slab segments. The slab is thought

942 to have been anchored at the 660 km discontinuity, which is preventing the roll back (Schepers et
943 al., 2017; Chen et al., 2019). The crustal shortening along the Arica bend in the Central Andes is
944 420 km, which is much greater than shortening values of 160 km and 150 km in the Southern and
945 Northern respectively (Arriagada et al., 2008; Schepers et al., 2017). There are also differences in
946 the style of deformation related to flat slabs including the inland development of thick-skinned
947 deformation east of the crest of the Andes. Another lateral variation related to the flat slab zones
948 is the absence of active volcanism. Several causes for the flattening of the slab have included
949 subduction of buoyant oceanic crust around the Nazca and Juan Fernandez Ridges or possible
950 changes in the thermal thickness of the overriding lithosphere (Pilger, 1981; Manea et al., 2012;
951 Schepers et al., 2017).
952 At a finer scale, there are lateral differences in the timing and nature of deformation along
953 the Andes. In the Northern Andes, crustal blocks are "escaping" northeastwards towards the free
954 Caribbean-North Andes boundary and away from the rigid South American Plate along the system
955 of large-scaled, strike-slip faults (Figure 9a) (Audemard et al., 2005; Audemard, 2009; Egbue &
956 Kellogg, 2010; Monod et al., 2010). The trench-parallel component of the oblique plate
957 convergence has been driving this escape for the last 1.8 Ma. This escape was likely triggered by
958 an increase in coupling between the upper and lower plate when the Carnegie Ridge entered the
959 subduction zone (Egbue & Kellogg, 2010).
960 The Central Andes segment is dominated by anomalous topography of the Altiplano-Puna
961 plateau, which was uplifted due to thermal softening of the lithosphere followed by crustal
962 shortening and accompanying arc magmatism during the orogeny (Allmendinger et al., 1997;
963 Coutand et al., 2001). Within the plateau region researchers have documented significant
964 differences in the timing of the surface uplift and crustal structure of adjacent blocks (e.g.; Bianchi
965 et al., 2013; Leier et al., 2013; Canavan et al., 2014). The fault boundaries of these blocks are
966 thought to be related to inherited basement faults, possibly bounding older accreted terranes
967 (Jordan et al., 1983) Towards the foreland, spatial location of the Cenozoic fault systems were
968 likely controlled by the presence of Paleozoic and Mesozoic basement structures (Coutand et al.,
969 2001; Gillis et al., 2006). The plateaus and the adjacent ranges in the Central Andes, define the
970 highest topographic features in the world within a non-collisional setting (Isacks, 1988).
971 Another feature unique to the southern Central Andes is the fragmentation and exhumation
972 of the retro-arc foreland basin (Sierras-Pampeanas) along inherited structures (Figure 9b) (Jordan

et al., 1983; Japas et al., 2016). Stronger coupling between the upper and lower plates in the flat-slab segments has been described as the driver behind inland propagation of deformation and subsequently the basin uplift (Ramos et al., 2002; Oriolo et al., 2014). Just to the south of the flat-slab segment, Giambiagi et al. (2012) documented an abrupt southward decrease in topographic uplift and crustal shortening. This sharp, lateral variation is driven by a strong lateral change in the upper plate rheology, which controls the degree of coupling between the upper and lower crust, such that a thick and more felsic crust has strongly coupled upper and lower slabs (Giambiagi et al., 2012).

Thick-skin deformation in the Central Andes terminates towards the south at the northern segment of the Southern Andes, which is characterized by trench-parallel, thin-skinned, fold and thrust deformation. The southern segment, however, is dominated by a system of strike-slip fault systems. The ENE-striking, transverse, dextral Callaqui-Copahue Mandolegue (CCM) fault is thought to decouple the contrasting deformation styles between the retro-arc thrust belt (north) and the Liquine-Ofqui Fault System (LOFS) in south (Folguera et al., 2004).The LOFS (Figure 9b) is a ~1200 km long, NNE-striking, right-lateral, reverse, intra-arc fault in the southern segment (Cembrano et al., 1996; Thomson, 2002; Vargas et al., 2013). Here, a series of NE-striking, en echelon, dextral, normal faults splay off from the LOFS and form a strike slip duplex between two sub-parallel fault branches of the LOFS (Cembrano et al., 1996). Another set of strike-slip faults cut the LOFS and associated faults and are called the Andean Transverse Faults (ATF). The ATF (Figure 9b) are NW-striking, reverse, sinistral faults, primarily formed on inherited basement structures (e.g.; Roquer et al., 2017; Sielfeld et al., 2019). Deformation partitioning occurs within these faults, whereby the trench-parallel component of the oblique convergence is accommodated by the LOFS and its splay faults and the ATFs accommodate the trench-perpendicular component (e.g.; Stanton-Yonge et al., 2016). In the northern termination of the LOFS, the strike-slip dominated domain sharply transitions into margin-parallel fold and thrust deformation (Figure 9b) (Stanton-Yonge et al., 2016). These strike-slip fault systems also form excellent conduits as well as reservoirs for magma and hydrothermal fluids and thereby control the locus of volcanic complexes (e.g.; Petrinovic et al., 2006; Pérez-Flores et al., 2016; Roquer et al., 2017; Sielfeld et al., 2019; Lupi et al., 2020; Piquer et al., 2020).

Effects of the subduction of oceanic fracture zones on seismic activity has also been observed in the central Andes. In the subducted Peruvian slab, generally deeper earthquakes are

generated around a subducted segment boundary, the Mendana Fracture Zone (Figure 9a) (Gutscher et al., 2000). Towards the south, a fracture zone in the down-going Nazca plate (most likely the Nazca Fracture zone) is thought to have induced a fracture in the over-riding plate that acted as a temporary lateral barrier during the initial seismic rupture propagation but subsequently allowed energy to pass through this vertical plane releasing the energy of the M_w 8.4 2001 Peru earthquake (Robinson et al., 2006). These examples indicate that transverse discontinuities in the lower plate (or subducting plate) can influence structures in the upper plate and can have great seismic implications.

7.2 Proposed Factors Controlling Lateral Heterogeneities

Along the Andean belt, lateral heterogeneities have been primarily expressed as variation in crustal shortening and topographic uplift (e.g.; Allmendinger et al., 1997; Arriagada et al., 2008; Giambiagi et al., 2012; Schepers et al., 2017), along-strike changes in the styles and timing of deformation (e.g.; Ramos et al., 2002; Bianchi et al., 2013; Leier et al., 2013; Canavan et al., 2014; Oriolo et al., 2014; Stanton-Yonge et al., 2016), laterally contrasting seismicity (Gutscher et al., 2000; Robinson et al., 2006), and as changes in volcanic activity (e.g.; Pérez-Flores et al., 2016; Roquer et al., 2017; Sielfeld et al., 2019; Lupi et al., 2020; Piquer et al., 2020). Researchers interpret that these heterogeneities are governed by the angle of lower plate subduction (flat versus steep slab), physiography of the lower plate, obliquity of the subduction vector, preexisting basement structures in the upper plate, and the rheology of the upper plate. The angle of the lower plate subduction controls the degree of coupling between the lower and upper plates (lower angle equals stronger coupling), which in turn impacts the nature and distribution of the upper plate deformation (e.g.; Ramos et al., 2002; Oriolo et al., 2014). Subduction of physiographical features in the lower plate also can change the amount of plate coupling and generate respective topographic and seismic signatures in the upper plate or it can influence the development of cross structures (Gutscher et al., 2000; Robinson et al., 2006). Oblique plate convergence in the Southern Andes has been accommodated by a system of strike-slip and transverse faults (e.g.; Stanton-Yonge et al., 2016). In the Northern Andes, however, the dynamic plate setting has favored crustal escape (e.g.; Egbue & Kellogg, 2010). Rheology of the upper plate dictates the amount of plate coupling and therefore, has controls on the rate and amount of crustal shortening and the overall topographic uplift (Giambiagi et al., 2012).

8 Other Orogens

Lateral heterogeneities have been documented in several other mountain belts around the world (Figure 1). While there are groups of along-strike variations common across multiple mountain belts, some of the heterogeneities are the result of the broad tectonic setting and the nature of the sedimentary cover, and therefore can be unique to only a few mountain belts. Comparable to the Appalachians, , the Mesozoic rift structures in the External Hellenides thrust belt in Greece were reactivated as transverse zones (e.g.; the Corinth Gulf, Ierapetra, and Omalos transverse zones), which partitioned the belt into a series of salients, recesses, and linear segments (Skourlis & Doutsos, 2003; Kokkalas & Doutsos, 2004; Chatzaras et al., 2013). These inherited structures also disrupted the lateral continuity of the foreland sedimentary sequences and served as crustal-scale lateral/oblique ramps during thrust propagation and thereby had a significant control on the nature and deformation style of the evolving taper wedge (Robertson et al., 1991; Doutsos et al., 2006; Chatzaras et al., 2013). Similarly, in the Urals, Precambrian aulacogens (failed rift arms) served as transverse basement structures, above which tear-faults and lateral ramps were developed during fold-thrust propagation (Rodgers, 1990; Brown et al., 1997; Perez-Estaun et al., 1997). Cross faults are common in the Apennines and are generally called anti-Apennine Faults (e.g.; Coltorti et al., 1996; Sorgi et al., 1998; Butler et al., 2006; Elter et al., 2011). The NNW-striking Apennine belt is underlain by the NNE-trending crustal tectonic lineaments (Valnerina Line, Ancona-Anzio Line, Ortona-Rocca Monfina Line). These large-scale lineaments act as structural barriers (zones of abrupt lateral changes in tectonic and structural style, wedge stratigraphy, and topography) during tectonic transport and laterally limit the propagation of seismic fault rupture (Pizzi & Galadini, 2009; Satolli et al., 2014). There are also smaller-scaled transverse basement structures, that may either serve as seismic segment boundaries/seismic loci or get reactivated as transfer zones (Valensise & Pantosti, 2001; Pizzi & Galadini, 2009). Furthermore, transfer zones in the Apennines are also known to form suitable loci for magma emplacement (Dini et al., 2008). On a much larger scale, the differential retreat along the adjacent segments of the Adriatic plate during the last 5 Ma has been manifested as a lithospheric tear/transfer zone across the Appennines (Scrocca, 2006), which may share a similar genesis to the Colorado Mineral Belt in the Cordilleran belt.

Cross structures have also been interpreted to have great economic and seismic impacts besides their influence in tectonic, stratigraphic, and structural evolution (e.g.; Mahoney et al., 2017). In

the Papua New Guinea fold-thrust belt, the Jurassic, extensional, transverse, crustal structures evolved as zones of economically significant copper-gold mineralization during their Late Miocene-Pliocene inversion (Davies, 1991; Corbett, 1994; Hill et al., 2002). Like in the Apennines and the Himalayas, active cross faults in the Taiwan mountains are known to serve as earthquake nucleation sites and as rupture segment boundaries (Deffontaines et al., 1997; Lacombe et al., 2001; Ching et al., 2011). These cross faults have genetically been linked to changing deformation style (thick-skinned vs thin-skinned) and to a lateral change in thickness of the deforming sedimentary sequences (Lacombe et al., 2001; Mouthereau et al., 2002; Mouthereau & Lacombe, 2006; Ching et al., 2007). Much similar to the Zagros belt, controls of the presence or absence of a decoupling layer on the style of the evolving taper wedge (narrow wedge with a high-taper angle, when decoupling layer is absent and vice-versa) have been noted in the Caucasus belt (Upper Jurassic salt and Middle-Lower Jurassic shales) in Russia (Sobornov, 1996), the Sulaiman belt (Paleozoic, Lower Cretaceous, and Eocene strata) in Pakistan (Jadoon et al., 1994), and the Parry Island belts (Ordovician salt) in the Canadian Arctic (Harrison & Bally, 1988).

9 Discussion

Despite the general temporal and spatial continuity of crustal deformation along convergent mountain belts, significant lateral heterogeneities have been observed in several orogenic belts from around the world. There are certain lateral variations, which are unique to only a few orogens such as the lithospheric tear in the Apennines and the asynchronous orogenic events in the Alps. More frequently, however, similar groups of lateral variations have been observed across multiple mountain belts. Generally, lateral heterogeneity in convergent mountain belt settings have been expressed as: 1) an along-strike change in deformation style (thick-skinned vs thin-skinned, imbrication vs duplexing/changes in ramp geometries); 2) variation in igneous activity and metamorphic grade; 3) variation in seismic activity; 4) differential topographic uplift/features along the strike; and/or 5) abrupt changes in thickness and facies of sedimentary sequences in both foreland basins and within the fold-thrust belt. Oftentimes such lateral variations are abrupt rather than gradual and are marked by geological structures, mostly faults, that are nearly orthogonal to the strike of the orogen, generically referred to as cross structures in this review. The causal factors/mechanisms behind the observed lateral heterogeneities are discussed in this section.

9.1 Irregular Continental Margins

The geometry of the continental margin(s), prior to the collision/convergence, has a profound effect on the geometry of the evolving orogenic belt. The orogenic front may mimic the continental margin geometry (Figure 4) such that any irregularities along the margin are reflected along the deformational font. This phenomenon has been proposed in the Appalachians. During the Iapetan rifting (plus the other rifting events) along the Laurentian margin, a series of embayments (concave oceanward) and promontories (convex oceanward) separated by transform faults were produced (Thomas, 2014). Along such an irregular margin, the depositional environment is bound to vary laterally. During subsequent orogenic events, promontories evolved into recesses (concave towards the foreland), embayments evolved into salients (convex towards the foreland), and the transform fault boundaries evolved into transverse zones or cross structures (Thomas, 2014). Kwon and Mitra (2004) have compiled five end-member models for the kinematic development of salients as a function of principal transport direction, amount of shortening, degree of vertical axis rotation, thrust displacement, and presence or absence of tear faults or lateral/oblique ramp boundaries. These models, however, can be viewed as second-order, structural controls on formation of orogenic curvatures.

Lin et al. (1994) further noted that a collisional event between two promontories (of two different landmasses) results in a narrower but stronger orogenic deformation and a higher grade of metamorphism than a promontory-embayment collision. It can be concluded that an irregularity along a continental margin may serve as a nucleation site for lateral heterogeneity.

9.2 Inherited Basement Structures

Inherited basement structures form a first-order control on formation of cross structures. Basement structures are primarily related to continental rifting, hyper-extension of rifted margins (e.g.; Ribes et al., 2019) , crustal sutures, or back-arc extension (Figure 10). Furthermore, it has been noted that a failed rift-arm (aulacogen) can also serves as an inherited basement structure and control structural evolution (Rodgers, 1990; Brown et al., 1997; Perez-Estaun et al., 1997). Crustal sutures mark boundaries between two continental blocks and form as a result of collisional tectonics or terrane accretion. Generally, suture zones consist of highly deformed rock units and form weaker zones within the crust (Hope & Eaton, 2002; Whitmeyer & Karlstrom, 2007). These zones are known to be intruded by igneous bodies during the subsequent crustal stabilization

(Whitmeyer & Karlstrom, 2007), and these intrusion boundaries can also behave as zone of weaknesses during various tectonic events (Simony & Carr, 1997; Bader, 2009).

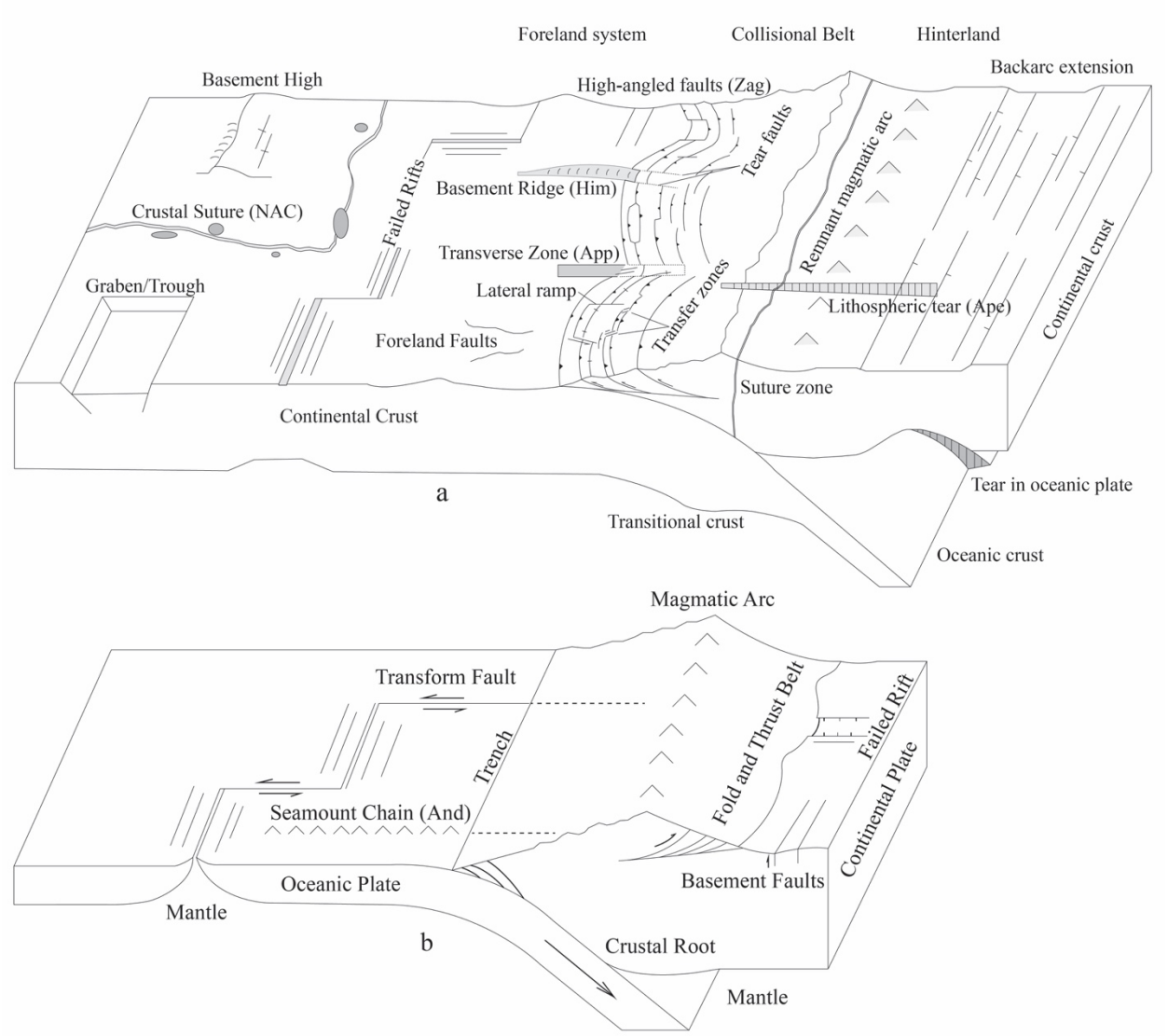

Figure 10: Various inherited basement structures and oceanic plate physiography in contractional settings. The gray ellipses in the 'Figure10a' represent igneous intrusions. The mountain belt that, in general, represents a certain structure are denoted in parenthesis.

And: Andes; Ape: Apennines; App: Appalachians; Him: Himalayas; NAC: North American Cordillera; Zag: Zagros.

9.2.1 Impacts of Basement Structures on Subsequent Sedimentation and Deformation

The presence of basement structures can greatly affect the foreland sedimentation and thereby have a strong control on the evolution of mountain belts as is seen in the Zagros, the Cordillera, and the Himalaya. Basement structures can isolate deposition centers in the foreland, which induces sharp lateral variations in both the thickness and facies of the sedimentary strata. A thicker foreland sedimentary sequence, when incorporated into the evolving taper wedge, will propagate much farther (salient) than a wedge consisting of a thinner sequence (recess) (e.g.; Paulsen & Marshak, 1999). Differential tectonic transport between the adjacent segments (salients and recesses) is often accommodated by cross structures such as tear faults, lateral ramps, and displacement transfer zones (Paulsen & Marshak, 1999). Orogen-parallel faults and folds are generally truncated at, or dragged into cross structures as seen in the Appalachians and the Cordillera (e.g.; Thomas, 2007; Whisner et al., 2014).

Similarly, lateral variations in sedimentary facies will also have a significant impact on the wedge evolution. An abrupt change in the structural elevation of decoupling layers results in lateral ramps (Thomas, 1990). Since thrust-ramp geometry is governed by the nature of the sedimentary column, any lateral variation in sedimentary facies is likely to be reflected in the thrust geometry (e.g.; Mitra, 1988). In a broader stratigraphic framework, if the presence of regional decollement horizons (units of salts, evaporites, and shales) varies laterally, then the deformation style in adjacent segments of the mountain belts will be very different. If a decollement horizon is present, then the taper angle will be low and propagate further than adjacent areas. Likewise, in the absence of such a horizon, the taper will build up to a larger angle in a narrower belt as in the Zagros (e,g,; Jadoon et al., 1994; Sobornov, 1996; Bahroudi & Koyi, 2003). The depth of these decollement horizons will also have a first order control on the fold geometry, such that a deeper horizon will result in folds with larger amplitude (Sepehr et al., 2006). Furthermore, the stratigraphic variation boundaries will also act as a lateral buttress to locally deflect the transport trajectories (Bahroudi & Koyi, 2003). If basement structures are reactivated during deposition, then syn-sedimentary faults and/or drape folds can form in the overlying sedimentary column (Thomas, 1990). These structures will also impact the fold-thrust belt evolution in a similar fashion to other cross-structures (e.g.; Zerlauth et al., 2014).

9.2.2 Reactivation of Basement Structures

Regardless of their origin, inherited basement structures can be broadly categorized into three groups: orogen-parallel, oblique, and transverse/cross basement structures. Various styles of preferential reactivation and inversion of basement structures have been discussed in the Apennines (Tavarnelli et al., 2004; Butler et al., 2006), and are also seen in other mountain belts. When orogen-parallel basement structures/faults are present, it is possible for them to be reactivated as reverse faults during orogenic compression (Figure 10a). It has, however, been noted that basement faults can be deformed under compression without inversion or reactivation (Pantet et al., 2020). In a reactivation scenario, the deformation between the basement and the overlying sedimentary cover is partially decoupled, whereby the basement deforms in thick-skinned style and the cover deforms as thin-skinned, fold and thrust belts (e.g.; Berberian, 1995; Lacombe et al., 2006). Discontinuities along the orogen-parallel basement structures will eventually result in laterally heterogeneous deformation style along the range. If the basement faults are steeply-dipping, then they often cut into the thin-skinned decollement faults of the sedimentary cover and act as frontal ramps during the upper, brittle deformation (e.g.; Bahroudi & Koyi, 2003). These orogen-parallel basement structures also accommodate convergence via strike-slip faulting under a favorable plate kinematic setting (e.g.; Authemayou et al., 2006). Margin perpendicular and oblique structures, however, either serve as lateral/oblique ramps or get reactivated as strike-slip faults with a dip-slip component based on their orientation in the stress field. Based on their aerial extent, these inherited structures can affect a few thrust sheets, or they can partition the entire mountain belt (Scrocca, 2006; Pizzi & Galadini, 2009; Satolli et al., 2014). Cross faults in the Himalayas may have had an origin in reactivated, margin-perpendicular basement faults and basement highs such as the Delhi-Hardwar ridge (Sahoo, 2000; Godin & Harris, 2014; Hubbard et al., 2018; Hubbard et al., 2021).

9.3 Rheology of the Crust

Variation in crustal rheology is another significant element in inducing lateral heterogeneities in orogenic belts, which itself is a function of its composition and thermal structure. In general, a weaker crust is more likely to buckle under contraction resulting in a high crustal relief, whereas a stronger crust will distribute deformation in more brittle manner (Allmendinger et al., 1997; Coutand et al., 2001). It has also been proposed that rheological heterogeneities along a continental

margin front could result in orogenic curvatures, such that a stronger segment better resists deformation and evolves as a salient (e.g.; Malekzade et al., 2016). As seen in the Zagros, frictional strength in hinterland faults, which is governed by crustal rheology, can influence the mode of deformation partitioning in the orogenic belt and thereby have a control on the style and distribution of deformation (e.g.; Vernant & Chéry, 2006). Thermal structure and rheology of the crust can vary laterally due to variations in arc magmatism. Therefore, previous tectonic events will also have an indirect impact on lateral heterogeneity of an orogen.

Giambiagi et al. (2012) proposed that a stronger coupling between the upper and lower crust deformation corresponds to a higher, surficial topography and greater crustal shortening. Crustal coupling is thought to be governed by crustal composition such that a thick and more felsic crust has a stronger coupling between the upper and lower units than a thin and mafic crust. Thus, if there is strong lateral variation in crustal properties due to tectonic events such as terrane accretion or rifting then such variation will be manifested as laterally heterogenous deformation segments.

In the Alps, intensive folding and uplift of the Tauern window has been linked to the northward encroachment of the Dolomite acting as an indenter (Rosenberg & Garcia, 2011), which indicates that rheology of both converging crustal blocks have an impact on the morpho-tectonic evolution of an orogen.. As Butler et al. (2006) pointed out, the correlation between precise lithospheric strength profiles and orogenic deformation would further elucidate our understanding about the role of upper crustal rheology during orogenesis.

9.4 Plate Dynamics and Physiography of the Lower Plate

Plate dynamics between the upper and lower plate as well as the lower plate structures can disrupt the lateral homogeneity of orogenic belt (Figure 10b). Effects of lateral change in the style of subduction in the deforming orogen have contributed to lateral heterogeneity in the Andes. Any transverse structure in the lower plate is likely to be inherited in the upper plate, such as the Colorado Mineral Belt and the lithospheric tear in the Apennines (e.g.; Figure 10a) (Scrocca, 2006; Chapin, 2012). These structures in the lower plate impartially dissect the orogen rather than controlling the deformation style. The dynamics of the lower plate, however, generally differs across these transverse structures, which impacts the foreland sedimentation and fold-thrust belt evolution (Chapin, 2012). A similar phenomenon has been observed in cases where oceanic fracture zones (Figure 10b), orthogonal to the subduction zone, get subducted and result in the

occurrence of cross faults in the over-riding plate. This scenario has been proposed on the Juan de Fuca plate subduction (Goldfinger, 1997), in Sumatra (Graindorge, 2008), and in the Andes (Robinson et al., 2006). Although not a cross structure, the Norumbega Fault System in the Appalachians has been regarded as a surface manifestation of a subducted oceanic ridge-transform system (Kuiper, 2016; Kuiper & Wakabayashi, 2018).

In orogens associated with oceanic subduction, variations in the relative rates of subduction versus convergence can create lateral heterogeneity in the over-riding plates as is seen in the Andes. When subduction outpaces convergence such that the convergent boundary retreats, back-arc extension occurs. These areas may have contrasting evolution when compared to adjacent areas where there is a better balance of the subduction versus convergence rates.

9.5 Obliquity of Plate Convergence

Lateral heterogeneity induced by oblique convergence is scale dependent. Obliquity of the plate convergence is generally accommodated by arrays of transtensional, transpressional, and strike-slip faults. In the Andes, transpressional cross faults are associated with mafic volcanism, while transtensional faults are linked with felsic magmatism as driven by magmatic viscosity difference (Petrinovic et al., 2006). At the scale of individual faults, these cross-faults disrupt the continuity of the fold-thrust belt as noted in the southern Andes and the Northern Calcareous Alps (Zerlauth et al., 2014; Stanton-Yonge et al., 2016). Lateral variation in the degree of oblique convergence itself, however, will also induce lateral heterogeneity in the orogenic belt due to an overall change in the stress field (McQuarrie et al., 2003; Vernant et al., 2004; Vernant & Chéry, 2006).

9.6 Further Implications of Cross Structures

Besides their role in foreland sedimentation and tectonic evolution of orogens, cross faults also have implications in the seismicity, mineralization, igneous activity, numerical modelling, and in topography of mountain belts. In the Zagros, a small seismic hazard has been linked to cross-faults (Berberian, 1995; Authemayou et al., 2006). Cross-faults in the Apennines are known to either serve as seismic segment boundaries or seismic loci (Valensise & Pantosti, 2001; Pizzi & Galadini, 2009). Similarly, in Taiwan, cross-faults are known to act as earthquake nucleation sites and as rupture segment boundaries (Deffontaines et al., 1997; Ching et al., 2011). Microseismicity in the

Himalayas has occurred along cross-strike trends, has terminated at cross-strike zones, and has made other spatial changes along cross-strike boundaries (Rajaure, 2013; Mugnier et al., 2017; Bilham, 2019; Mendoza, 2019). A transverse fault in the down-going Nazca plate had an enormous impact during the 2001 Peru earthquake (Robinson et al., 2003). From the economic standpoint, cross-faults form excellent conduits as well as reservoirs for magma and hydrothermal fluids (McMechan, 2012), which makes them target sites for economic mineral deposits. In the Papua New Guinea fold-thrust belt, transverse zones form sites of economically significant copper-gold deposits (Davies, 1991; Corbett, 1994; Hill et al., 2002). The Colorado Mineral Belt is another example of valuable mineral accumulation along a cross-structure (Chapin, 2012). Moreover, cross-structures can form potential traps for oil and gas accumulation, which, in some areas makes them an important site for hydrocarbon exploration (Wheeler, 1980; Séjourné & Malo, 2007; Bader, 2009). Fault systems can form excellent conduits and reservoirs for magmatic fluids and therefore can control the locus of volcanic complexes in convergent settings (e.g.; Petrinovic et al., 2006; Pérez-Flores et al., 2016; Roquer et al., 2017; Sielfeld et al., 2019; Lupi et al., 2020; Piquer et al., 2020). Thermo-mechanical tectonic models could potentially be rectified by changing the lithospheric parametric values along the strike such that they agree with the lateral variation in crustal deformation, as can be observed on the surface. Finally, cross-structures also have a major control on the geomorphologic evolution of mountain belts. In the Himalayan front, cross faults spatially coincide with river channels (Sahoo, 2000; Srivastava, 2018). The anti-Apennine faults have distinct topographic signatures (Coltorti et al., 1996). Cross-faults can be zones of weaknesses, and therefore, can also amplify erosional hazards, especially in active mountain belts.

10 Conclusions

While convergent mountain belts are dominated by spatially and temporally continuous orogen-parallel structures, geological and geophysical data shows that various forms of lateral heterogeneity, often marked by cross structures, are ubiquitous in most orogenic settings. In general, lateral heterogeneities along orogens have been manifested as: 1) along-strike changes in deformation style; 2) variation in igneous activity or metamorphic grade; 3) variation in seismic activity; 4) changes in topography and geomorphology; and 5) abrupt lateral stratigraphic changes. Common drivers behind these lateral heterogeneities include the geometry of the continental margin, inherited basement structures, lateral variation in stratigraphy of deforming sedimentary sequences, variation in crustal rheology, along-strike changes in plate tectonic setting,

physiography of the lower plate, and obliquity of plate convergence. In most settings, these factors are interrelated and simultaneously influence the morpho-tectonic evolution of an orogen. Apart from their influence on foreland sedimentation and orogenic evolution, lateral heterogeneity and cross structures can have an impact on patterns of seismicity, natural resource occurrence, and natural hazards. We therefore stress the importance of documenting heterogeneity, mapping cross structures, and understanding the role these lateral changes play in mountain belt development along convergent margins.

References

Aleinikoff, J. N., Zartman, R. E., Walter, M., Rankin, D. W., Lyttle, P. T., & Burton, W. C. (1995). U-Pb ages of metarhyolites of the Catoctin and Mount Rogers Formations, central and southern Appalachians: Evidence for two pulses of Iapetan rifting. *American Journal of Science, 295*(4), 428-454. doi:https://doi.org/10.2475/ajs.295.4.428

Allen, M. B., & Armstrong, H. A. (2008). Arabia–Eurasia collision and the forcing of mid-Cenozoic global cooling. *Palaeogeography, Palaeoclimatology, Palaeoecology, 265*(1-2), 52-58. doi:https://doi.org/10.1016/j.palaeo.2008.04.021

Allmendinger, R. W., Jordan, T. E., Kay, S. M., & Isacks, B. L. (1997). The evolution of the Altiplano-Puna plateau of the Central Andes. *Annual Review of Earth and Planetary Sciences, 25*(1), 139-174. doi:https://doi.org/10.1146/annurev.earth.25.1.139

Anderson, H. E., & Davis, D. W. (1995). U–Pb geochronology of the Moyie sills, Purcell Supergroup, southeastern British Columbia: implications for the Mesoproterozoic geological history of the Purcell (Belt) basin. *Canadian Journal of Earth Sciences, 32*(8), 1180-1193. doi:https://doi.org/10.1139/e95-097

Angermann, D., Klotz, J., & Reigber, C. (1999). Space-geodetic estimation of the Nazca-South America Euler vector. *Earth and Planetary Science Letters, 171*(3), 329-334. doi:https://doi.org/10.1016/S0012-821X(99)00173-9

Arriagada, C., Roperch, P., Mpodozis, C., & Cobbold, P. (2008). Paleogene building of the Bolivian Orocline: Tectonic restoration of the central Andes in 2-D map view. *Tectonics, 27*(6). doi:https://doi.org/10.1029/2008TC002269

Audemard, F. A. (2009). Key issues on the post-Mesozoic southern Caribbean plate boundary. In K. James, M. Lorente, & J. Pindell (Eds.), *Origin and Evolution of the Caribbean Plate* (Vol. 328, pp. 569-586). London: Geological Society, Special Publications.

Audemard, F. A., Romero, G., Rendon, H., & Cano, V. (2005). Quaternary fault kinematics and stress tensors along the southern Caribbean from fault-slip data and focal mechanism solutions. *Earth-Science Reviews, 69*(3-4), 181-233. doi:https://doi.org/10.1016/j.earscirev.2004.08.001

1332 Authemayou, C., Chardon, D., Bellier, O., Malekzadeh, Z., Shabanian, E., & Abbassi, M. R.
1333 (2006). Late Cenozoic partitioning of oblique plate convergence in the Zagros fold-and-
1334 thrust belt (Iran). *Tectonics, 25*(3). doi:https://doi.org/10.1029/2005TC001860
1335 Avouac, J.-P. (2003). Mountain building, erosion, and the seismic cycle in the Nepal Himalaya.
1336 *Advances in geophysics, 46*, 1-80. doi:https://doi.org/10.1016/S0065-2687(03)46001-9
1337 Bader, J. W. (2008). Structural and tectonic evolution of the Cherokee Ridge arch, south-central
1338 Wyoming: implications for recurring strike-slip along the Cheyenne Belt suture zone.
1339 *Rocky Mountain Geology, 43*(1), 23-40. doi:https://doi.org/10.2113/gsrocky.43.1.23
1340 Bader, J. W. (2009). Structural and tectonic evolution of the Douglas Creek arch, the Douglas
1341 Creek fault zone, and environs, northwestern Colorado and northeastern Utah
1342 Implications for petroleum accumulation in the Piceance and Uinta basins. *Rocky*
1343 *Mountain Geology, 44*(2), 121-145. doi:https://doi.org/10.2113/gsrocky.44.2.121
1344 Bahroudi, A., & Koyi, H. A. (2003). Effect of spatial distribution of Hormuz salt on deformation
1345 style in the Zagros fold and thrust belt: an analogue modelling approach. *Journal of the*
1346 *Geological Society, 160*(5), 719-733. doi:https://doi.org/10.1144/0016-764902-135
1347 Bartosch, T., Stüwe, K., & Robl, J. (2017). Topographic evolution of the Eastern Alps: The
1348 influence of strike-slip faulting activity. *Lithosphere, 9*(3), 384-398.
1349 doi:https://doi.org/10.1130/L594.1
1350 Bayona, G., Thomas, W. A., & Van der Voo, R. (2003). Kinematics of thrust sheets within
1351 transverse zones: a structural and paleomagnetic investigation in the Appalachian thrust
1352 belt of Georgia and Alabama. *Journal of Structural Geology, 25*(8), 1193-1212.
1353 doi:https://doi.org/10.1016/S0191-8141(02)00162-1
1354 Beck, R. A., Vondra, C. F., Filkins, J. E., & Olander, J. D. (1988). Syntectonic sedimentation and
1355 Laramide basement thrusting, Cordilleran foreland; timing of deformation. In C. J.
1356 Schmidt Jr & W. J. Perry (Eds.), *Interaction of the Rocky Mountain Foreland and the*
1357 *Cordilleran Thrust Belt* (Vol. 171, pp. 465-488): Geological Society of America Memoir.
1358 Behrmann, J. H. (1988). Crustal-scale extension in a convergent orogen: the Sterzing-Steinach
1359 mylomte zone in the Eastern Alps. *Geodinamica Acta, 2*(2), 63-73.
1360 doi:https://doi.org/10.1080/09853111.1988.11105157
1361 Benvenuto, G. L., & Price, R. A. (1979). Structural evolution of the Hosmer thrust sheet,
1362 southeastern British Columbia. *Bulletin of Canadian Petroleum Geology, 27*(3), 360-394.
1363 Berberian, M. (1995). Master "blind" thrust faults hidden under the Zagros folds: active
1364 basement tectonics and surface morphotectonics. *Tectonophysics, 241*(3-4), 193-224.
1365 doi:https://doi.org/10.1016/0040-1951(94)00185-C
1366 Berberian, M., & King, G. C. P. (1981). Towards a paleogeography and tectonic evolution of
1367 Iran. *Canadian Journal of Earth Sciences, 18*(2), 210-265.
1368 doi:https://doi.org/10.1139/e81-019
1369 Berger, Z., Boast, M., & Mushayandebvu, M. (2008). The contribution of integrated HRAM
1370 studies to exploration and exploitation of unconventional plays in North America.
1371 *Reservoir, Canadian Society of Petroleum Geologist, 35*(10), 42-48.
1372 Bernoulli, D. (2007). The pre-Alpine geodynamic evolution of the Southern Alps: a short
1373 summary. *Bulletin für angewandte Geologie, 12*(2), 3-10.
1374 Berra, F., & Carminati, E. (2010). Subsidence history from a backstripping analysis of the
1375 Permo-Mesozoic succession of the Central Southern Alps (Northern Italy). *Basin*
1376 *Research, 22*(6), 952-975. doi:https://doi.org/10.1111/j.1365-2117.2009.00453.x

1377 Bertotti, G., Picotti, V., Bernoulli, D., & Castellarin, A. (1993). From rifting to drifting: tectonic
1378 evolution of the South-Alpine upper crust from the Triassic to the Early Cretaceous.
1379 *Sedimentary Geology, 86*(1-2), 53-76. doi:https://doi.org/10.1016/0037-0738(93)90133-P
1380 Bianchi, M., Heit, B., Jakovlev, A., Yuan, X., Kay, S., Sandvol, E., Alonso, R. N., Coira, B.,
1381 Brown, L., & Kind, R. (2013). Teleseismic tomography of the southern Puna plateau in
1382 Argentina and adjacent regions. *Tectonophysics, 586*, 65-83.
1383 doi:http://dx.doi.org/10.1016/j.tecto.2012.11.016
1384 Bielenstein, H. U. (1969). *The Rundle thrust sheet, Banff, Alberta—a structural analysis.*
1385 (Ph.D.). Queen's University, Kingston, Ontario.
1386 Bigi, S., Carminati, E., Aldega, L., Trippetta, F., & Kavoosi, M. A. (2018). Zagros fold and
1387 thrust belt in the Fars province (Iran) I: Control of thickness/rheology of sediments and
1388 pre-thrusting tectonics on structural style and shortening. *Marine and Petroleum*
1389 *Geology, 91*, 211-224. doi:https://doi.org/10.1016/j.marpetgeo.2018.01.005
1390 Bilham, R. (2019). Himalayan earthquakes: a review of historical seismicity and early 21st
1391 century slip potential. In P. J. Treloar & M. P. Searle (Eds.), *Himalayan Tectonics: a*
1392 *Modern Synthesis* (Vol. 483, pp. 423-482). London: Geological Society of London
1393 Special Publication.
1394 Bilham, R., Gaur, V. K., & Molnar, P. (2001). Himalayan seismic hazard. *Science, 293*.
1395 doi:https://doi.org/10.1126/science.1062584
1396 Boyer, S. E. (1995). Sedimentary basin taper as a factor controlling the geometry and advance of
1397 thrust belts. *American Journal of Science, 295*(10), 1220-1254.
1398 doi:https://doi.org/0.2475/ajs.295.10.1220
1399 Boyer, S. E., & Elliott, D. (1982). Thrust systems. *AAPG Bulletin, 66*(9), 1196-1230.
1400 doi:https://doi.org/10.1306/03B5A77D-16D1-11D7-8645000102C1865D
1401 Brack, P. (1981). Structures in the southwestern border of the Adamello intrusion (Alpi
1402 Bresciane, Italy). *Schweizerische Mineralogische und Petrographische Mitteilungen,*
1403 *61(1)*, 37-50. doi:http://pascal-
1404 francis.inist.fr/vibad/index.php?action=getRecordDetail&idt=PASCALGEODEBRGM82
1405 20070062
1406 Brewer, M. C. (2004). *Geometric and Kinematic Evolution of the Bessemer Transverse Zone,*
1407 *Alabama Alleghanian Thrust Belt.* (Ph.D.). University of Kentucky,
1408 Brown, D., Alvarez-Marrón, J., Perez-Estaun, A., Gorozhanina, Y., Baryshev, V., & Puchkov, V.
1409 (1997). Geometric and kinematic evolution of the foreland thrust and fold belt in the
1410 southern Urals. *Tectonics, 16*(3), 551-562. doi:https://doi.org/10.1029/97TC00815
1411 Burchfiel, B. C., Cowan, D. S., & Davis, G. A. (1992). Tectonic overview of the Cordilleran
1412 orogen in the western United States. In B. C. Burchfiel, W. Lipman, & M. L. Zoback
1413 (Eds.), *The Cordilleran Orogen: Conterminous US* (Vol. G3, pp. 107-168): Geoogical
1414 Society of America.
1415 Burrard, S. G. (1915). Origin of the Indo-Gangetic trough, commonly called Himalayan
1416 foredeep. *Proceedings of the Royal Society of Londong, 91A*, 220-238.
1417 doi:https://doi.org/10.1098/rspa.1915.0014
1418 Butler, R. W. H., Tavarnelli, E., & Grasso, M. (2006). Structural inheritance in mountain belts:
1419 an Alpine–Apennine perspective. *Journal of Structural Geology, 28*(11), 1893-1908.
1420 doi:https://doi.org/10.1016/j.jsg.2006.09.006
1421 Calais, E., Nocquet, J.-M., Jouanne, F., & Tardy, M. (2002). Current strain regime in the
1422 Western Alps from continuous Global Positioning System measurements, 1996–2001.

Geology, 30(7), 651-654. doi:https://doi.org/10.1130/0091-7613(2002)030<0651:CSRITW>2.0.CO;2

Campani, M., Mancktelow, N., Seward, D., Rolland, Y., Müller, W., & Guerra, I. (2010). Geochronological evidence for continuous exhumation through the ductile-brittle transition along a crustal-scale low-angle normal fault: Simplon Fault Zone, central Alps. *Tectonics, 29*(3). doi:https://doi.org/10.1029/2009TC002582

Canavan, R. R., Carrapa, B., Clementz, M. T., Quade, J., DeCelles, P. G., & Schoenbohm, L. M. (2014). Early Cenozoic uplift of the Puna Plateau, Central Andes, based on stable isotope paleoaltimetry of hydrated volcanic glass. *Geology, 42*(5), 447-450. doi:https://doi.org/101130/G35239.1

Carosi, R., Montomoli, C., Rubatto, D., Visoná, D. (2010). Late Oligocene high-temperature shear zones in the core of the Higher Himalayan Crystallines (lower Dolpo, Western Nepal). *Tectonics, 29*. doi:https://doi.org/10.1029/2008TC002400

Castellarin, A., & Cantelli, L. (2000). Neo-Alpine evolution of the southern Eastern Alps. *Journal of Geodynamics, 30*(1-2), 251-274. doi:https://doi.org/10.1016/j.tecto.2005.10.019

Castellarin, A., Vai, G. B., & Cantelli, L. (2006). The Alpine evolution of the Southern Alps around the Giudicarie faults: A Late Cretaceous to Early Eocene transfer zone. *Tectonophysics, 414*(1), 203-223. doi:https://doi.org/10.1016/j.tecto.2005.10.019

Cawood, P. A., & Botsford, J. W. (1991). Facies and structural contrasts across Bonne Bay cross-strike discontinuity, western Newfoundland. *American Journal of Science, 291*(8), 737-759. doi:https://doi.org/10.2475/ajs.291.8.737

Cembrano, J., Hervé, F., & Lavenu, A. (1996). The Liquiñe Ofqui fault zone: a long-lived intra-arc fault system in southern Chile. *Tectonophysics, 259*(1-3), 55-66. doi:https://doi.org/10.1016/0040-1951(95)00066-6

Chapin, C. E. (2012). Origin of the Colorado mineral belt. *Geosphere, 8*(1), 28-43. doi:https://doi.org/10.1130/GES00694.1

Chapple, W. M. (1978). Mechanics of thin-skinned fold-and-thrust belts. *Geological Society of America Bulletin, 89*(8), 1189-1198. doi:https://doi.org/10.1130/0016-7606(1978)89<1189:MOTFB>2.0.CO;2

Chatzaras, V., Xypolias, P., Kokkalas, S., & Koukouvelas, I. (2013). Tectonic evolution of a crustal-scale oblique ramp, Hellenides thrust belt, Greece. *Journal of Structural Geology, 57*, 16-37. doi:https://doi.org/10.1016/j.jsg.2013.10.003

Chauvet, A., Onézime, J., Charvet, J., & Barbanson, L. (2004). Syn-to late-tectonic stockwork emplacement within the spanish section of the iberian pyrite belt: Structural, textural, and mineralogical constraints in the tharsis and la zarza areas. *Economic Geology, 99*(8), 1781-1792. doi:https://doi.org/10.2113/gsecongeo.99.8.1781

Chen, Y.-W., Wu, J., & Suppe, J. (2019). Southward propagation of Nazca subduction along the Andes. *Nature, 565*(7740), 441-447. doi:https://doi.org/10.1038/s41586-018-0860-1

Ching, K.-E., Johnson, K. M., Rau, R.-J., Chuang, R. Y., Kuo, L.-C., & Leu, P.-L. (2011). Inferred fault geometry and slip distribution of the 2010 Jiashian, Taiwan, earthquake is consistent with a thick-skinned deformation model. *Earth and Planetary Science Letters, 301*(1-2), 78-86. doi:https://doi.org/10.1016/j.epsl.2010.10.021

Ching, K.-E., Rau, R.-J., Lee, J.-C., & Hu, J.-C. (2007). Contemporary deformation of tectonic escape in SW Taiwan from GPS observations, 1995–2005. *Earth and Planetary Science Letters, 262*(3-4), 601-619. doi:https://doi.org/10.1016/j.epsl.2007.08.017

1469 Colman-Sadd, S. P. (1978). Fold development in Zagros simply folded belt, Southwest Iran.
1470 *AAPG Bulletin, 62*(6), 984-1003. doi:https://doi.org/10.1306/C1EA4F81-16C9-11D7-
1471 8645000102C1865D
1472 Colman-Sadd, S. P., Cawood, P. A., Dunning, G. R., Hall, J. M., Kean, B. F., O'Brien, B. H., &
1473 O'Brien, S. J. (1992). *Lithoprobe East in Newfoundland (Burgeo Transect): A cross-*
1474 *section through the southwest New- foundland Appalachians* (Vol. 92-A7).
1475 Coltorti, M., Farabollini, P., Gentili, B., & Pambianchi, G. (1996). Geomorphological evidence
1476 for anti-Apennine faults in the Umbro-Marchean Apennines and in the peri-Adriatic
1477 basin, Italy. *Geomorphology, 15*(1), 33-45. doi:https://doi.org/10.1016/0169-
1478 555X(95)00117-N
1479 Coney, P. J., & Reynolds, S. J. (1977). Cordilleran benioff zones. *Nature, 270*(5636), 403-406.
1480 doi:https://doi.org/10.1038/270403a0
1481 Constenius, K. N. (1996). Late Paleogene extensional collapse of the Cordilleran foreland fold
1482 and thrust belt. *Geological Society of America Bulletin, 108*(1), 20-39.
1483 doi:https://doi.org/10.1130/0016-7606(1996)108<0020:LPECOT>2.3.CO;2
1484 Cook, B. S., & Thomas, W. A. (2009). Superposed lateral ramps in the Pell City thrust sheet,
1485 Appalachian thrust belt, Alabama. *Journal of Structural Geology, 31*(9), 941-949.
1486 doi:https://doi.org/10.1016/j.jsg.2009.06.001
1487 Cooley, M. A., Price, R. A., Dixon, J. M., & Kyser, T. K. (2011). Along-strike variations and
1488 internal details of chevron-style, flexural-slip thrust-propagation folds within the southern
1489 Livingstone Range anticlinorium, a paleohydrocarbon reservoir in southern Alberta
1490 Foothills, Canada. *AAPG Bulletin, 95*(11), 1821-1849.
1491 doi:https://doi.org/10.1306/01271107097
1492 Corbett, G. J. (1994). *Regional structural control of selected Cu/Au occurrences in Papua New*
1493 *Guinea.* Paper presented at the Proceedings of the Papua New Guinea Geology,
1494 Exploration and Mining Conference, Melbourne.
1495 Cotton, J. T., & Koyi, H. A. (2000). Modeling of thrust fronts above ductile and frictional
1496 detachments: Application to structures in the Salt Range and Potwar Plateau, Pakistan.
1497 *Geological Society of America Bulletin, 112*(3), 351-363.
1498 doi:https://doi.org/10.1130/0016-7606(2000)112<351:MOTFAD>2.0.CO;2
1499 Coutand, I., Cobbold, P. R., de Urreiztieta, M., Gautier, P., Chauvin, A., Gapais, D., Rossello, E.
1500 A., & López-Gamundí, O. (2001). Style and history of Andean deformation, Puna
1501 plateau, northwestern Argentina. *Tectonics, 20*(2), 210-234.
1502 doi:https://doi.org/10.1029/2000TC900031
1503 Dahl, P. S., Holm, D. K., Gardner, E. T., Hubacher, F. A., & Foland, K. A. (1999). New
1504 constraints on the timing of Early Proterozoic tectonism in the Black Hills (South
1505 Dakota), with implications for docking of the Wyoming province with Laurentia.
1506 *Geological Society of America Bulletin, 111*(9), 1335-1349.
1507 doi:https://doi.org/10.1130/0016-7606(1999)111<1335:NCOTTO>2.3.CO;2
1508 Dahlen, F. A. (1990). Critical taper model of fold-and-thrust belts and accretionary wedges.
1509 *Annual Review of Earth and Planetary Sciences, 18*(1), 55-99.
1510 doi:https://doi.org/10.1146/annurev.ea.18.050190.000415
1511 Davies, H. L. (1991). *Regional geologic setting of some mineral deposits of the New Guinea*
1512 *Orogen.* Paper presented at the Papua New Guinea Geology, Exploration and Mining
1513 Conference; Rabaul, Papua New Guinea, 1991.

1514 DeCelles, P. G. (2004). Late Jurassic to Eocene evolution of the Cordilleran thrust belt and
1515 foreland basin system, western USA. *American Journal of Science, 304*(2), 105-168.
1516 doi:https://doi.org/10.2475/ajs.304.2.105
1517 DeCelles, P. G., Carrapa, B., Ojha, T. P., Gehrels, G. E., & Collins, D. (2020). Structural and
1518 thermal evolution of the Himalayan thrust belt in midwestern Nepal. *Geological Society*
1519 *of America Special Paper, 547*, 1-77. doi:https://doi.org/10.1130/2020.2547(01)
1520 Decelles, P. G., Gray, M., Ridgway, K., Cole, R., Pivnik, D., Pequera, N., & Srivastava, P.
1521 (1991). Controls on synorogenic alluvial-fan architecture, Beartooth Conglomerate
1522 (Palaeocene), Wyoming and Montana. *Sedimentology, 38*(4), 567-590.
1523 doi:https://doi.org/10.1111/j.1365-3091.1991.tb01009.x
1524 DeCelles , P. G., Robinson, D. M., Quade, J., Ojha, T. P., Garzione, C. N., Copeland, P., & N.,
1525 U. B. (2001). Stratigraphy, structure, and tectonic evolution of the Himalayan fold-thrust
1526 belt in western Nepal. *Tectonics, 20*, 487-509. doi:https://doi.org/10.1029/2000TC001226
1527 Deffontaines, B., Lacombe, O., Angelier, J., Chu, H., Mouthereau, F., Lee, C., Deramond, J.,
1528 Lee, J., Yu, M., & Liew, P. (1997). Quaternary transfer faulting in the Taiwan Foothills:
1529 evidence from a multisource approach. *Tectonophysics, 274*(1-3), 61-82.
1530 doi:https://doi.org/10.1016/S0040-1951(96)00298-3
1531 Dewey, J. F., & Bird, J. M. (1970). Mountain belts and the new global tectonics. *Journal of*
1532 *Geophysical Research, 75*(14), 2625-2647. doi:https://doi.org/10.1029/JB075i014p02625
1533 Dewey, J. F., Holdsworth, R. E., & Strachan, R. A. (1998). Transpression and transtension
1534 zones. In R. E. Holdworth, R. A. Strachan, & J. F. Dewey (Eds.), *Continental*
1535 *Transpressional and Transtensional Tectonics* (Vol. 135, pp. 1-14): Geological Society,
1536 London, Special Publications.
1537 Dickinson, W. R. (2004). Evolution of the North American cordillera. *Annual Reviwe of Earth*
1538 *and Planetary Sciences, 32*, 13-45.
1539 doi:https://doi.org/10.1146/annurev.earth.32.101802.120257
1540 Dickinson, W. R., & Snyder, W. S. (1978). Plate tectonics of the Laramide orogeny. In V. W.
1541 Matthews (Ed.), *Laramide folding associated with block faulting in the Western United*
1542 *States* (Vol. 151, pp. 355-366): Geoloical Society of America Memoir.
1543 Diehl, T., Singer, J., Hetényi, G., Grujic, D., Clinton, J., Giardini, D., Kissling,E., GANSSER
1544 Working Group. (2017). Seismotectonics of Bhutan: Evidence for segmentation of the
1545 Eastern Himalayas and link to foreland deformation. *Earth and Planetary Science*
1546 *Letters, 471*, 54-65. doi:https://doi.org/10.1016/j.epsl.2017.04.038
1547 Dini, A., Westerman, D., Innocenti, F., & Rocchi, S. (2008). Magma emplacement in a transfer
1548 zone: the Miocene mafic Orano dyke swarm of Elba Island, Tuscany, Italy. *Geological*
1549 *Society, London, Special Publications, 302*(1), 131-148.
1550 doi:https://doi.org/10.1144/SP302.10
1551 Divyadarshini, A. a. S., Vi. (2019). Investigating topographic metrics to decipher structural
1552 model and morphotectonic evolution of the Frontal Siwalik Ranges, Central Himalaya,
1553 Nepal. *Geomorphology, 337*, 31-52. doi:10.1016/j.geomorph.2019.03.028
1554 Domeier, M. (2016). A plate tectonic scenario for the Iapetus and Rheic oceans. *Gondwana*
1555 *Research, 36*, 275-295. doi:https://doi.org/10.1016/j.gr.2015.08.003
1556 Doutsos, T., Koukouvelas, I., & Xypolias, P. (2006). A new orogenic model for the External
1557 Hellenides. In A. H. F. Robertson & D. Mountrakis (Eds.), *Tectonic development of the*
1558 *Eastern Mediterranean Region* (Vol. 260, pp. 507-520): Geological Society, London,
1559 Special Publications.

1560 Drahovzal, J. A., & Thomas, W. A. (1976). *Cross-strike structural discontinuities in the*
1561 *Appalachians of Alabama: Geological Society of America Abstracts with Programs* (Vol.
1562 8).
1563 Drake, A. A. J., Sinha, A. K., Larid, J., & Guy, R. E. (1989). The Taconian Orogen. In R. D.
1564 Hatcher Jr, W. A. Thomas, & G. W. Viele (Eds.), *The Appalachian-Ouachita Orogen in*
1565 *the United States, The Geology of North America* (Vol. F-2, pp. 101-177): Geological
1566 Society of America.
1567 Drukpa, D., Velasco, A.A., Doser, D. (2006). Seismicity in the Kingdom of Bhutan (1937–
1568 2003): Evidence for crustal transcurrent deformation. *Journal of Geophysical Research,*
1569 *111*, B06301. doi:https://doi/org/10.1029/2004JB003087
1570 Dubey, A. K., Mishra, R and Bhakuni, S.S. (2001). Erratic shortening from balanced cross
1571 sections of the western Himalayan foreland basin causes and implications for basin
1572 evolution. *Journal of Asian Earth Sciences, 19*, 765-777.
1573 doi:https://doi.org/10.1016/S1367-9120(01)00010-4
1574 Duncan, C., Masek, J., & Fielding, E. (2003). How steep are the Himalaya? Characteristics and
1575 implications of along-strike topographic variations. *Geology, 31*(1), 75-78.
1576 doi:https://doi.org/10.1130/0091-7613(2003)031<0075:HSATHC>2.0.CO;2
1577 Dunkl, I., Kuhlemann, J., Reinecker, J., & Frisch, W. (2005). Cenozoic relief evolution of the
1578 Eastern Alps—constraints from apatite fission track age-provenance of Neogene
1579 intramontane sediments. *Austrian Journal of Earth Sciences, 98*, 92-105.
1580 Duvall, M. J., Waldron, J.W.F., Godin, L., Najman, Y. (2020). Active strike-slip faults and an
1581 outer frontal thrust in the Himalayan foreland basin. *Proceedings of the National*
1582 *Academy of Sciences, 117*(30), 17615-17621.
1583 doi:https://doi.org/10.1073/pnas.2001979117
1584 Edey, A., Allen, M., & Nilfouroushan, F. (2020). Kinematic variation within the Fars Arc,
1585 eastern Zagros, and the development of fold-and-thrust belt curvature. *Tectonics, 39*(8),
1586 e2019TC005941. doi:https://doi.org/10.1029/2019TC005941
1587 Egbue, O., & Kellogg, J. (2010). Pleistocene to present North Andean "escape". *Tectonophysics,*
1588 *489*(1-4), 248-257. doi:https://doi.org/10.1016/j.tecto.2010.04.021
1589 Elliott, D. (1976). The motion of thrust sheets. *Journal of Geophysical Research, 81*(5), 949-963.
1590 doi:https://doi.org/10.1029/JB081i005p00949
1591 Elter, F. M., Piero, E., Claudio, E., Elena, E., Katharina, K. R., Matteo, P., & Stefano, S. (2011).
1592 Strike-slip geometry inferred from the seismicity of the Northern-Central Apennines
1593 (Italy). *Journal of Geodynamics, 52*(5), 379-388.
1594 doi:https://doi.org/10.1016/j.jog.2011.03.003
1595 Eugster, P., Thiede, R.C., Scherler, D., Stubner, K., Sobel, E.R., Strecker, M.R. (2018).
1596 Segmentation of the Main Himalayan Thrust Revealed by Low-Temperature
1597 Thermochronometry in the Western Indian Himalaya. *Tectonics, 37*, 2710-2726.
1598 doi:https://doi.org/10.1029/2017TC004752
1599 Fakhari, M. D., Axen, G. J., Horton, B. K., Hassanzadeh, J., & Amini, A. (2008). Revised age of
1600 proximal deposits in the Zagros foreland basin and implications for Cenozoic evolution
1601 of the High Zagros. *Tectonophysics, 451*(1-4), 170-185.
1602 doi:https://doi.org/10.1016/j.tecto.2007.11.064
1603 Falcon, N. L. (1974). Southern Iran: Zagros Mountains. *Geological Society, London, Special*
1604 *Publications, 4*(1), 199-211. doi:https://doi.org/10.1144/GSL.SP.2005.004.01.11

1605 Farzipour-Saein, A., Nilfouroushan, F., & Koyi, H. (2013). The effect of basement
1606 step/topography on the geometry of the Zagros fold and thrust belt (SW Iran): an analog
1607 modeling approach. *International Journal of Earth Sciences, 102*(8), 2117-2135.
1608 doi:https://doi.org/10.1007/s00531-013-0921-5
1609 Fermor, P. (1999). Aspects of the three-dimensional structure of the Alberta Foothills and Front
1610 Ranges. *GSA bulletin, 111*(3), 317-346. doi:https://doi.org/10.1130/0016-
1611 7606(1999)111<0317:AOTTDS>2.3.CO;2
1612 Festa, A., Balestro, G., Borghi, A., De Caroli, S., & Succo, A. (2020). The role of structural
1613 inheritance in continental break-up and exhumation of Alpine Tethyan mantle (Canavese
1614 Zone, Western Alps). *Geoscience Frontiers, 11*(1), 167-188.
1615 doi:https://doi.org/10.1016/j.gsf.2018.11.007
1616 Fiigenschuh, B., Seward, D., & Mancktelow, N. (1997). Exhumation in a convergent orogen: the
1617 western Tauern window. *Terra nova, 9*(5-6), 213-217. doi:https://doi.org/10.1111/j.1365-
1618 3121.1997.tb00015.x
1619 Folguera, A., Ramos, V. A., Hermanns, R. L., & Naranjo, J. (2004). Neotectonics in the foothills
1620 of the southernmost central Andes (37–38 S): Evidence of strike-slip displacement along
1621 the Antiñir-Copahue fault zone. *Tectonics, 23*(5).
1622 doi:https://doi.org/10.1029/2003TC001533
1623 Fondriest, M., Aretusini, S., Di Toro, G., & Smith, S. A. (2015). Fracturing and rock
1624 pulverization along an exhumed seismogenic fault zone in dolostones: The Foiana Fault
1625 Zone (Southern Alps, Italy). *Tectonophysics, 654*, 56-74.
1626 doi:http://dx.doi.org/10.1016/j.tecto.2015.04.015
1627 Foo, W. K. (1979). *Evolution of transverse structures linking the Purcell Anticlinorium to the*
1628 *western Rocky Mountains near Canal Flats, British Columbia.* (MSc). Queen's
1629 University, Kingston,
1630 Foster, D. A., Doughty, P. T., Kalakay, T. J., Fanning, C. M., Coyner, S., Grice, W. C., & Vogl,
1631 J. (2007). Kinematics and timing of exhumation of metamorphic core complexes along
1632 the Lewis and Clark fault zone, northern Rocky Mountains, USA. *Special Papers-*
1633 *Geological Society of America, 434*, 207. doi:https://doi.org/10.1130/2007.2434(10)
1634 Foster, D. A., Mueller, P. A., Mogk, D. W., Wooden, J. L., & Vogl, J. J. (2006). Proterozoic
1635 evolution of the western margin of the Wyoming craton: Implications for the tectonic and
1636 magmatic evolution of the northern Rocky Mountains. *Canadian Journal of Earth*
1637 *Sciences, 43*(10), 1601-1619. doi:https://doi.org/10.1139/E06-052
1638 Frisch, W., Kuhlemann, J., Dunkl, I., & Brügel, A. (1998). Palinspastic reconstruction and
1639 topographic evolution of the Eastern Alps during late Tertiary tectonic extrusion.
1640 *Tectonophysics, 297*(1-4), 1-15. doi:https://doi.org/10.1016/S0040-1951(98)00160-7
1641 Gaetani, M., Gianotti, R., Jadoul, F., Ciarapica, G., & Cirilli, S. (1986). Carbonifero superiore,
1642 Permiano et Triassico nell'area Lariana. *Memorie della Società Geologica Italiana, 32*, 5-
1643 48. doi:http://pascal-
1644 francis.inist.fr/vibad/index.php?action=getRecordDetail&idt=7204188
1645 Galliski, M., & Viramonte, J. (1988). The Cretaceous paleorift in northwestern Argentina: a
1646 petrologic approach. *Journal of South American earth sciences, 1*(4), 329-342.
1647 doi:https://doi.org/10.1016/0895-9811(88)90021-1
1648 Gansser, A. (1964). *Geology of the Himalayas*. New York: Wiley Interscience.
1649 Gaupp, R., & Batten, D. (1983). Depositional setting of middle to Upper Cretaceous sediments in
1650 the Northern Calcareous Alps from palynological evidence. *Neues Jahrbuch für Geologie*

und Paläontologie-Monatshefte, 585-600. doi:https://doi.org/10.1127/njgpm/1983/1983/585

Ghiglione, M. C., Suarez, F., Ambrosio, A., Da Poian, G., Cristallini, E. O., Pizzio, M. F., & Reinoso, R. M. (2009). Structure and evolution of the Austral Basin fold-thrust belt, southern Patagonian Andes. *Revista de la Asociación Geológica Argentina, 65*(1), 215-226.

Giambiagi, L., Mescua, J., Bechis, F., Tassara, A., & Hoke, G. (2012). Thrust belts of the southern Central Andes: Along-strike variations in shortening, topography, crustal geometry, and denudation. *Bulletin, 124*(7-8), 1339-1351. doi:https://doi.org/10.1130/B30609.1

Gifford, J. N., Mueller, P. A., Foster, D. A., & Mogk, D. W. (2014). Precambrian crustal evolution in the Great Falls tectonic zone: Insights from xenoliths from the Montana Alkali Province. *The Journal of Geology, 122*(5), 531-548. doi:https://doi.org/10.1086/677262

Gillis, R. J., Horton, B. K., & Grove, M. (2006). Thermochronology, geochronology, and upper crustal structure of the Cordillera Real: Implications for Cenozoic exhumation of the central Andean plateau. *Tectonics, 25*(6). doi:https://doi.org/10.1029/2005TC001887

Godin, L., & Harris, L. B. (2014). Tracking basement cross-strike discontinuities in the Indian crust beneath the Himalayan orogen using gravity data – relationship to upper crustal faults. *Geophysical Journal International, 198*, 198-215. doi:https://doi.org/10.1093/gji/ggu131

Goldfinger, C., Kulm, L.D., Yeats, R.S., McNeill, L., and Hummon, C. (1997). Oblique strike-slip faulting of the central Cascadia submarine forearc. *Journal of Geophysical Research, 102*(B4), 8217-8243. doi:https://doi.org/10.1029/96JB02655

Graindorge, D., Klingelhoefer, F., Sibuiet, J.C., McNeill, L., Henstock, T., Dean, S., Gutscher, M., Dessa, J.X., Permana, H., and 15 others. (2008). Impact of lower plate structure on upper plate deformation at the NW Sumatran convergent margin from seafloor morphology. *Earth and Planetary Science Letters, 275*, 201-210. doi:https://doi.org/10.1016/j.epsl.2008.04.053

Grosjean, G., Sue, C., & Burkhard, M. (2004). Late Neogene extension in the vicinity of the Simplon fault zone (central Alps, Switzerland). *Eclogae Geologicae Helvetiae, 97*(1), 33-46. doi:https://doi.org/10.1007/s00015-004-1114-9

Grujic, D., Hollister, L.S., and Parrish, R.P. (2002). Himalayan metamorphic sequence as an orogenic channel: Insight from Bhutan. *Earth and Planetary Science Letters, 198*, 177-191. doi:https://doi.org/10.1016S0012-821X(02)00482-X.

Guillot, S., Mahéo, G., De Sigoyer, J., Hattori, K., & Pecher, A. (2008). Tethyan and Indian subduction viewed from the Himalayan high-to ultrahigh-pressure metamorphic rocks. *Tectonophysics, 451*(1-4), 225-241. doi:https://doi.org/10.1016/j.tecto.2007.11.059

Gutscher, M. A., Spakman, W., Bijwaard, H., & Engdahl, E. R. (2000). Geodynamics of flat subduction: Seismicity and tomographic constraints from the Andean margin. *Tectonics, 19*(5), 814-833. doi:https://doi.org/10.1029/1999TC001152

Handy, M. R., Schmid, S. M., Bousquet, R., Kissling, E., & Bernoulli, D. (2010). Reconciling plate-tectonic reconstructions of Alpine Tethys with the geological–geophysical record of spreading and subduction in the Alps. *Earth-Science Reviews, 102*(3-4), 121-158. doi:https://doi.org/10.1007/s00531-014-1060-3

1696 Harrison, J., & Bally, A. (1988). Cross-sections of the Parry Islands fold belt on Melville Island,
1697 Canadian Arctic Islands: Implications for the timing and kinematic history of some thin-
1698 skinned decollement systems. *Bulletin of Canadian Petroleum Geology, 36*(3), 311-332.
1699 Harrison, J. E., Griggs, A. B., & Wells, J. D. (1974). *Tectonic features of the Precambrian Belt*
1700 *basin and their influcence on post-Belt structures* (Vol. 886): United States Geological
1701 Survey Professional Paper.
1702 Harvey, J. E., Burbank, D.W., Bookhagen, B. (2015). Along-strike changes in Himalayan thrust
1703 geometry: Topographic and tectonic discontinuities in western Nepal. *Lithosphere, 7*(5),
1704 511-518. doi:https://doi.org/10.1130/L444.1
1705 Hatcher, J. R. D. (1972). Developmental model for the southern Appalachians. *Geological*
1706 *Society of America Bulletin, 83*(9), 2735-2760.
1707 Hatcher, J. R. D. (2010). The Appalachian orogen: A brief summary. In R. P. Tollo, M. J.
1708 Bartholomew, J. P. Hibbard, & P. M. Karabinos (Eds.), *From Rodinia to Pangea: The*
1709 *Lithotectonic Record of the Appalachian Region: Geological Society of America Memoir*
1710 *206* (pp. 1-19).
1711 Hatcher, J. R. D., Thomas, W. A., Geiser, P. A., Snoke, A. W., Mosher, S., & Wiltschko, D. V.
1712 (1989). Alleghanian orogen. In R. D. Hatcher Jr, W. A. Thomas, & G. W. Viele (Eds.),
1713 *The Appalachian-Ouachita Orogen in the United States, The Geology of North America*
1714 (Vol. F-2, pp. 233-319): Geological Society of America.
1715 Hauck, M. L., Nelson, K.D., Brown, L.D., Wenjin, Z., and Ross, A.R. (1998). Crustal structure
1716 of the Himalayan orogen at ~90° east longitude from Project INDEPTH deep reflection
1717 profiles. *Tectonics, 17*, 481-500. doi:https://doi.org/10.1029/98TC01314
1718 Haynes, S. J., & McQuillan, H. (1974). Evolution of the Zagros suture zone, southern Iran.
1719 *Geological Society of America Bulletin, 85*(5), 739-744. doi:https://doi.org/10.1130/0016-
1720 7606(1974)85<739:EOTZSZ>2.0.CO;2
1721 Haynes, S. J., & Reynolds, P. (1980). Early development of Tethys and Jurassic ophiolite
1722 displacement. *Nature, 283*(5747), 561-563. doi:https://doi.org/10.1038/283561a0
1723 Hessami, K., Koyi, H. A., & Talbot, C. J. (2001). The significance of strike-slip faulting in the
1724 basement of the Zagros fold and thrust belt. *Journal of petroleum Geology, 24*(1), 5-28.
1725 doi:https://doi.org/10.1111/j.1747-5457.2001.tb00659.x
1726 Hibbard, J. P., van Staal, C. R., Rankin, D. W., & Williams, H. (2006). *Lithotectonic map of the*
1727 *Appalachian orogen, Canada–United States of America, Geological Survey of Canada,*
1728 *Map 2096A, scale 1:1,500,000*.
1729 Hill, K. C., Kendrick, R. D., Crowhurst, P. V., & Gow, P. A. (2002). Copper-gold mineralisation
1730 in New Guinea: Tectonics, lineaments, thermochronology and structure. *Australian*
1731 *Journal of Earth Sciences, 49*(4), 737-752. doi:https://doi.org/10.1046/j.1440-
1732 0952.2002.00944.x
1733 Hodges, K. V. (2000). Tectonics of the Himalaya and southern Tibet from two perspectives.
1734 *Geological Society of America Bulletin, 112*(3), 324-350.
1735 doi:https://doi.org/10.1130/0016-7606(2000)112<324:TOTHAS>2.0.CO;2
1736 Hoffman, P. F. (1988). Early Proterozoic Assembly. *Annual Review of Earth and Planetary*
1737 *Sciences, 6*, 543-603. doi:https://doi.org/10.1146/annurev.ea.16.050188.002551
1738 Hofmann, F., Schlatter, R., & Weh, M. (2000). Erläuterungen zu Blatt 97: Beggingen (LK 1011)
1739 des Geologischen Atlas der Schweiz 1: 25,000. *Bundesamt für Wasser und Geologie,*
1740 *Bern*, 113.

1741 Hogan, J. P., & Gilbert, M. C. (1998). The Southern Oklahoma aulacogen: A Cambrian analog
1742 for Mid-Proterozoic AMCG (anorthosite-mangerite-charnockite-granite) complexes? In
1743 H. J.P. & G. M.C (Eds.), *Basement tectonics 12. Proceedings of the International*
1744 *Conferences on Basement Tectonics* (Vol. 6, pp. 39-78): Springer.
1745 Hope, J., & Eaton, D. (2002). Crustal structure beneath the Western Canada Sedimentary Basin:
1746 constraints from gravity and magnetic modelling. *Canadian Journal of Earth Sciences,*
1747 *39*(3), 291-312. doi:https://doi.org/10.1139/e01-060
1748 Horváth, F., & Cloetingh, S. A. P. L. (1996). Stress-induced late stage subsidence anomalies in
1749 the Pannonian Basin. *Tectonophysics, 266*, 287-300.
1750 Höy, T., & Heyden, P. v. d. (1988). Geochemistry, geochronology, and tectonic implications of
1751 two quartz monzonite intrusions, Purcell Mountains, southeastern British Columbia.
1752 *Canadian Journal of Earth Sciences, 25*(1), 106-115. doi:https://doi.org/10.1139/e88-011
1753 Hubbard, J., Almeida, R., Foster, A., Sapkota, S. N., Burgi, P., & Tapponnier, P. (2016).
1754 Structural segmentation controlled the 2015 MW 7.8 Gorkha earthquake rupture in
1755 Nepal. *Geology, 44*(8), 639-642. doi:https://doi.org/10.1130/G38077.1
1756 Hubbard, M., Gajurel, A. P., Mukul, M., & Seifert, N. (2018). *Cross faults and their role in*
1757 *Himalayan Structural Evolution*. Paper presented at the Geological Society of America
1758 Abstracts with Programs.
1759 Hubbard, M., Mukul, M., Gajurel, A. P., Ghosh, A., Srivastava, V., Giri, B., Seifert, N., &
1760 Mendoza, M. M. (2021). Orogenic Segmentation and Its Role in Himalayan Mountain
1761 Building. *Frontiers in Earth Science, 9*(259).
1762 doi:https://doi.org/10.3389/feart.2021.641666
1763 Hubbard, M. S. (1999). Norumbega fault zone: part of an orogen-parallel strike-slip system,
1764 northern Appalachians. In A. Ludman & D. P. J. West (Eds.), *Normumberga Fault*
1765 *System of the Northern Appalachians* (Vol. 331, pp. 155-166). Boulder, Colorado:
1766 Geological Society of America Special Paper.
1767 Hubbard, M. S., & Mancktelow, N. S. (1992). Lateral displacement during Neogene convergence
1768 in the western and central Alps. *Geology, 20*(10), 943-946.
1769 doi:https://doi.org/10.1130/0091-7613(1992)020<0943:LDDNCI>2.3.CO;2
1770 Hunziker, J. C., Frey, M., Clauer, N., Dallmeyer, R. D., Friedrichsen, H., Flehmig, W.,
1771 Hochstrasser, K., Roggwiler, P. T., & Schwander, H. (1986). The evolution of illite to
1772 muscovite: mineralogical and isotopic data from the Glarus Alps, Switzerland.
1773 *Contributions to Mineralogy and Petrology, 92*(2), 157-180.
1774 doi:https://doi.org/10.1007/BF00375291
1775 Husseini, M. I. (1988). The Arabian infracambrian extensional system. *Tectonophysics, 148*(1-
1776 2), 93-103. doi:https://doi.org/10.1016/0040-1951(88)90163-1
1777 Hyndman, D. W., Alt, D., & Sears, J. W. (1988). Post-Archean metamorphic and tectonic
1778 evolution of western Montana and northern Idaho. In W. G. Ernst (Ed.), *Metamorphism*
1779 *and crustal evolution of the western United States* (Vol. 7, pp. 332-361). Englewood
1780 Cliffs, New Jersey: Prentice Hall.
1781 Hynes, A., & Rivers, T. (2010). Protracted continental collision—Evidence from the Grenville
1782 orogen. *Canadian Journal of Earth Sciences, 47*(5), 591-620.
1783 doi:https://doi.org/10.1139/E10-003
1784 Isacks, B. L. (1988). Uplift of the central Andean plateau and bending of the Bolivian orocline.
1785 *Journal of Geophysical Research: Solid Earth, 93*(B4), 3211-3231.
1786 doi:https://doi.org/10.1029/ JB093iB04p03211

1787 Jackson, J. A. (1980). Reactivation of basement faults and crustal shortening in orogenic belts.
1788 *Nature, 283*(5745), 343-346. doi:https://doi.org/10.1038/283343a0
1789 Jadoon, I. A. K., Lawrence, R. D., & Lillie, R. J. (1994). Seismic data, geometry, evolution, and
1790 shortening in the active Sulaiman fold-and-thrust belt of Pakistan, southwest of the
1791 Himalayas. *AAPG Bulletin, 78*(5), 758-774. doi:https://doi.org/10.1306/A25FE3AB-
1792 171B-11D7-8645000102C1865D
1793 Japas, M. S., Ré, G. H., Oriolo, S., & Vilas, J. F. (2016). Basement-involved deformation
1794 overprinting thin-skinned deformation in the Pampean flat-slab segment of the southern
1795 Central Andes, Argentina. *Geological Magazine, 153*(5-6), 1042-1065.
1796 doi:https://doi.org/10.1017/S001675681600056X
1797 Jessup, M. J., Newell, D. L., Cottle, J. M., Berger, A. L., & Spotila, J. A. (2008). Orogen-parallel
1798 extension and exhumation enhanced by denudation in the trans-Himalayan Arun River
1799 gorge, Ama Drime Massif, Tibet-Nepal. *Geology, 36*(7), 587-590.
1800 doi:https://doi.org/10.1130/g24722a.1
1801 Jordan, T. E., Isacks, B., Ramos, V. A., & Allmendinger, R. W. (1983). Mountain building in the
1802 Central Andes. *Episodes, 3*(3), 20-26.
1803 Joudaki, M., Farzipour-Saein, A., & Nilfouroushan, F. (2016). Kinematics and surface fracture
1804 pattern of the Anaran basement fault zone in NW of the Zagros fold–thrust belt.
1805 *International Journal of Earth Sciences, 105*(3), 869-883.
1806 doi:https://doi.org/10.1007/s00531-015-1209-8
1807 Karlstrom, K. E., & Houston, R. S. (1984). The Cheyenne belt: Analysis of a Proterozoic suture
1808 in southern Wyoming. *Precambrian Research, 25*(4), 415-446.
1809 doi:https://doi.org/10.1016/0301-9268(84)90012-3
1810 Kendrick, E., Bevis, M., Smalley Jr, R., Brooks, B., Vargas, R. B., Lauría, E., & Fortes, L. P. S.
1811 (2003). The Nazca–South America Euler vector and its rate of change. *Journal of South*
1812 *American earth sciences, 16*(2), 125-131. doi:https://doi.org/10.1016/S0895-
1813 9811(03)00028-2
1814 Kent, P. E. (1979). The emergent Hormuz salt plugs of southern Iran. *Journal of petroleum*
1815 *Geology, 2*(2), 117-144. doi:https://doi.org/10.1111/j.1747-5457.1979.tb00698.x
1816 Keppie, J. D., & Krogh, T. E. (1999). U-Pb Geochronology of Devonian Granites in the Meguma
1817 Terrane of Nova Scotia, Canada: Evidence for Hotspot Melting of a Neoproterozoic
1818 Source. *The Journal of Geology, 107*(5), 555-568. doi:10.1086/314369
1819 Khadivi, S., Mouthereau, F., Larrasoaña, J. C., Vergés, J., Lacombe, O., Khademi, E., Beamud,
1820 E., Melinte-Dobrinescu, M., & Suc, J. P. (2010). Magnetochronology of synorogenic
1821 Miocene foreland sediments in the Fars arc of the Zagros Folded Belt (SW Iran). *Basin*
1822 *Research, 22*(6), 918-932. doi:https://doi.org/10.1111/j.1365-2117.2009.00446.x
1823 Kley, J., Rossello, E. A., Monaldi, C. R., & Habighorst, B. (2005). Seismic and field evidence
1824 for selective inversion of Cretaceous normal faults, Salta rift, northwest Argentina.
1825 *Tectonophysics, 399*(1-4), 155-172. doi:https://doi.org/10.1016/j.tecto.2004.12.020
1826 Kokkalas, S., & Doutsos, T. (2004). Kinematics and strain partitioning in the southeast
1827 Hellenides (Greece). *Geological Journal, 39*(2), 121-140.
1828 doi:https://doi.org/10.1002/gj.947
1829 Koop, W. J., & Stoneley, R. (1982). Subsidence history of the Middle East Zagros basin,
1830 Permian to recent. *Philosophical Transactions of the Royal Society A Mathematical and*
1831 *Physical Sciences, 305*(1489), 149-168. doi:https://doi.org/10.1098/rsta.1982.0031

1832 Kralik, M., Klima, K., & Riedmüller, G. (1987). Dating fault gouges. *Nature, 327*(6120), 315-
1833 317. doi:https://doi.org/10.1038/327315a0
1834 Kuiper, Y. D. (2016). Development of the Norumbega fault system in mid-Paleozoic New
1835 England, USA: An integrated subducted oceanic ridge model. *Geology, 44*(6), 455-458.
1836 doi:https://doi.org/10.1130/G37599.1
1837 Kuiper, Y. D., & Wakabayashi, J. (2018). A comparison between mid-Paleozoic New England,
1838 USA, and the modern western USA: Subduction of an oceanic ridge-transform fault
1839 system. *Tectonophysics, 745*, 278-292. doi:https://doi.org/10.1016/j.tecto.2018.08.020
1840 Kwon, S., & Mitra, G. (2004). Strain distribution, strain history, and kinematic evolution
1841 associated with the formation of arcuate salients in fold-thrust belts: The example of the
1842 Provo salient, Sevier orogen, Utah. In A. J. Sussman & A. B. Weil (Eds.), *Orogenic*
1843 *Curvature: Integrating Paleomagnetic and Structural Analyses* (Vol. 383, pp. 205-223):
1844 Geological Society of America Special Paper.
1845 Kwon, S., & Mitra, G. (2006). Three-dimensional kinematic history at an oblique ramp,
1846 Leamington zone, Sevier belt, Utah. *Journal of Structural Geology, 28*(3), 474-493.
1847 doi:https://doi.org/10.1016/j.jsg.2005.12.011
1848 Lacombe, O., Mouthereau, F., Angelier, J., & Deffontaines, B. (2001). Structural, geodetic and
1849 seismological evidence for tectonic escape in SW Taiwan. *Tectonophysics, 333*(1-2),
1850 323-345. doi:https://doi.org/10.1016/S0040-1951(00)00281-X
1851 Lacombe, O., Mouthereau, F., Kargar, S., & Meyer, B. (2006). Late Cenozoic and modern stress
1852 fields in the western Fars (Iran): implications for the tectonic and kinematic evolution of
1853 central Zagros. *Tectonics, 25*(1), 1-27. doi:https://doi.org/10.1029/2005TC001831
1854 Larson, K. P., Cottle, J.M. (2014). Midcrustal discontinuities and the assembly of the
1855 Himalayan midcrust. *Tectonics, 33*, 718-740. doi:https://doi.org/10.1002/2013TC003452
1856 Larson, K. P., Price, R. A., & Archibald, D. A. (2006). Tectonic implications of 40Ar/39Ar
1857 muscovite dates from the Mt. Haley stock and Lussier River stock, near Fort Steele,
1858 British Columbia. *Canadian Journal of Earth Sciences, 43*(11), 1673-1684.
1859 doi:https://doi.org/10.1139/E06-048
1860 Laubscher, H. P. (1971). Das Alpen-Dinariden-Problem und die Palinspastik der südlichen
1861 tethys. *Geologische rundschau, 60*(3), 813-833. doi:https://doi.org/10.1007/BF02046522
1862 Laubscher, H. P. (1985). Large-scale, thin-skinned thrusting in the southern Alps: Kinematic
1863 models. *Geological Society of America Bulletin, 96*(6), 710-718.
1864 doi:https://doi.org/10.1130/0016-7606(1985)96<710:LTTITS>2.0.CO;2
1865 Lawton, T. F., Sprinkel, D. A., Decelles, P. G., Mitra, G., Sussman, A. J., & Weiss, M. P. (1997).
1866 Stratigraphy and structure of the Sevier thrust belt and proximal foreland-basin system in
1867 central Utah: A transect from the Sevier Desert to the Wasatch Plateau. In K. P. Link &
1868 B. J. Kowallis (Eds.), *Brigham Young University Geology Studies Field Trip Guide Book,*
1869 *Part 2* (Vol. 42, pp. 33-68): Geological Society of America Annual Meeting.
1870 Le Garzic, E., Vergés, J., Sapin, F., Saura, E., Meresse, F., & Ringenbach, J. (2019). Evolution
1871 of the NW Zagros Fold-and-Thrust Belt in Kurdistan Region of Iraq from balanced and
1872 restored crustal-scale sections and forward modeling. *Journal of Structural Geology, 124*,
1873 51-69. doi:https://doi.org/10.1016/j.jsg.2019.04.006
1874 Leier, A., McQuarrie, N., Garzione, C., & Eiler, J. (2013). Stable isotope evidence for multiple
1875 pulses of rapid surface uplift in the Central Andes, Bolivia. *Earth and Planetary Science*
1876 *Letters, 371*, 49-58. doi:https://doi.org/10.1016/j.epsl.2013.04.025

Lemieux, S., Ross, G. M., & Cook, F. A. (2000). Crustal geometry and tectonic evolution of the Archean crystalline basement beneath the southern Alberta Plains, from new seismic reflection and potential-field studies. *Canadian Journal of Earth Sciences, 37*(11), 1473-1491. doi:https://doi.org/10.1139/e00-065

Li, Z. X., Bogdanova, S. V., Collins, A. S., Davidson, A., De Waele, B., Ernst, R. E., Fitzsimons, I. C. W., Fuck, R. A., Gladkochub, D. P., Jacobs, J., Karlstrom, K. E., Lu, S., Natapov, L. M., Pease, V., Pisarevsky, S. A., Thrane, K., & Vernikovsky, V. (2008). Assembly, configuration, and break-up history of Rodinia: A synthesis. *Precambrian Research, 160*(1), 179-210. doi:https://doi.org/10.1016/j.precamres.2007.04.021

Likerman, J., Burlando, J. F., Cristallini, E. O., & Ghiglione, M. C. (2013). Along-strike structural variations in the Southern Patagonian Andes: insights from physical modeling. *Tectonophysics, 590*, 106-120. doi:https://doi.org/10.1016/j.tecto.2013.01.018

Lin, S., Staal, C. R. v., & Dubé, B. t. (1994). Promontory-promontory collision in the Canadian Appalachians. *Geology, 22*(10), 897-900. doi:https://doi.org/10.1130/0091-7613(1994)022<0897:PPCITC>2.3.CO;2

Linzer, H.-G., Ratschbacher, L., & Frisch, W. (1995). Transpressional collision structures in the upper crust: the fold-thrust belt of the Northern Calcareous Alps. *Tectonophysics, 242*(1-2), 41-61. doi:https://doi.org/10.1016/0040-1951(94)00152-Y

Llambías, E. J., Kleinman, L. E., & Salvarradi, J. A. (1993). El magmatismo Gondwánico. In V. Ramos (Ed.), *Rela- torio Geología y Recursos Naturales de Mendoza* (Vol. 1, pp. 53-64). Buenos Aires: Servicio Geológico Minero Argentino (SEGEMAR).

Long, S., McQuarrie, N., Tobgay, T., Grujic, D. (2011). Geometry and crustal shortening of the Himalayan fold-thrust belt, eastern and central Bhutan. *Geological Society of America Bulletin, 123*(7/8), 1427-1447. doi:https://doi.org/10.1130/B30203.1

Lupi, M., Trippanera, D., Gonzalez, D., D'amico, S., Acocella, V., Cabello, C., Stef, M. M., & Tassara, A. (2020). Transient tectonic regimes imposed by megathrust earthquakes and the growth of NW-trending volcanic systems in the Southern Andes. *Tectonophysics, 774*, 228204. doi:https://doi.org/10.1016/j.tecto.2019.228204

Mahoney, L., Hill, K., McLaren, S., & Hanani, A. (2017). Complex fold and thrust belt structural styles: Examples from the Greater Juha area of the Papuan Fold and Thrust Belt, Papua New Guinea. *Journal of Structural Geology, 100*, 98-119. doi:https://doi.org/10.1016/j.jsg.2017.05.010

Malekzade, Z., Bellier, O., Abbassi, M. R., Shabanian, E., & Authemayou, C. (2016). The effects of plate margin inhomogeneity on the deformation pattern within west-Central Zagros Fold-and-Thrust Belt. *Tectonophysics, 693*, 304-326. doi:http://dx.doi.org/10.1016/j.tecto.2016.01.030

Malusà, M. G. (2004). *Post-metamorphic evolution of the Western Alps: kinematic constraints from a multidisciplinary approach.* (PhD). University of Turin, Turin, Italy.

Mancktelow, N., Zwingmann, H., Campani, M., Fügenschuh, B., & Mulch, A. (2015). Timing and conditions of brittle faulting on the Silltal-Brenner fault zone, Eastern Alps (Austria). *Swiss Journal of Geosciences, 108*(2-3), 305-326. doi:https://doi.org/10.1007/s00015-015-0179-y

Mancktelow, N. S. (1992). Neogene lateral extension during convergence in the Central Alps: evidence from interrelated faulting and backfolding around the Simplonpass (Switzerland). *Tectonophysics, 215*(3-4), 295-317. doi:https://doi.org/10.1016/0040-1951(92)90358-D

1923 Mancktelow, N. S., Stöckli, D. F., Grollimund, B., Müller, W., Fügenschuh, B., Viola, G.,
1924 Seward, D., & Villa, I. M. (2001). The DAV and Periadriatic fault systems in the Eastern
1925 Alps south of the Tauern window. *International Journal of Earth Sciences, 90*(3), 593-
1926 622. doi:https://doi.org/10.1007/s005310000190
1927 Manea, V. C., Pérez-Gussinyé, M., & Manea, M. (2012). Chilean flat slab subduction controlled
1928 by overriding plate thickness and trench rollback. *Geology, 40*(1), 35-38.
1929 doi:10.1130/g32543.1
1930 Marshak, S., & Wilkerson, M. S. (1992). Effect of overburden thickness on thrust belt geometry
1931 and development. *Tectonics, 11*(3), 560-566. doi:https://doi.org/10.1029/92TC00175
1932 McGugan, A. (1987). "Horses" and transverse faults in the Lewis thrust sheet, Elk range,
1933 Kananaskis valley, Rocky mountain front ranges, Southwestern Alberta. *Bulletin of*
1934 *Canadian Petroleum Geology, 35*(3), 358-361.
1935 doi:https://doi.org/10.35767/gscpgbull.35.3.358
1936 McMechan, M. (2001). Large-scale duplex structures in the McConnell thrust sheet, Rocky
1937 Mountains, Southwest Alberta. *Bulletin of Canadian Petroleum Geology, 49*(3), 408-425.
1938 doi:https://doi.org/10.2113/49.3.408
1939 McMechan, M. (2007). Nature, origin and tectonic significance of anomalous transverse
1940 structures, southeastern Skeena Fold Belt, British Columbia. *Bulletin of Canadian*
1941 *Petroleum Geology, 55*(4), 262-274. doi:https://doi.org/10.2113/gscpgbull.55.4.262
1942 McMechan, M. E. (2000). Walker Creek fault zone, central Rocky Mountains, British
1943 Columbia—southern continuation of the Northern Rocky Mountain Trench fault zone.
1944 *Canadian Journal of Earth Sciences, 37*(9), 1259-1273. doi:https://doi.org/10.1139/e00-
1945 038
1946 McMechan, M. E. (2012). Deep transverse basement structural control of mineral systems in the
1947 southeastern Canadian Cordillera. *Canadian Journal of Earth Sciences, 49*(5), 693-708.
1948 doi:https://doi.org/10.1139/E2012-013
1949 McMechan, M. E., & Price, R. A. (1982). Transverse folding and superposed deformation,
1950 Mount Fisher area, southern Canadian Rocky Mountain thrust and fold belt. *Canadian*
1951 *Journal of Earth Sciences, 19*(5), 1011-1024. doi:https://doi.org/10.1139/e82-084
1952 McQuarrie, N. (2004). Crustal scale geometry of the Zagros fold–thrust belt, Iran. *Journal of*
1953 *Structural Geology, 26*(3), 519-535. doi:https://doi.org/10.1016/j.jsg.2003.08.009
1954 McQuarrie, N., Stock, J. M., Verdel, C., & Wernicke, B. P. (2003). Cenozoic evolution of
1955 Neotethys and implications for the causes of plate motions. *Geophysical Research*
1956 *Letters, 30*(20). doi: https://doi.org/10.1029/2003GL017992
1957 McQuarrie, N., & van Hinsbergen, D. J. J. (2013). Retrodeforming the Arabia-Eurasia collision
1958 zone: Age of collision versus magnitude of continental subduction. *Geology, 41*(3), 315-
1959 318. doi:https://doi.org/10.1130/G33591.1
1960 McQuillan, H. (1991). The role of basement tectonics in the control of sedimentary facies,
1961 structural patterns and salt plug emplacements in the Zagros fold belt of southwest Iran.
1962 *Journal of Southeast Asian Earth Sciences, 5*(1-4), 453-463.
1963 doi:https://doi.org/10.1016/0743-9547(91)90061-2
1964 Mendoza, M. M., Ghosh, A., Karplus, M.S., Klemperer, S.L., Sapkota, S.N., Adhikari, L.B.,
1965 Velasco, A. (2019). Duplex in the Main Himalayan Thrust illuminated by aftershocks of
1966 the 2015 Mw 7.8 Gorkha earthquake. *Nature geoscience, 12*, 1018-1022.
1967 doi:https://doi.org/10.1038/s41561-019-0474-8

1968 Mescua, J. F., & Giambiagi, L. B. (2012). Fault inversion vs. new thrust generation: a case study
1969 in the Malargüe fold-and-thrust belt, Andes of Argentina. *Journal of Structural Geology,*
1970 *35*, 51-63. doi:https://doi.org/10.1016/j.jsg.2011.11.011
1971 Mitra, S. (1988). Three-dimensional geometry and kinematic evolution of the Pine Mountain
1972 thrust system, southern Appalachians. *Geological Society of America Bulletin, 100*(1),
1973 72-95. doi:https://doi.org/10.1130/0016-7606(1988)100<0072:TDGAKE>2.3.CO;2
1974 Moffat, I. W., & Spang, J. H. (1984). Origin of transverse faulting, Rocky Mountain Front
1975 Ranges, Canmore, Alberta. *Bulletin of Canadian Petroleum Geology, 32*(2), 147-161.
1976 doi:https://doi.org/10.35767/gscpgbull.32.2.147
1977 Mogk, D. W., Mueller, P. A., & Wooden, J. L. (1992). The nature of Archean terrane
1978 boundaries: an example from the northern Wyoming Province. *Precambrian Research,*
1979 *55*(1-4), 155-168. doi:https://doi.org/10.1016/0301-9268(92)90020-O
1980 Monod, B., Dhont, D., & Hervouët, Y. (2010). Orogenic float of the Venezuelan Andes.
1981 *Tectonophysics, 490*(1-2), 123-135. doi:https://doi.org/10.1016/j.tecto.2010.04.036
1982 Mouthereau, F., Deffontaines, B., Lacombe, O., & Angelier, J. (2002). Variations along the
1983 strike of the Taiwan thrust belt: Basement control on structural style, wedge geometry,
1984 and kinematics. In T. Byrne & C.-S. Liu (Eds.), *Geology and Geophysics of an Arc-*
1985 *Continent collision, Taiwan, Republic of China* (Vol. 358, pp. 35-58). Boulder, Colorado:
1986 Geological Society of America Special Paper.
1987 Mouthereau, F., & Lacombe, O. (2006). Inversion of the Paleogene Chinese continental margin
1988 and thick-skinned deformation in the Western Foreland of Taiwan. *Journal of Structural*
1989 *Geology, 28*(11), 1977-1993. doi:https://doi.org/10.1016/j.jsg.2006.08.007
1990 Mouthereau, F., Lacombe, O., & Vergés, J. (2012). Building the Zagros collisional orogen:
1991 timing, strain distribution and the dynamics of Arabia/Eurasia plate convergence.
1992 *Tectonophysics, 532*, 27-60. doi:https://doi.org/10.1016/j.tecto.2012.01.022
1993 Mpodozis, C., & Ramos, V. (1989). The Andes of Chile and Argentina. In G. Ericksen, M.
1994 Cañas, & J. Reinemund (Eds.), *Geology of the Andes and its Relation to Hydrocarbon*
1995 *and Mineral Resources* (Vol. 11, pp. 59-90): Circum-Pacific Council for Energy and
1996 Mineral Resources.
1997 Mueller, P. A., Heatherington, A. L., Kelly, D. M., Wooden, J. L., & Mogk, D. W. (2002).
1998 Paleoproterozoic crust within the Great Falls tectonic zone: Implications for the assembly
1999 of southern Laurentia. *Geology, 30*(2), 127-130. doi:https://doi.org/10.1130/0091-
2000 7613(2002)030<0127:PCWTGF>2.0.CO;2
2001 Mugnier, J. L., Jouanne, F., Bhattarai, R., Cortes-Aranda, J., Gajurel, A., Leturmy, P., Robert,
2002 X., Upreti, B., & Vassallo, R. (2017). Segmentation of the Himalayan megathrust around
2003 the Gorkha earthquake (25 April 2015) in Nepal. *Journal of Asian Earth Sciences, 141*,
2004 236-252. doi:https://doi.org/10.1016/j.jseaes.2017.01.015
2005 Mugnier, J. L., Leturmy, P., Mascle, G., Huyghe, P., Chalaron, E., Vidal, G., Husson, L., &
2006 Delcaillau, B. (1999). The Siwaliks of western Nepal 1: Geometry and kinematics.
2007 *Journal of Asian Earth Sciences, 17*, 629-642. doi:https://doi.org/10.1016/S1367-
2008 9120(99)00038-3
2009 Mukherjee, S., Talbot, C. J., & Koyi, H. A. (2010). Viscosity estimates of salt in the Hormuz and
2010 Namakdan salt diapirs, Persian Gulf. *Geological Magazine, 147*(4), 497-507.
2011 doi:https://doi/org/10.1017/S001675680999077X

2012 Mukul, M. (2010). First-order kinematics of wedge-scale active Himalayan deformation: insights
2013 from Darjiling-Sikkim-Tibet (DaSiT) wedge. *Journal of Asian Earth Sciences, 39*, 645-
2014 657. doi:https://doi.org/10.1016/j.jseaes.2010.04.029
2015 Mukul, M., Jade, S., Ansari, K., Matin, A, Joshi, V. (2018). Structural insights from geodetic
2016 Global Positioning System measurements in the Darjiling-Sikkim Himalaya. *Journal of*
2017 *Structural Geology, 114*, 346-356. doi:https://doi.org/10.1016/j.jsg.2018.03.007
2018 Müller, W., Mancktelow, N. S., & Meier, M. (2000). Rb–Sr microchrons of synkinematic mica
2019 in mylonites: an example from the DAV fault of the Eastern Alps. *Earth and Planetary*
2020 *Science Letters, 180*(3-4), 385-397. doi:https://doi.org/10.1016/S0012-821X(00)00167-9
2021 Müller, W., Prosser, G., Mancktelow, N. S., Villa, I. M., Kelley, S. P., Viola, G., & Oberli, F.
2022 (2001). Geochronological constraints on the evolution of the Periadriatic Fault System
2023 (Alps). *International Journal of Earth Sciences, 90*(3), 623-653.
2024 doi:https://doi.org/10.1007/s005310000187
2025 Murphy, J. B., & Keppie, J. D. (2005). The Acadian Orogeny in the Northern Appalachians.
2026 *International Geology Review, 47*(7), 663-687. doi:https://doi.org/10.2747/0020-
2027 6814.47.7.663
2028 Murphy, J. B., Waldron, J. W., Kontak, D. J., Pe-Piper, G., & Piper, D. J. (2011). Minas Fault
2029 Zone: Late Paleozoic history of an intra-continental orogenic transform fault in the
2030 Canadian Appalachians. *Journal of Structural Geology, 33*(3), 312-328.
2031 doi:https://doi.org/10.1016/j.jsg.2010.11.012
2032 Nabelek, J., G. Hetenyi, J. Vergne, S. Sapkota, B. Kafle, M. Jiang, H. Su, J. Chen, and B.-S.
2033 Huang, and the Hi-CLIMB Team. (2009). Underplating in the Himalaya-Tibet collision
2034 zone revealed by the Hi-CL IMB experiment. *Science, 325*, 1371-1374.
2035 doi:https://doi.org/10.1126/science.1167719
2036 Norris, D. (2001). Slickenlines and the kinematics of the Crowsnest Deflection in the southern
2037 Rocky Mountains of Canada. *Journal of Structural Geology, 23*(6-7), 1089-1102.
2038 doi:https://doi.org/10.1016/S0191-8141(00)00180-2
2039 O'Brien, T. M., & van der Pluijm, B. A. (2012). Timing of Iapetus Ocean rifting from Ar
2040 geochronology of pseudotachylytes in the St. Lawrence rift system of southern Quebec.
2041 *Geology, 40*(5), 443-446. doi:10.1130/g32691.1
2042 O'Neill, J. M., & Lopez, D. A. (1985). Character and regional significance of Great Falls
2043 tectonic zone, east-central Idaho and west-central Montana. *AAPG Bulletin, 69*(3), 437-
2044 447. doi:https://doi.org/10.1306/AD462506-16F7-11D7-8645000102C1865D
2045 Oldham, R. D. (1917). Structure of the Himalayas and Indo-Gangetic plains. *Memoir of the*
2046 *Geological Survey of India, 156*.
2047 Oldow, J. S., Bally, A. W., Lallemant, H. G. A., & Leeman, W. P. (1989). Phanerozoic evolution
2048 of the North American Cordillera, United States and Canada. In A. W. Bally & A. R.
2049 Palmer (Eds.), *The geology of North America: an overview* (Vol. A, pp. 139-232):
2050 Geological Society of America, The Geology of North America.
2051 Oriolo, S., Japas, M. S., Cristallini, E. O., & Giménez, M. (2014). Cross-strike structures
2052 controlling magmatism emplacement in a flat-slab setting (Precordillera, Central Andes
2053 of Argentina). *Geological Society, London, Special Publications, 394*(1), 113-127.
2054 doi:https://doi.org/10.1144/sp394.6
2055 Oswald, P., Ortner, H., & Gruber, A. (2019). Deformation around a detached half-graben
2056 shoulder during nappe stacking (Northern Calcareous Alps, Austria). *Swiss Journal of*
2057 *Geosciences, 112*(1), 23-37. doi:https://doi.org/10.1007/s00015-018-0333-4

2058 Pantet, A., Epard, J.-L., & Masson, H. (2020). Mimicking Alpine thrusts by passive deformation
2059 of synsedimentary normal faults: a record of the Jurassic extension of the European
2060 margin (Mont Fort nappe, Pennine Alps). *Swiss Journal of Geosciences, 113*(1), 13.
2061 doi:10.1186/s00015-020-00366-2
2062 Pash, R. R., Sarkarinejad, K., Ghoochaninejad, H. Z., Motamedi, H., & Yazdani, M. (2020).
2063 Accommodation of the different structural styles in the foreland fold-and-thrust belts:
2064 northern Dezful Embayment in the Zagros belt, Iran. *International Journal of Earth*
2065 *Sciences*, 1-12. doi:https://doi.org/10.1007/s00531-020-01844-6
2066 Paul, H., Mitra, S., Bhattacharya, S.N., Suresh, G. (2015). Active transverse faulting within
2067 underthrust Indian crust beneath the Sikkim Himalaya. *Geophysics Journal International,*
2068 *201*(2), 1070-1081. doi:https://doi.org/10.1093/gji/ggv058
2069 Paulsen, T., & Marshak, S. (1997). Structure of the Mount Raymond transverse zone at the
2070 southern end of the Wyoming salient, Sevier fold-thrust belt, Utah. *Tectonophysics,*
2071 *280*(3-4), 199-211. doi:https://doi.org/10.1016/S0040-1951(97)00205-9
2072 Paulsen, T., & Marshak, S. (1998). Charleston transverse zone, Wasatch Mountains, Utah:
2073 Structure of the Provo salient's northern margin, Sevier fold-thrust belt. *Geological*
2074 *Society of America Bulletin, 110*(4), 512-522. doi:https://doi.org/10.1130/0016-
2075 7606(1998)110<0512:CTZWMU>2.3.CO;2
2076 Paulsen, T., & Marshak, S. (1999). Origin of the Uinta recess, Sevier fold–thrust belt, Utah:
2077 influence of basin architecture on fold–thrust belt geometry. *Tectonophysics, 312*(2-4),
2078 203-216. doi:https://doi.org/10.1016/S0040-1951(99)00182-1
2079 Perello, P., Delle Piane, L., Piana, F., Morelli, M., Damiano, A., & Venturini, G. (2004). New
2080 constraints on late to post-Oligocene deformation history of the Western Alps: data from
2081 Middle Susa valley and High Maurienne valley. *Abstract, 32nd IGC—Firenze, 247*.
2082 Perez-Estaun, A., Alvarez-Marron, J., Brown, D., Puchkov, V., Gorozhanina, Y., & Baryshev, V.
2083 (1997). Along-strike structural variations in the foreland thrust and fold belt of the
2084 southern Urals. *Tectonophysics, 276*(1-4), 265-280. doi:https://doi.org/10.1016/S0040-
2085 1951(97)00060-7
2086 Pérez-Flores, P., Cembrano, J., Sánchez-Alfaro, P., Veloso, E., Arancibia, G., & Roquer, T.
2087 (2016). Tectonics, magmatism and paleo-fluid distribution in a strike-slip setting: Insights
2088 from the northern termination of the Liquiñe–Ofqui fault System, Chile. *Tectonophysics,*
2089 *680*, 192-210. doi:http://dx.doi.org/10.1016/j.tecto.2016.05.016
2090 Perrone, G., Cadoppi, P., Tallone, S., & Balestro, G. (2011). Post-collisional tectonics in the
2091 Northern Cottian Alps (Italian Western Alps). *International Journal of Earth Sciences,*
2092 *100*(6), 1349-1373. doi:https://doi.org/10.1007/s00531-010-0534-1
2093 Petrinovic, I., Riller, U., Brod, J., Alvarado, G., & Arnosio, M. (2006). Bimodal volcanism in a
2094 tectonic transfer zone: evidence for tectonically controlled magmatism in the southern
2095 Central Andes, NW Argentina. *Journal of Volcanology and Geothermal Research,*
2096 *152*(3-4), 240-252. doi:https://doi.org/10.1016/j.jvolgeores.2005.10.008
2097 Pfiffner, O. A. (2014). *Geology of the Alps*: John Wiley & Sons.
2098 Picotti, V., Casolari, E., Castellarin, A., Mosconi, A., Cairo, E., Pessina, C., & Sella, M. (1997).
2099 Structural evolution of the eastern Lombardian Prealps: Alpine inversion of a Mesozoic
2100 rifted margin. *Agip SpA, San Donato Milanese, 102*.
2101 Pilger, R. H. J. (1981). Plate reconstructions, aseismic ridges, and low-angle subduction beneath
2102 the Andes. *GSA bulletin, 92*(7), 448-456. doi:10.1130/0016-
2103 7606(1981)92<448:Praral>2.0.Co;2

Pilkington, M., Miles, W., Ross, G., & Roest, W. (2000). Potential-field signatures of buried Precambrian basement in the Western Canada Sedimentary Basin. *Canadian Journal of Earth Sciences, 37*(11), 1453-1471. doi:https://doi.org/10.1139/e00-020

Piquer, J., Rivera, O., Yañez, G., & Oyarzun, N. (2020). The Piuquencillo Fault System: a long-lived, Andean-transverse fault system and its relationship with magmatic and hydrothermal activity. *Solid Earth Discussions*, 1-34. doi:https://doi.org/10.5194/se-2020-142

Pizzi, A., & Galadini, F. (2009). Pre-existing cross-structures and active fault segmentation in the northern-central Apennines (Italy). *Tectonophysics, 476*(1-2), 304-319. doi:https://doi.org/10.1016/j.tecto.2009.03.018

Plint, H. E., & Jamieson, R. A. (1989). Microstructure, metamorphism and tectonics of the western Cape Breton Highlands, Nova Scotia. *Journal of Metamorphic Geology, 7*(4), 407-424. doi:https://doi.org/10.1111/j.1525-1314.1989.tb00606.x

Polinski, R. K., & Eisbacher, G. H. (1992). Deformation partitioning during polyphase oblique convergence in the Karawanken Mountains, southeastern Alps. *Journal of Structural Geology, 14*(10), 1203-1213. doi:https://doi.org/10.1016/0191-8141(92)90070-D

Pomella, H., Stipp, M., & Fügenschuh, B. (2012). Thermochronological record of thrusting and strike-slip faulting along the Giudicarie fault system (Alps, Northern Italy). *Tectonophysics, 579*, 118-130. doi:https://doi.org/10.1016/j.tecto.2012.04.015

Prey, S. (1989). Ein steilstehendes Störungssystem als Westbegrenzung des Tauernfensters. *Journal of Geologische Bundesanstalt, 132*(4), 745-749.

Price, R. A. (1981). The Cordilleran foreland thrust and fold belt in the southern Canadian Rocky Mountains. *Geological Society, London, Special Publications, 9*(1), 427-448. doi:https://doi.org/10.1144/GSL.SP.1981.009.01.39

Pride, K. R., Lecouteur, P. C., & Mawer, A. B. (1986). Geology and mineralogy of the Aley carbonatite, Ospika River area, British Columbia. *Canadian Institute of Mining Bulletin, 79*(891), 32-32.

Prosser, G. (1998). Strike-slip movements and thrusting along a transpressive fault zone: The North Giudicarie line (Insubric line, northern Italy). *Tectonics, 17*(6), 921-937. doi:https://doi.org/10.1029/1998TC900010

Raiverman, V., Kunte, S.V., and Mukherjea, A. (1983). Basin geometry, Cenozoic sedimentation and hydrocarbon in northwestern Himalaya and Indo-Gangetic plains. *Petroleum Geology of Asia Journal, 6*(4), 67-92.

Rajaure, S., Sapkota, S.N., Adhikari, L.B., Koirala, B., Bhattarai, M., Tiwari, D.R., Gautam, U., Shrestha, P., Maske, S., Avouac, J.P., Bollinger, L., Pandey, M.R. (2013). Double difference relocation of local earthquakes in the Nepal Himalaya. *Journal of the Nepal Geological Society, 46*, 133-142.

Ramos, V. A. (1988). The tectonics of the Central Andes (30°–33°S latitude). In S. Clark, D. Burchfiel, & D. Suppe (Eds.), *Processes in Continental Lithospheric Deformation* (Vol. 218, pp. 31-54): Geological Society of America Special Paper.

Ramos, V. A., Cristallini, E. O., & Pérez, D. J. (2002). The Pampean flat-slab of the Central Andes. *Journal of South American earth sciences, 15*(1), 59-78. doi:https://doi.org/10.1016/S0895-9811(02)00006-8

Ramos, V. A., & Folguera, A. (2009). Andean flat-slab subduction through time. *Geological Society, London, Special Publications, 327*(1), 31-54. doi:10.1144/sp327.3

2149 Rankin, D. W. (1976). Appalachian salients and recesses: Late Precambrian continental breakup
2150 and the opening of the Iapetus Ocean. *Journal of Geophysical Research, 81*(32), 5605-
2151 5619. doi:https://doi.org/10.1029/JB081i032p05605
2152 Rao, M. B. R. (1973). The subsurface geology of the Indo-Gangetic plains. *Journal of The*
2153 *Geological Society of India, 14*(3), 217-242.
2154 Ratschbacher, L., Merle, O., Davy, P., & Cobbold, P. (1991). Lateral extrusion in the Eastern
2155 Alps, part 1: boundary conditions and experiments scaled for gravity. *Tectonics, 10*(2),
2156 245-256. doi:https://doi.org/10.1029/90TC02622
2157 Regard, V., Bellier, O., Thomas, J.-C., Bourles, D., Bonnet, S., Abbassi, M., Braucher, R.,
2158 Mercier, J., Shabanian, E., & Soleymani, S. (2005). Cumulative right-lateral fault slip
2159 rate across the Zagros—Makran transfer zone: role of the Minab—Zendan fault system in
2160 accommodating Arabia—Eurasia convergence in southeast Iran. *Geophysical Journal*
2161 *International, 162*(1), 177-203. doi:https://doi.org/10.1111/j.1365-246X.2005.02558.x
2162 Reiter, F., Freudenthaler, C., Hausmann, H., Ortner, H., Lenhardt, W., & Brandner, R. (2018).
2163 Active seismotectonic deformation in front of the Dolomites indenter, Eastern Alps.
2164 *Tectonics, 37*(12), 4625-4654. doi:https://doi.org/10.1029/2017TC004867
2165 Reynolds, M. W. (1979). Character and Extent of Basin-Range Faultin, Western Montana and
2166 East-Central Idaho. In G. W. Newman & H. D. Goode (Eds.), *Basin and Range*
2167 *Symposium and Great Basin Field Conference* (pp. 185-193). Denver: Rocky Mountain
2168 Association of Geologists.
2169 Ribes, C., Manatschal, G., Ghienne, J.-F., Karner, G. D., Johnson, C. A., Figueredo, P. H.,
2170 Incerpi, N., & Epin, M.-E. (2019). The syn-rift stratigraphic record across a fossil hyper-
2171 extended rifted margin: the example of the northwestern Adriatic margin exposed in the
2172 Central Alps. *International Journal of Earth Sciences, 108*(6), 2071-2095.
2173 doi:10.1007/s00531-019-01750-6
2174 Ring, U. (1994). The kinematics of the late Alpine Muretto fault and its relation to dextral
2175 transpression across the Periadriatic Line. *Eclogae Geologicae Helvetiae, 87*(3), 811-831.
2176 Ring, U., & Gerdes, A. (2016). Kinematics of the Alpenrhein-Bodensee graben system in the
2177 Central Alps: Oligocene/Miocene transtension due to formation of the Western Alps arc.
2178 *Tectonics, 35*(6), 1367-1391. doi:https://doi.org/10.1002/2015TC004085
2179 Rivers, T. (2008). Assembly and preservation of lower, mid, and upper orogenic crust in the
2180 Grenville Province—Implications for the evolution of large hot long-duration orogens.
2181 *Precambrian Research, 167*(3), 237-259.
2182 doi:https://doi.org/10.1016/j.precamres.2008.08.005
2183 Rivers, T. (2012). Upper-crustal orogenic lid and mid-crustal core complexes: signature of a
2184 collapsed orogenic plateau in the hinterland of the Grenville Province 1This article is one
2185 of a series of papers published in CJES Special Issue: In honour of Ward Neale on the
2186 theme of Appalachian and Grenvillian geology. *Canadian Journal of Earth Sciences,*
2187 *49*(1), 1-42. doi:https://doi.org/10.1139/e11-014
2188 Rivers, T. (2015). Tectonic Setting and Evolution of the Grenville Orogen: An Assessment of
2189 Progress Over the Last 40 Years. *Geoscience Canada, 42*(1), 77-124.
2190 doi:10.12789/geocanj.2014.41.057
2191 Robertson, A. H. F., Clift, P. D., Degnan, P. J., & Jones, G. (1991). Palaeogeographic and
2192 palaeotectonic evolution of the Eastern Mediterranean Neotethys. *Palaeogeography,*
2193 *Palaeoclimatology, Palaeoecology, 87*(1-4), 289-343. doi:https://doi.org/10.1016/0031-
2194 0182(91)90140-M

2195 Robinson, D. P., Das, S., & Watts, A. B. (2006). Earthquake rupture stalled by a subducting
2196 fracture zone. *Science, 312*(5777), 1203-1205.
2197 doi:https://doi.org/10.1126/science.1125771
2198 Robl, J., & Stüwe, K. (2005). Continental collision with finite indenter strength: 2. European
2199 Eastern Alps. *Tectonics, 24*(4). doi:https://doi.org/10.1029/2004TC001741
2200 Rodgers, J. (1990). Fold-and-thrust belts in sedimentary rocks. Part 1: Typical examples.
2201 *American Journal of Science, 290*(4), 321-359. doi:https://doi.org/10.2475/ajs.290.4.321
2202 Ronemus, C. B., Orme, D. A., Campbell, S., Black, S. R., & Cook, J. (2020).
2203 Mesoproterozoic−Early Cretaceous provenance and paleogeographic evolution of the
2204 Northern Rocky Mountains: Insights from the detrital zircon record of the Bridger Range,
2205 Montana, USA. *GSA bulletin*. doi:10.1130/b35628.1
2206 Root, K. G. (1987). *Geology of the Delphine Creek area, southeastern British Columbia:*
2207 *implications for the Proterozoic and Paleozoic development of the Cordilleran Divergent*
2208 *Margin.* (Ph.D.). University of Calgary, Calgary, Alberta.
2209 Roquer, T., Arancibia, G., Rowland, J., Iturrieta, P., Morata, D., & Cembrano, J. (2017). Fault-
2210 controlled development of shallow hydrothermal systems: Structural and mineralogical
2211 insights from the Southern Andes. *Geothermics, 66*, 156-173.
2212 doi:http://dx.doi.org/10.1016/j.geothermics.2016.12.003
2213 Rosenberg, C. L., Brun, J.-P., & Gapais, D. (2004). Indentation model of the Eastern Alps and
2214 the origin of the Tauern Window. *Geology, 32*(11), 997-1000.
2215 doi:https://doi.org/10.1130/G20793.1
2216 Rosenberg, C. L., & Garcia, S. (2011). Estimating displacement along the Brenner Fault and
2217 orogen-parallel extension in the Eastern Alps. *International Journal of Earth Sciences,*
2218 *100*(5), 1129-1145. doi:https://doi.org/10.1007/s00531-011-0645-3
2219 Ross, G., Parrish, R., Villeneuve, M., & Bowring, S. (1991). Geophysics and geochronology of
2220 the crystalline basement of the Alberta Basin, western Canada. *Canadian Journal of*
2221 *Earth Sciences, 28*(4), 512-522. doi:https://doi.org/10.1139/e91-045
2222 Royden, L., Horváth, F., Nagymarosy, A., & Stegena, L. (1983). Evolution of the Pannonian
2223 basin system: 2. Subsidence and thermal history. *Tectonics, 2*(1), 91-137.
2224 doi:https://doi.org/10.1029/TC002i001p00091
2225 Royden, L. H. (1993). Evolution of retreating subduction boundaries formed during continental
2226 collision. *Tectonics, 12*(3), 629-638. doi:https://doi.org/10.1029/92TC02641
2227 Sadeghi, S., & Yassaghi, A. (2016). Spatial evolution of Zagros collision zone in Kurdistan, NW
2228 Iran: Constraints on Arabia–Eurasia oblique convergence. *Solid Earth, 7*(2), 659-659.
2229 doi:https://doi.org/10.5194/se-7-659-2016
2230 Sahoo, P. K., Kumar, S., and Singh, R.P. (2000). Neotectonic study of Ganga and Yamuna tear
2231 faults, NW Himalaya, using remote sensing and GIS. *International Journal of Remote*
2232 *Sensing, 21*(3), 499-518. doi:https://doi.org/10.1080/014311600210713
2233 Saleeby, J. B. (2003). Segmentation of the Laramide slab—Evidence from the southern Sierra
2234 Nevada region. *Geological Society of America Bulletin, 115*(6), 655-668.
2235 doi:https://doi.org/10.1130/0016-7606(2003)115<0655:SOTLSF>2.0.CO;2
2236 Saleeby, J. B., Busby-Spera, C., Oldow, J. S., Dunne, G. C., Wright, J. E., Cowan, D. S., Walker,
2237 R. W., & Alllmendinger, R. W. (1992). Early Mesozoic tectonic evolution of the western
2238 US Cordillera. In B. C. Burchfiel, W. Lipman, & M. L. Zoback (Eds.), *The Cordilleran*
2239 *Orogen, Conterminous U.S., The Geology of North America G3* (pp. 107-168):
2240 Geological Society of America.

2241 Salfity, J. A., & Marquillas, R. A. (1994). Tectonic and sedimentary evolution of the Cretaceous-
2242 Eocene Salta Group basin, Argentina. In J. A. Salfity (Ed.), *Cretaceous tectonics of the*
2243 *Andes* (pp. 266-315): Vieweg+Teubner Verlag, Wiesbaden.
2244 Sarkarinejad, K., Pash, R. R., Motamedi, H., & Yazdani, M. (2018). Deformation and kinematic
2245 evolution of the subsurface structures: Zagros foreland fold-and-thrust belt, northern
2246 Dezful Embayment, Iran. *International Journal of Earth Sciences, 107*(4), 1287-1304.
2247 doi:https://doi.org/10.1007/s00531-017-1532-3
2248 Sastri, V. V., Bhandari, L.L., Raju, A.T.R., Datta, A.K. (1971). Tectonic framework and
2249 subsurface stratigraphy of the Ganga Basin. *Journal of The Geological Society of India,*
2250 *12*(3), 222-233.
2251 Satolli, S., Pace, P., Viandante, M. G., & Calamita, F. (2014). Lateral variations in tectonic style
2252 across cross-strike discontinuities: an example from the Central Apennines belt (Italy).
2253 *International Journal of Earth Sciences, 103*(8), 2301-2313.
2254 doi:https://doi.org/10.1007/s00531-014-1052-3
2255 Schepers, G., Van Hinsbergen, D. J., Spakman, W., Kosters, M. E., Boschman, L. M., &
2256 McQuarrie, N. (2017). South-American plate advance and forced Andean trench retreat
2257 as drivers for transient flat subduction episodes. *Nature communications, 8*, 15249.
2258 doi:https://doi.org/10.1038/ncomms15249
2259 Schmid, S. M., Aebli, H. R., Heller, F., & Zingg, A. (1989). The role of the Periadriatic Line in
2260 the tectonic evolution of the Alps. *Geological Society, London, Special Publications,*
2261 *45*(1), 153-171. doi:https://doi.org/10.1144/gsl.Sp.1989.045.01.08
2262 Schmid, S. M., Fügenschuh, B., Kissling, E., & Schuster, R. (2004). Tectonic map and overall
2263 architecture of the Alpine orogen. *Eclogae Geologicae Helvetiae, 97*(1), 93-117.
2264 doi:https://doi,org/10.1007/s00015-004-1113-x
2265 Schmid, S. M., Pfiffner, O.-A., Froitzheim, N., Schönborn, G., & Kissling, E. (1996).
2266 Geophysical-geological transect and tectonic evolution of the Swiss-Italian Alps.
2267 *Tectonics, 15*(5), 1036-1064. doi: https://doi.org/10.1029/96TC00433
2268 Schönborn, G. (1992). Kinematics of a transverse zone in the Southern Alps, Italy. In K. R.
2269 McClay (Ed.), *Thrust Tectonics* (pp. 299-310). Dordrecht: Springer Netherlands.
2270 Schumacher, M. E. (1990). Alpine basement thrusts in the Eastern Seengebirge, Southern Alps
2271 (Italy Switzerland). *Eclogae Geologicae Helvetiae, 83*(3), 645-663.
2272 Scrocca, D. (2006). Thrust front segmentation induced by differential slab retreat in the
2273 Apennines (Italy). *Terra nova, 18*(2), 154-161. doi: https://doi.org/10.1111/j.1365-
2274 3121.2006.00675.x
2275 Searle, M. P., Simpson, R. L., Law, R. D., Parrish, R. R., & Waters, D. J. (2003). The structural
2276 geometry, metamorphic and magmatic evolution of the Everest massif, High Himalaya of
2277 Nepal–South Tibet. *Journal of the Geological Society, 160*(3), 345-366. doi:
2278 https://doi.org/10.1144/0016-764902-126
2279 Sears, J. W., Hendrix, M., Waddell, A., Webb, B., Nixon, B., King, T., Roberts, E., & Lerman,
2280 R. (2000). Structural and stratigraphic evolution of the Rocky Mountain foreland basin in
2281 central-western Montana. In S. Roberts & D. Winston (Eds.), *Geologic Field Trips,*
2282 *Western Montana and Adjacent Areas. Edited by S. Roberts and D. Winston. Rocky*
2283 *Mountain Section Geological Society of America Annual Meeting* (pp. 131-156).
2284 Missoula: University of Montana.
2285 Sears, J. W., & Hendrix, M. S. (2004). Lewis and Clark line and the rotational origin of the
2286 Alberta and Helena salients, North American Cordillera. In A. Sussman & A. Weil

(Eds.), *Orogenic Curvature: Integrating Paleomagnetic and Structural Analyses: Geological Society of America Special Paper* (Vol. 383, pp. 173-186).

Seifert, N. (2019). *Structural analysis of the Benkar Fault Zone, a cross structure in the higher Himalaya of the Khumbu Region, eastern Nepal.* (MS). Montana State University, Bozeman, Montana.

Séjourné, S., & Malo, M. (2007). Pre-, syn-, and post-imbrication deformation of carbonate slices along the southern Quebec Appalachian front—implications for hydrocarbon exploration. *Canadian Journal of Earth Sciences, 44*(4), 543-564. doi:https://doi.org/10.1139/E06-106

Selverstone, J. (1988). Evidence for east-west crustal extension in the Eastern Alps: Implications for the unroofing history of the Tauern Window. *Tectonics, 7*(1), 87-105. doi:https://doi.org/10.1029/TC007i001p00087

Sepehr, M., Cosgrove, J., & Moieni, M. (2006). The impact of cover rock rheology on the style of folding in the Zagros fold-thrust belt. *Tectonophysics, 427*(1-4), 265-281. doi:https://doi.org/10.1016/j.tecto.2006.05.021

Sepehr, M., & Cosgrove, J. W. (2004). Structural framework of the Zagros fold–thrust belt, Iran. *Marine and Petroleum Geology, 21*(7), 829-843. doi:https://doi.org/10.1016/j.marpetgeo.2003.07.006

Sielfeld, G., Ruz, J., Brogi, A., Cembrano, J., Stanton-Yonge, A., Pérez-Flores, P., & Iturrieta, P. (2019). Oblique-slip tectonics in an active volcanic chain: A case study from the Southern Andes. *Tectonophysics, 770*, 228221. doi:https://doi.org/10.1016/j.tecto.2019.228221

Silver, C. R. P., Murphy, M. A., Taylor, M. H., Gosse, J., & Baltz, T. (2015). Neotectonics of the Western Nepal Fault System: Implications for Himalayan strain partitioning. *Tectonics, 34*(12), 2494-2513. doi:https://doi.org/10.1002/2014TC003730

Simony, P. S., & Carr, S. D. (1997). Large lateral ramps in the Eocene Valkyr shear zone: extensional ductile faulting controlled by plutonism in southern British Columbia. *Journal of Structural Geology, 19*(6), 769-784. doi:https://doi.org/10.1016/S0191-8141(97)00011-4

Sims, P. K., Bankey, V., & Finn, C. (2001). *Preliminary Precambrian basement map of Colorado: A geologic interpretation of the aeromagnetic map*: U.S. Geological Survey.

Skourlis, K., & Doutsos, T. (2003). The Pindos Fold-and-thrust belt (Greece): inversion kinematics of a passive continental margin. *International Journal of Earth Sciences, 92*(6), 891-903. doi:https://doi.org/10.1007/s00531-003-0365-4

Sobornov, K. O. (1996). Lateral variations in structural styles of tectonic wedging in the northeastern Caucasus, Russia. *Bulletin of Canadian Petroleum Geology, 44*(2), 385-399.

Sorgi, C., Deffontaines, B., Hippolyte, J. C., & Cadet, J. P. (1998). An integrated analysis of transverse structures in the northern Apennines, Italy. *Geomorphology, 25*(3-4), 193-206. doi:https://doi.org/10.1016/S0169-555X(98)00041-5

Soucy La Roche, R., and Godin, L. (2019). Inherited cross-strike faults and Oligocene-early Miocene segmentation of the Main Himalayan Thrust, West Nepal. *Journal of Geophysical Research Solid Earth, 124*, 7429-7444. doi:https://doi.org/10.1029/2019JB017467

Southworth, C. S. (1986). Side-looking airborne radar image map showing cross-strike structural discontinuities and lineaments of the central Appalachians. In *Miscellaneous Field Studies Map. doi: https://doi.org/10.3133/mf1891*.

2333 Sperner, B., Ratschbacher, L., & Nemčok, M. (2002). Interplay between subduction retreat and
2334 lateral extrusion: Tectonics of the Western Carpathians. *Tectonics, 21*(6), 1-1-1-24.
2335 doi:https://doi.org/10.1029/2001TC901028
2336 Srivastava, V., Mukul, M., Barnes, J.B., Mukul, M. (2018). Geometry and kinematics of Main
2337 Frontal thrust-related fault propagation folding in the Mohand Range, northwest
2338 Himalaya. *Journal of Structural Geology, 115*, 1-18.
2339 doi:https://doi.org/10.1016/j.jsg.2018.06.022
2340 Stampfli, G. M., & Borel, G. D. (2002). A plate tectonic model for the Paleozoic and Mesozoic
2341 constrained by dynamic plate boundaries and restored synthetic oceanic isochrons. *Earth*
2342 *and Planetary Science Letters, 196*(1), 17-33. doi:https://doi.org/10.1016/S0012-
2343 821X(01)00588-X
2344 Stanton-Yonge, A., Griffith, W., Cembrano, J., St. Julien, R., & Iturrieta, P. (2016). Tectonic role
2345 of margin-parallel and margin-transverse faults during oblique subduction in the Southern
2346 Volcanic Zone of the Andes: Insights from Boundary Element Modeling. *Tectonics,*
2347 *35*(9), 1990-2013. doi:https://doi.org/10.1002/2016TC004226
2348 Steck, A. (2008). Tectonics of the Simplon massif and Lepontine gneiss dome: deformation
2349 structures due to collision between the underthrusting European plate and the Adriatic
2350 indenter. *Swiss Journal of Geosciences, 101*(2), 515-546.
2351 doi:https://doi.org//10.1007/s00015-008-1283-z
2352 Stocklin, J. (1968). Structural history and tectonics of Iran: A review. *AAPG Bulletin, 52*(7),
2353 1229-1258. doi:https://doi.org/10.1306/5D25C4A5-16C1-11D7-8645000102C1865D
2354 Sue, C., & Tricart, P. (2003). Neogene to ongoing normal faulting in the inner western Alps: a
2355 major evolution of the late alpine tectonics. *Tectonics, 22*(5).
2356 doi:https://doi.org/10.1029/2002TC001426
2357 Talbot, C. J., & Alavi, M. (1996). The past of a future syntaxis across the Zagros. *Geological*
2358 *Society, London, Special Publications, 100*(1), 89-109.
2359 Tavarnelli, E., Butler, R. W. H., Decandia, F. A., Calamita, F., Grasso, M., Alvarez, W., Renda,
2360 P., Crescenti, U., & D'offizi, S. (2004). *Implications of fault reactivation and structural*
2361 *inheritance in the Cenozoic tectonic evolution of Italy*. Paper presented at the
2362 International Geological Congress 32.
2363 Tchalenko, J., & Braud, J. (1974). Seismicity and structure of the Zagros (Iran): the Main Recent
2364 Fault between 33 and 35 N. *Philosophical Transactions of the Royal Society of London.*
2365 *Series A, Mathematical and Physical Sciences, 277*(1262), 1-25.
2366 doi:https://doi.org/10.1098/rsta.1974.0044
2367 Thomas, W. A. (1977). Evolution of Appalachian-Ouachita salients and recesses from reentrants
2368 and promontories in the contineral margin. *American Journal of Science, 277*, 1233-
2369 1278. doi:http://dx.doi.org/10.2475/ajs.277.10.1233.
2370 Thomas, W. A. (1990). Controls on locations of transverse zones in thrust belts. *Eclogae*
2371 *Geologicae Helvetiae, 83*(3), 727-744.
2372 Thomas, W. A. (1991). The Appalachian-Ouachita rifted margin of southeastern North America.
2373 *Geological Society of America Bulletin, 103*(3), 415-431.
2374 doi:https://doi.org/10.1130/0016-7606(1991)103<0415:TAORMO>2.3.CO;2
2375 Thomas, W. A. (2007). Role of the Birmingham basement fault in thin-skinned thrusting of the
2376 Birmingham anticlinorium, Appalachian thrust belt in Alabama. *American Journal of*
2377 *Science, 307*(1), 46-62. doi:https://doi.org/10.2475/01.2007.03

Thomas, W. A. (2014). A mechanism for tectonic inheritance at transform faults of the Iapetan margin of Laurentia. *Geoscience Canada*, 321-344. doi:http://dx.doi.org/10.12789/geocanj.2014.41.048

Thomas, W. A., & Bayona, G. (2002). Palinspastic restoration of the Anniston transverse zone in the Appalachian thrust belt, Alabama. *Journal of Structural Geology, 24*(4), 797-826. doi:https://doi.org/10.1016/S0191-8141(01)00117-1

Thompson, R. I. (1989). Stratigraphy, tectonic evolution and structural analysis of the Halfway River map area (94B), northern Rocky Mountains, British Columbia. *Geological Survey of Canada, 425*, 1-119.

Thomson, S. N. (2002). Late Cenozoic geomorphic and tectonic evolution of the Patagonian Andes between latitudes 42˚ S and 46˚ S: An appraisal based on fission-track results from the transpressional intra-arc Liquiñe-Ofqui fault zone. *Geological Society of America Bulletin, 114*(9), 1159-1173. doi:https://doi.org/10.1130/0016-7606(2002)114<1159:LCGATE>2.0.CO;2

Tricart, P. (1984). From passive margin to continental collision; a tectonic scenario for the Western Alps. *American Journal of Science, 284*(2), 97-120. doi:https://doi.org/10.2475/ajs.284.2.97

Tull, J. F., & Holm, C. S. (2005). Structural evolution of a major Appalachian salient-recess junction: Consequences of oblique collisional convergence across a continental margin transform fault. *Geological Society of America Bulletin, 117*(3-4), 482-499. doi:https://doi.org/10.1130/B25578.1

Urbanek, C., Frank, W., Grasemann, B., & Decker, K. (2002). Eoalpine versus Tertiary deformation: Dating of heterogeneously partitioned strain (Tauern Window, Austria). Pangeo Austria: Erdwissenschaften in€ Osterreich 28.-30.6. 2002 (Program and abstract). *Institute for geology and paleontology University of Salzburg*.

Valdiya, K. S. (1976). Himalayan transverse faults and folds and their parallelism with subsurface structures of North Indian plains. *Tectonophysics, 32*, 353-386. doi:https://doi.org/10.1016/0040-1951(76)90069-X

Valensise, G., & Pantosti, D. (2001). The investigation of potential earthquake sources in peninsular Italy: a review. *Journal of Seismology, 5*(3), 287-306. doi:https://doi.org/10.1023/A:1011463223440

van der Beek, P., Litty, C., Baudin, M., Mercier, J., Robert, X., Hardwick, E. (2016). Contrasting tectonically driven exhumation and incision patterns, western versus central Nepal Himalaya. *Geology, 44*(4), 327-330. doi:https://doi.org10.1130/G37579.1

van Staal, C. R., Whalen, J. B., McNicoll, V. J., Pehrsson, S., Lissenberg, C. J., Zagorevski, A., van Breemen, O., & Jenner, G. A. (2007). The Notre Dame arc and the Taconic orogeny in Newfoundland. In R. D. Hatcher, Jr., M. P. Carlson, J. H. McBride, & J. R. Martínez Catalán (Eds.), *4-D Framework of Continental Crust: Geological Society of America Memoir 200* (pp. 511-552).

Vargas, G., Rebolledo, S., Sepúlveda, S. A., Lahsen, A., Thiele, R., Townley, B., Padilla, C., Rauld, R., Herrera, M. J., & Lara, M. (2013). Submarine earthquake rupture, active faulting and volcanism along the major Liquiñe-Ofqui Fault Zone and implications for seismic hazard assessment in the Patagonian Andes. *Andean Geology, 40*(1), 141-171. doi:https://doi.org/10.5027/andgeoV40n1-a07

Vergani, G., Tankard, J., Belotti, J., & Welsink, J. (1995). Tectonic evolution and paleogeography of the Neuquén Basin, Argentina. In A. Tankard, R. Suárez, & H.

Welsink (Eds.), *Petroleum Basins of South America* (Vol. 62): American Association of Petroleum Geologists.

Vernant, P., & Chéry, J. (2006). Mechanical modelling of oblique convergence in the Zagros, Iran. *Geophysical Journal International, 165*(3), 991-1002. doi:https://doi.org/10.1111/j.1365-246X.2006.02900.x

Vernant, P., Nilforoushan, F., Hatzfeld, D., Abbassi, M., Vigny, C., Masson, F., Nankali, H., Martinod, J., Ashtiani, A., & Bayer, R. (2004). Present-day crustal deformation and plate kinematics in the Middle East constrained by GPS measurements in Iran and northern Oman. *Geophysical Journal International, 157*(1), 381-398. doi:https://doi.org/10.1111/j.1365-246X.2004.02222.x

Viola, G., Mancktelow, N. S., & Seward, D. (2001). Late Oligocene-Neogene evolution of Europe-Adria collision: New structural and geochronological evidence from the Giudicarie fault system (Italian Eastern Alps). *Tectonics, 20*(6), 999-1020. doi:https://doi.org/10.1029/2001tc900021

Waldron, J. W., Barr, S. M., Park, A. F., White, C. E., & Hibbard, J. (2015). Late Paleozoic strike-slip faults in Maritime Canada and their role in the reconfiguration of the northern Appalachian orogen. *Tectonics, 34*(8), 1661-1684. doi:https://doi.org/10.1002/2015TC003882

Wallace, C. A., Lidke, D. J., & Schmidt, R. G. (1990). Faults of the central part of the Lewis and Clark line and fragmentation of the Late Cretaceous foreland basin in west-central Montana. *Geological Society of America Bulletin, 102*(8), 1021-1037. doi:https://doi.org/10.1130/0016-7606(1990)102<1021:FOTCPO>2.3.CO;2

Weil, A. B., Yonkee, A., & Schultz, M. (2016). Tectonic evolution of a Laramide transverse structural zone: Sweetwater Arch, south central Wyoming. *Tectonics, 35*(5), 1090-1120. doi:https://doi.org/10.1002/2016TC004122

Weinberg, R. F. (2016). Himalayan leucogranites and migmatites: nature, timing and duration of anatexis. *Journal of Metamorphic Geology, 34*(8), 821-843. doi:https://doi.org/10.1111/jmg.12204

West Jr, D. P., & Hubbard, M. S. (1997). Progressive localization of deformation during exhumation of a major strike-slip shear zone: Norumbega fault zone, south-central Maine, USA. *Tectonophysics, 273*(3-4), 185-201. doi:https://doi.org/10.1016/S0040-1951(96)00306-X

Wheeler, R. L. (1980). Cross-strike structural discontinuities: possible exploration tool for natural gas in Appalachian overthrust belt. *AAPG Bulletin, 64*(12), 2166-2178. doi:https://doi.org/10.1306/2F91975B-16CE-11D7-8645000102C1865D

Whisner, S. C., Schmidt, C. J., & Whisner, J. B. (2014). Structural analysis of the Lombard thrust sheet and adjacent areas in the Helena salient, southwest Montana, USA. *Journal of Structural Geology, 69*, 351-376. doi:http://dx.doi.org/10.1016/j.jsg.2014.08.006

Whitmeyer, S. J., & Karlstrom, K. E. (2007). Tectonic model for the Proterozoic growth of North America. *Geosphere, 3*(4), 220-259. doi:https://doi.org/10.1130/GES00055.1

Williams, H., & Cawood, P. (1986). Relationships along the eastern margin of the Humber Arm allochthon between Georges Lake and Corner Brook, Newfoundland. *Current Research, Part A. Geological Survey of Canada, Paper, 86*, 759-765.

Wooden, J., & Mueller, P. (1988). Pb, Sr, and Nd isotopic compositions of a suite of Late Archean, igneous rocks, eastern Beartooth Mountains: implications for crust-mantle

evolution. *Earth and Planetary Science Letters, 87*(1-2), 59-72. doi:https://doi.org/10.1016/0012-821X(88)90064-7

Yeats, R. S., and Lillie, R.J. (1991). Contemporary tectonics of the Himalayan frontal fault system: folds, blind thrusts and the 1905 Kangra earthquake. *Journal of Structural Geology, 13*(2), 215-225.

Yonkee, W. A., & Weil, A. B. (2015). Tectonic evolution of the Sevier and Laramide belts within the North American Cordillera orogenic system. *Earth-Science Reviews, 150*, 531-593. doi:http://dx.doi.org/10.1016/j.earscirev.2015.08.001

Zanchetta, S., D'Adda, P., Zanchi, A., Barberini, V., & Villa, I. M. (2011). Cretaceous-Eocene compression in the central Southern Alps (N Italy) inferred from 40Ar/39Ar dating of pseudotachylytes along regional thrust faults. *Journal of Geodynamics, 51*(4), 245-263. doi:https://doi.org/10.1016/j.jog.2010.09.004

Zanchi, A., D'Adda, P., Zanchetta, S., & Berra, F. (2012). Syn-thrust deformation across a transverse zone: the Grem–Vedra fault system (central Southern Alps, N Italy). *Swiss Journal of Geosciences, 105*(1), 19-38. doi:https://doi.rog/10.1007/s00015-011-0089-6

Zerlauth, M., Ortner, H., Pomella, H., Pfiffner, O. A., & Fügenschuh, B. (2014). Inherited tectonic structures controlling the deformation style: an example from the Helvetic nappes of the Eastern Alps. *Swiss Journal of Geosciences, 107*(2-3), 157-175. doi:https://doi.org/10.1007/s00015-014-0167-7

Zhao, W., K. D. Nelson, the Project INDEPTH Team. (1993). Deep seismic reflection evidence for continental underthrusting beneath southern Tibet. *Nature geoscience, 366*, 557-559. doi:https://doi.org/10.1038/366557a0